SYNTHESIS AND REACTIVITY OF N-HETEROCYCLIC CHALCOGENONE COMPLEXES OF COPPER AND SILVER

by

Alexander M. Allen

A thesis submitted to the faculty of
The University of North Carolina at Charlotte
in partial fulfillment of the requirements
for the degree of Master of Science in Chemistry

Charlotte

2018

Approved by:

_____
Dr. Daniel Rabinovich

_____
Dr. Thomas A. Schmedake

_____
Dr. Christopher M. Bejger

_____
Dr. Miguel Pando

ABSTRACT

ALEXANDER M. ALLEN. Synthesis and reactivity of N-heterocyclic chalcogenone complexes of copper and silver. (Under the direction of DR. DANIEL RABINOVICH)

This presentation outlines the synthesis and characterization of several unusual two-coordinate copper(I) and silver(I) complexes supported by bulky N-heterocyclic thione (NHT) and selone (NHSe) ligands. More specifically, copper(I) complexes of the general formula (IArE)CuX (E = S, Se; Ar = Xy, Mes, Dipp; X = Cl, Br, I) have been prepared and fully characterized using a variety of spectroscopic and analytical techniques. Similarly, rare examples of homoleptic silver(I) complexes with NHT or NHSe ligands, $[Ag(IArE)_2]X$ (X = NO_3, BF_4, ClO_4, PF_6, or SbF_6), have also been isolated and fully characterized. The molecular structures of several (IArE)CuX and $[Ag(IArE)_2]X$ complexes have been determined by X-ray crystallography, which confirms the monomeric nature for both series of compounds in the solid state. Many of the silver(I) complexes are currently being assessed for potential biological activity against various cancer cell lines.

ACKNOWLEDGEMENTS

I am beyond grateful for all of the wonderful people I have met and all of the experiences I've had in my time at UNC Charlotte. I have learned valuable life lessons that I will carry with me forever, and truly learned how to connect with myself. Unlike many other things throughout my life, I was determined that I would finish this program regardless of what it took. Nevertheless, it was an amazing journey that I will never forget. Thanks to Dr. Daniel Rabinovich for being the best advisor I could have ever hoped for. From the day I joined his lab, he saw something in me and challenged me to become the researcher I am now. He's made me set new standards for myself which have been permanently instilled within me. He allowed me to not only excel, but gave me confidence in myself. If it weren't for him, I would have never committed to entering the Master's program in the first place.

I also would have never started this program if it weren't for Mr. Ernest Ritchie, my former high school chemistry teacher. Thanks to him for his detailed explanations, countless anecdotal stories, and laughs. He helped me discover my fascination with chemistry, eventually inspiring me to devote my career and life to it. I would also obviously like to thank my parents for being such an influence on me throughout my life. Most of all, you raised me to have an open mind, which has allowed me to see the world through my own eyes. I could always count on you both to be there whenever I needed help or just needed to talk. The guidance you gave me has made me strive to be the best person I can possibly be. If I can become half the parent either of you were, I'll be doing pretty good. I would also like to thank the rest of my family who was always there to

motivate and encourage me. I would especially like to acknowledge my grandfather's influential role in my life. I truly admired him and he was part of my decision to pursue chemistry and to continue onto my Master's degree.

Maison, Akshar, Riley, and Mattison have all taught me the meaning of true friendship and gave me the encouragement to get through some of my toughest times. Above all else, they helped me realize that sometimes I'm too hard on myself and sometimes I just need to relax. Just know that I would do anything in the world for each of you.

Thank you to the DR group and everyone who has helped me along the way. This never would have been possible without the hard work and dedication of several students that I had the pleasure working with. Mustafa, Kirk, and Bryant, you all put up with me and helped me in more ways than you'll ever realize. Sarah, Hussain, Evan, Flannery, Michelle, Mil, Sanjit, Raahil, Ryan, Emery, and Zoe, thanks for being amazing lab mates and assisting me with my research in any way you could. I will always owe my success to you all. Marissa, thank you for always being there to show me things I didn't know and to have friendly conversation with. Margaret, thanks for training me in the lab and teaching me everything you knew. You're all so bright and it's been a pleasure getting to know you all personally. I wish you all luck and success in your lives.

I would also like to thank my committee members, Drs. Schmedake, Bejger, and Pando, for providing guidance to me and helping me develop my skills as a researcher. Thanks to Mrs. Rabinovich for the positive words of encouragement when I was stressed. Dr. Ogle, thanks for letting me use your five-decimal place balance so often! I also thank Dr. Afonin and Justin Halman for their help and collaboration with the biological testing.

That was an amazing experience that made me a more well-rounded researcher. Victoria, thank you for always being around to talk to on a daily basis and giving me words of encouragement. I wish you luck in your future endeavors. Last but certainly not least, I would like to thank Dr. James Golen (UMass Dartmouth) for his invaluable contribution to obtain all the crystal structures presented in this work.

TABLE OF CONTENTS

LIST OF FIGURES

LIST OF TABLES

LIST OF SCHEMES

LIST OF ABBREVIATIONS

AIF	Apoptosis Inducing Factor
DCM	Dichloromethane
DMSO	Dimethyl Sulfoxide
Dipp	2,6-diisopropylphenyl
DNA	Deoxyribonucleic acid
EA	Elemental Analysis
ESI-MS	Electrospray Ionization Mass Spectrometry
FT–IR	Fourier Transform Infrared Spectroscopy
h	hour(s)
IC_{50}	Half maximal inhibitory concentration
Mes	2,4,6-trimethylphenyl (mesityl)
MeCN	acetonitrile
MTT	3-(4,5-dimethylthiazol-2-yl)-2,5diphenyltetrazolium bromide
NHC	N-Heterocyclic Carbene
NHE	N-Heterocyclic Chalcogenone
NHT	N-Heterocyclic Thione
NHSe	N-Heterocyclic Selone
NHTe	N-Heterocyclic Telone
NMR	Nuclear Magnetic Resonance
ppm	parts per million

PTA	1,3,5-triaza-7-phosphaadamantane
THF	tetrahydrofuran
TMS	tetramethylsilane
XRD	X-Ray Diffraction
Xy	2,6-dimethylphenyl (2,6-xylyl)

CHAPTER 1: INTRODUCTION

1.1. Carbenes

A carbene consists of a divalent carbon atom bonded to two other atoms, that leads to the carbon having two unshared electrons (Figure 1.1). Carbenes have been theorized to exist *in situ* since 1903 when German chemist Eduard Buchner studied the cyclopropanation of ethyl diazoacetate.[1] In the following decades, many others argued that the presence of a methylene intermediate in several organic transformation reactions was evident.[2,3] In 1964, Fischer and Maasböl reported the first metal-carbon double bond with the synthesis of $(CO)_5W{=}C(Ph)(OMe)$.[4] The existence of such a species was heavily debated due to the inability to effectively isolate a stable carbene for many years to come until this was achieved by Arduengo in 1991 with the isolation of a free, stable N-heterocyclic carbene (NHC).[5] Now, carbenes have a well-planted place in chemistry on both a microscale and industrial scale.

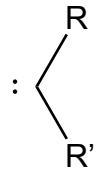

Figure 1.1. The general form of a carbene.

Carbenes as a whole can be divided into two classes that effectively explain their reactivity towards a set of chemical species. Singlet and triplet carbenes can be distinguished by their electronic spins and display disparate reactivity characteristics.[6] A singlet carbene is a divalent carbon atom that is sp^2 hybridized due to the electrons being spin-paired (Figure 1.2). This type of carbene prefers a bent molecular geometry and those with unfilled p-orbitals can be electrophilic.

The second type of carbene, triplet carbenes, have unpaired electrons and can be observed via electron spin resonance spectroscopy due to this.[7] Triplet carbenes exhibit more of a radical-like reactivity while singlet carbenes tend to be more nucleophilic. Their reactivity also varies upon the substituent groups and can coordinate with many metals and main-group elements.

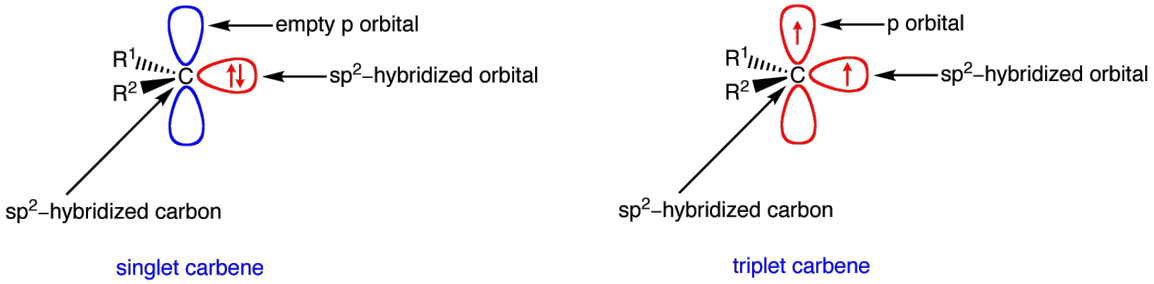

Figure 1.2. Diagram of a singlet vs. triplet carbene.

1.2. *N*-Heterocyclic Carbenes (NHCs)

With a heterocycle being simply a cyclic compound consisting of at least two different atoms, the variation in structure can be expansive with all having different reactivity. Nitrogen-containing heterocycles are thus given the description of an *N*-heterocycle. NHCs are in their own class and are relatively well studied, more recently for their involvement in catalytic transformations at an industrial level and for many metal-NHC complexes exhibiting biological activity.[8]

The structure of a typical NHC can vary in the number of atoms that constitute the "backbone", the substituents appended to the nitrogen or carbon atoms, and the number and placement of the nitrogen atoms in the ring.[9] NHCs with only one nitrogen atom are known and NHCs with three nitrogen atoms are fairly common, with the most common being triazoles. The largest class of NHCs are of the five-membered ring type and the

placement of the atoms in the ring has a large effect on the electronic properties of the molecule. With the expansive list of known NHCs, only those of the five-membered variety will be discussed in this work.

It is understood that NHCs benefit from aromaticity and due to this require less steric bulk for electronic stabilization of the heteroatoms. This suggests that unsaturated NHCs (imidazolylidenes) (Figure 1.3) do not require as much steric bulk for electronic stabilization as saturated NHCs (imidazolinylidenes).

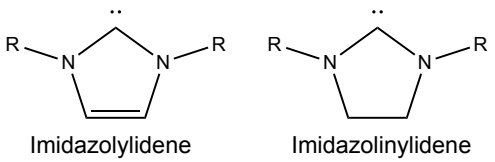

Figure 1.3. Structure of imidazolylidene (unsaturated backbone) versus imidazolinylidene (saturated backbone).

Generally, the substituents on the nitrogen atoms are indeed bulky, which provide excellent kinetic stabilization and disfavor dimerization. Despite this, NHCs bearing just hydrogen atoms are known, especially for asymmetrical versions. Regardless of the bulky groups attached to the ring, it is important to note that the greatest electronic stabilization comes from the nitrogen atoms, given their σ-electron-withdrawing and π-electron-donating nature (Figure 1.4). The increased electronegativity when compared to carbon leads to an inductive effect in the direction of the nitrogen atom(s) to increase the s-character in singlet carbenes by stabilizing the σ-nonbonding orbital. The pπ-pπ electron-donation into the empty p-orbital of the carbene carbon creates a mesomeric effect, the primary stabilizing effect for the carbene. This is very often described as a "push-pull" mechanism, and accurately so.

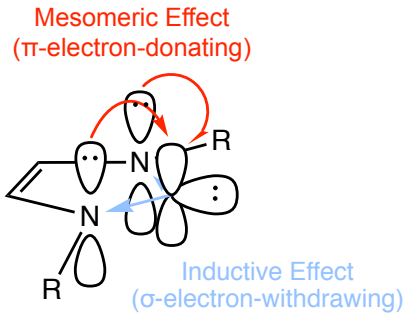

Figure 1.4. Inductive and mesomeric effects within a typical NHC.

Additionally, the π donation into the empty p-orbital on the carbene carbon forces the lone pair of electrons on the carbon to be in the same plane as the ring in singlet carbenes. As a result, NHCs are usually referred to as more nucleophilic due to their σ–donating fashion and in turn can coordinate to many metals and nonmetals.

Unsaturated NHCs tend to be slightly more stable as a result of the π-electrons in the backbone (C=C) and aromaticity confirmed by charge density studies and inner-shell electron loss spectroscopy.[10,11] These studies showed that the precursor imidazolium salts tend to show more aromaticity than the NHC and their metal complexes. The π delocalization by the inductive and mesomeric effects seen in NHCs also increases the stabilization energy by 70 kcal mol^{-1} and about a 20 kcal mol^{-1} favorable difference for unsaturated NHCs over saturated ones, suggesting possibly a cyclic electron delocalization occurring across the entire ring.[12]

1.3. *N*-Heterocyclic Thione (NHT) and Selone (NHSe) Ligands

Similar to traditional NHCs, ligands bearing a heavy chalcogen (S, Se, Te) are very good σ-donors and more polarizable due to their lowered electronegativity.[13] Although the atomic radius of selenium is larger than that of sulfur, the electronegativities of the two are about the same. Oxygen, however, with its high

electronegativity prefers to bind to lithophiles, such as the alkali metals and early transition metals. Due to resonance, chalcogen donor ligands gain electronic stability that allows a strong C=E (E = S, Se) bond that is shorter than traditional C-E single bonds and longer that C=E double bonds.[14] Conversely, when studying C-O bonds, oxygen's polar nature allows for a more highly polarized σ-bond in the direction of the oxygen atom. The more highly polarized the carbon-chalcogen bond, the higher the magnitude of the negative charge. This idea helps explain why the larger chalcogens have decreased σ-polarization and reduced negative charge, resulting in less polar C-E bonds. When viewing the resonance structures of the NHT and NHSe ligands, we can observe the zwitterionic resonance structures that depict C^{+}-E^{-} dative covalent bonds (Figure 1.5). The less polar C-E bonds of sulfur and selenium tend to prefer the zwitterionic form, whereas oxygen prefers a more of a C=E double bond.

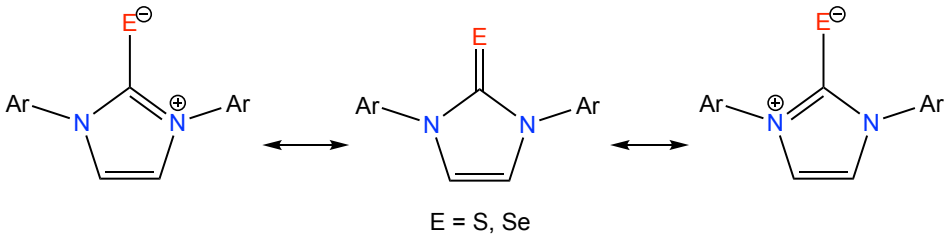

Figure 1.5. Resonance forms of the IArE ligands.

1.4. Project Goals

The overall objective for this project is to synthesize a series of N-heterocyclic thione and selone ligands and explore their reactivity specifically with copper(I) and silver(I). The general nomenclature for the NHT and NHSe ligands is IArE, where 'I' signifies the presence of the imidazole backbone, 'Ar' describes the aromatic substituents bound to the nitrogen atoms, and 'E' is the chalcogen donor, sulfur or selenium (Figure 1.6). The

aromatic substituents in this project are 2,6-dimethylphenyl (Xy), 2,4,6-trimethylphenyl (Mes), and 2,6-diisopropylphenyl (Dipp).

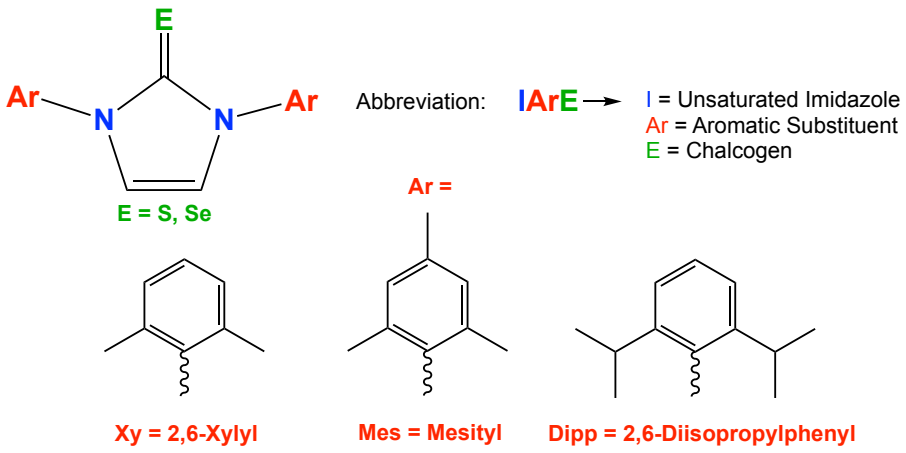

Figure 1.6. General diagram to explain the nomenclature for the NHT and NHSe ligands.

Utilizing the plethora of past and current research on NHCs in a variety of settings it is of interest to determine in what ways a ligand bearing a sulfur or selenium donor atom can outperform these previously reported complexes. The reactivity of this set of ligands with copper(I) and silver(I) will be investigated through the synthesis of a number of new complexes. It has also been of interest to synthesize new or rare mononuclear, linear two-coordinate silver(I) complexes and conduct biological studies. Due to a vast array of evidence that many silver(I)-NHC complexes possess antimicrobial and anticancer activity, it is of interest to examine the reactivity of our NHT and NHSe ligands with silver in an attempt to create a series of potentially cytotoxic complexes.[8,15-17] Once synthesized, cell studies will be completed in an attempt to assess the capabilities of our ligands to show anticancer potential and compare our results directly with that of many complexes reported in primary literature. It is reported that it is the Ag^{+} ions that

are able to cause damage to cancer cells and halt their proliferation in the human body. It is our hypothesis that due to our ligands improved donation into empty d orbitals of the d^{10} metals, we can create a slower, more sustained release of Ag^{+} ions at the cancer site, enhancing its capability. This concept is discussed in greater detail in Chapter 3.

1.5. Introduction to Metallodrugs

Metallodrugs have been well-investigated in recent years due to their ever-growing applications across many different fields. To date, metallodrugs have found practical use as therapeutics for such conditions as arthritis, diabetes, cardiovascular diseases, and cancer. Additionally, metallodrugs have more recently been used as diagnostic tools to assist in imaging biological targets through the use of radioactive isotopes of various transition metals.[18,19] Regardless of the application, metallodrugs are an expanding field in medicine, and quite interestingly, a large portion of these drugs have high toxicity in the human body. Current research is focused towards creating safer alternatives by exploring less toxic routes in terms of more safe metals and striving to understand the mechanism of action within the human body.

By observing metallodrugs developed over the recent decades, it is evident that there is no uniform design or framework proven to be superior. Traditionally, when designing a drug, it is essential to determine the method of action by which the disease proliferates and then locate a molecular target for the metallodrug to reach. In order to determine a target, it is crucial to understand how the metal is uptaken in the body, how it is transported, its function, and how it is excreted.[20] There are several ways by which these drugs function in the body, but most notably it is through interactions with organic acids, proteins, sugars, or DNA fragments.[21] Many of the essential amino acids contain

donor atoms in their side chains which allows for interactions with the metallodrug or its ligands. Similarly, in proteins, the various N-terminuses of many natural proteins allow for interaction with a metal center.[22] Consequently, bonded metal ions alter the proteins structure and alter its normal functions. In DNA, metal ions are able to bond with all four nitrogenous bases of the nucleotides and create intrastrand cross-links, inhibiting replication.[23] Alternatively, small drug molecules are able to intercalate between the base pairs of DNA, altering its normal structure, similar to how some poisons work. Very commonly the metal ions can interact with the amino acid side-chains of proteins as well to create a protein-DNA cross-link.[24]

Metal-based drugs can vary in the coordination number, geometry, and redox states, allowing for tunability. Not to mention, for all of these drugs, the metal center dictates how the drug will interact in the body. As noted, a key advantage of metallodrugs over traditional organic molecules for the treatment of diseases is the ability to fine tune ligands or create multiple "generations" of drugs based on slight structural modifications to alter toxicity, lipophilicity, thermodynamic stability, and ultimately increase the drug's pharmacokinetics.[25] By changing the ligands coordinated to the metal center, different areas of the cell can be targeted, which completely determines the mechanism of action. Obviously, a huge concern of emerging metallodrugs is how the metal complex degrades in the body and what happens to the metal and ligand(s) throughout its time in the body.

Traditionally, drug design is a process that is carefully completed once an understanding of the biological target is obtained. Once a clear target is identified, a mechanism of action must be hypothesized that limits the amount of side effects to the patient. This lengthy process occurs through innovative drug design, borrowing ideas

from nature, or pure chance (like the discovery of cisplatin), followed by rigorous testing. Regardless, drug design is a whole area of research in itself, and far outside the scope or practicality of this thesis. In our case, active searching in literature allowed our group to assess current work around Ag(I)-NHCs and employ this in a unique and facile way to generate a novel series of cytotoxic complexes.

1.6. Evolution of Metallodrugs in Recent Decades

It was 1967 when Barnett Rosenberg discovered the formation of cisplatin (*cis*-diamminedichloroplatinum(II)) while investigating the effect of an electrical field on bacterial growth.[26] After noting that the bacterial cells were elongated and cell division was halted, Rosenberg noted that the drug "differs from that of other reported methods" and knew that the complex had unique properties. Cisplatin (formed as a byproduct from the platinum electrodes used in the study) was later found to create DNA-crosslinks. In 1969, Rosenberg *et al.* promptly tested the antitumor activity of four platinum compounds, with cisplatin being one of these.[27] It was concluded through these series of tests that platinum compounds do possess antitumor activity, but it was noted at the time that the mechanism of action was unknown.

Since then, cancer research has been very prevalent in primary literature and a myriad of chemotherapeutic drugs have been developed as a result. Since cancer research is a lucrative and flourishing field, browsing even recent advancements can be a daunting task. Needless to say, there have been thousands of organic and inorganic drugs introduced in recent years with no signs of slowing down. To touch on this subject, platinum-based drugs will be discussed first. Since the discovery of the antitumor potential of cisplatin, platinum-based drugs have been a subject of interest. Square-planar

complexes of Pt(II) seem to be the most prevalent, with many of these complexes categorized as later 'generations' of Pt-based drugs. Currently, 50% of all chemotherapeutic regimens employ Pt-based drugs, whether they are administered independently or in combination with other chemotherapeutic drugs to decrease acquired resistance in the body.[28] The only FDA-approved Pt-based drugs used to treat cancer are cisplatin, carboplatin, and oxaliplatin – all three of these are used worldwide (Figure 1.7).

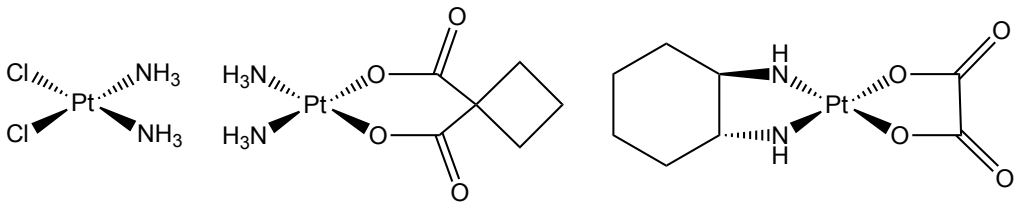

Figure 1.7. Molecular structures of cisplatin (left), carboplatin (middle), and oxaliplatin (right).

Platinum-based drugs exhibit serious side effects (nephrotoxicity, neurotoxicity, ototoxicity, nausea, vomiting, diarrhea, ototoxicity, myelosuppression) which is a driving force to explore drugs utilizing a different metal center.[29]

Ruthenium is another promising metal for the design of chemotherapeutic drugs due to its role in a variety of biochemical processes. It is less toxic than Pt-based drugs, but acts similarly to target DNA. The range of oxidation states (II-IV) and typical octahedral geometry allow for the tuning of the complexes' electronic and steric properties.[30] Perhaps the most promising of the Ru-based drugs is NAMI-A ([Him]trans-[$RuCl_4$(DMSO-S)(imidazole)]) and was the first ruthenium compound tested on humans (Figure 1.8).[19] This drug is the only Ru-based drug that made it to phase II of clinical trials and was found to have antimetastatic properties.[31]

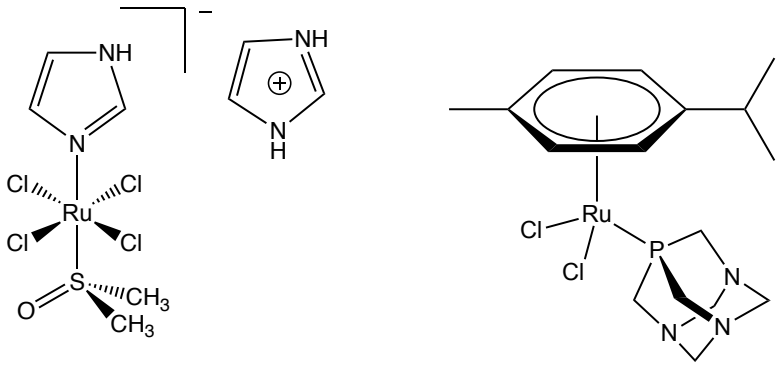

Figure 1.8. NAMI-A (left) and RAPTA-C (right).

Also worth discussing when mentioning Ru-based complexes are RAPTA compounds. This class of ruthenium-arene compounds possess a 1,3,5-triaza-7-phosphatricyclo-[3.3.1.1]decane (PTA) ligand which allows for water solubility, with the most popular being RAPTA-C ([Ru(η^6-p-cymene)Cl_2(PTA)]) (Figure 1.8). No Ru-based complexes have been used commercially, despite being flaunted as a replacement to toxic Pt-based drugs.

With platinum- and ruthenium-based metallodrugs being the most common and thoroughly studied, the focus of more recent work has been finding alternatives. Not only does a complex need to have lower toxicity, it must be stable enough to make it to the target of interest, be transported easily in blood and through membranes, bind to DNA but not proteins, kill or damage only cancerous cells, and offer toxicity in areas that are resistant to cisplatin and its derivatives. This is quite an expansive list and few transition metals have shown significant promise. In order to satisfy these requirements, not only must the correct transition metal be chosen, but the ligands must be chosen carefully. The ligand systems are what dictate the lipophilicity/hydrophilicity of the complex, solubility in different mediums, and its ability to permeate through cell membranes. All of these are

important and ensure that the metallodrug reaches its target and enhances its practicality for *in vivo* applications.

1.7. Silver NHC Complexes with Biological Activity

Focusing solely on anticancer applications, few metals other than platinum and ruthenium show promise. Of these, the most notable are zinc, copper, silver, and gold. For the purpose of expediency, the primary focus of this work will be recent advancements in silver-based anticancer complexes.

Silver is suggested to exhibit low toxicity when compared with other transition metals and is widely utilized for its antibacterial properties (Table 1.1). The earliest reported use of silver was in 69 B.C. when $AgNO_3$ was used to treat *ophthalmia neonatorum*, a form of conjunctivitis that affects newborns.[32]

Table 1.1. Comparison of the properties of Pt(II), Au(I), and Ag(I) metallodrugs in anticancer and antibacterial drugs.[33]

	Pt(II)	Au(I)	Ag(I)
Anticancer drugs			
Efficacy	High	High (*in vitro*)	High (*in vitro*)
Cytotoxicity	High	High (*in vitro*)	Low (*in vitro*)
Drawbacks	Many	Many	Not known
Resistance	Yes	Yes	Not known
Bioavailability	Scarce	Scarce	Low
Antibacterial drugs			
Efficacy	High (*in vitro*)	High (*in vitro*)	High
Human toxicity	Under assessment	Not reported	No
Resistance	Not known	Not known	No

Traditionally, silver was known to help heal infections, burns, wounds, and prevent contagious diseases, and it was used extensively until the development of antibiotics around 1940. More recently, silver has found applications in ointments, socks, airplane tray tables, and shower curtains – all used to kill or prevent the formation of bacteria.

Bacterial resistance to silver is rare and is theorized to be a result of silver undergoing multiple mechanisms within a cell to trigger cell death.[34] There is no known biological role for silver in the human body and excess silver ions easily form AgCl with chloride ions found throughout the body to reduce cytotoxicity to normal cells.[35]

Current work seems to suggest that complexes of gold and silver use a different mechanism of action compared to other metal-based drugs. They do not target DNA but instead target the mitochondrial membrane of cancer cells or inhibit thiol-containing proteins or enzymes.[36] More specifically, silver complexes are found to inhibit thioredoxin reductase (TrxR) to trigger mitochondria-initiated apoptosis.[37] TrxR is a selenoenzyme that is essential for cell growth and survival. By catalyzing the reduction of thioredoxin (Trx) and other oxidized dithiols, TrxR allows for ribonucleotide reductase to produce deoxyribonucleotides, which is necessary for DNA synthesis.[38] However, the full mechanism has yet to be fully elucidated. The cytotoxicity of silver compounds comes mainly from the silver ion and the ligands mostly act as tunable scaffolds to modify the lipophilicity or hydrophilicity. Having the ability to make these modifications can have drastic effects on the efficacy of the complex when completing *in vitro* studies. Metal-ligand interactions are also important when mentioning this area of research as ligand exchange reactions within the cell can also have an impact on the interactions with individual cellular components. It is also suggested that the slower the release of Ag^{+} ions in the cancer cell, the higher the cytotoxic effect. It was our hypothesis that the use of our sterically-demanding ligands, with their strong electron-donating properties that form strong Ag(I)-E (E = S or Se) bonds, would create a series of promising chemotherapeutic agents that offer advantages unparalleled in current works. With many silver complexes

outperforming cisplatin in various cell lines, this was obviously an area that was of utmost importance to pursue.

Knowing that strong coordination to the Ag(I) center is essential, an overwhelming majority of anticancer Ag(I) complexes employ the use of NHC ligands.[33] Silver complexes that do not contain some sort of nitrogenous heterocycle are known, but do not tend to exhibit as significant effects, and are more common for antibacterial applications. Due to their strong σ-donating abilities, silver-NHCs display a moderate ability to slow the metal release once in the cell. It has been reported that including chlorides or other electron-withdrawing substituents on an imidazole backbone can increase the stability of Ag-NHC complexes from hours to weeks in the aqueous solution phase.[17] This also happens to be the first report of a Ag(I)-NHC displaying anticancer potential which came in 2008 when Youngs *et al.* reported testing a series of three complexes derived from 4,5-dichloro-1H-imidazole against OVCAR-3 (ovarian), MB157 (breast), and HeLa (cervical) cell lines (Figure 1.9).[17] All three complexes were found to be active against the ovarian and breast cancer lines. It is believed that the presence of electron-withdrawing groups on the imidazole backbone such as chlorides can decrease the electron density at the carbene carbon, allowing for a higher degree of back-bonding to the empty p-orbital of the carbene carbon atom from the metal, along with improved carbene-to-metal donation forming a stronger Ag-C bond, and therefore a slower release of the cytotoxic Ag^{+} ion.

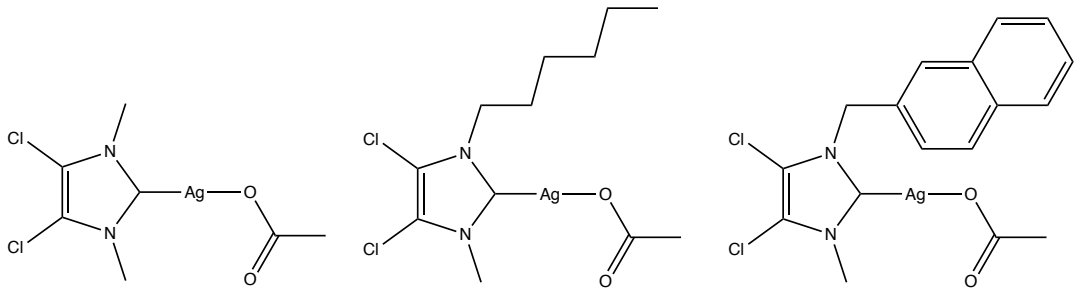

Figure 1.9. Series of Ag(I)-NHC complexes synthesized by Youngs *et al*.[17]

Benzimidazole-based complexes are proposed to accumulate in a cell's mitochondria and depolarize their membrane, ultimately resulting in self-induced apoptosis by means of damaging the endoplasmic reticulum and translocating the apoptosis inducing factor (AIF) from the internal portion of the mitochondrial membrane to the cytosol and eventually the nucleus.[39] Other Ag-NHC complexes were found to lower the mitochondria inner membrane potential ($\Delta\Psi_m$) which causes the release of varying mitochondrial proteins, followed by an apoptosis pathway. Combining these two effects may be even more effective by ensuring that cells are unable to avoid programmed cell death. In the same publication by Roland *et al*., several Ag-NHC complexes were reported to display IC_{50} values in the nanomolar range. More specifically, the two most promising complexes that were tested were of similar nature, (Figure 1.10). As one example, against the cancer cell line HL60 (promyelocytic leukemia) IPrAgCl and SIPrAgCl displayed IC_{50} values of 35 ± 5 nM and 58 ± 1 nM, respectively. Compared to cisplatin with an IC_{50} value of 5.9 μM, the results are surely promising as the number of Ag-NHC complexes displaying equal or comparable cytotoxic ability are not present in literature.

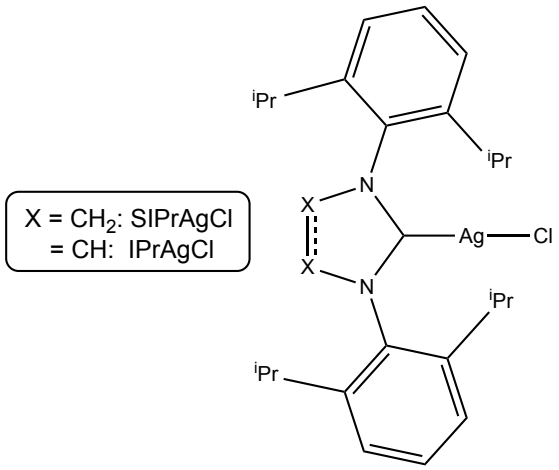

Figure 1.10. Molecular structure of SIPrAgCl/IPrAgCl that exhibited cytotoxicity in the nanomolar range against the HL60 cell line.[39]

Studies have also been completed that vary the length and steric hindrance of the substituents appended to the back carbon atoms of the imidazole. In a study by Bjørsvik *et al.*, the effect of increasing the length of an alkyl group on an imidazole ligand was investigated through the use of two similar alkyl-substituted Ag-NHCs on HL60 and MOLM-13 leukemic cells.[40] N-1-Phenyl-N-3-methyl-4-methylimidazolium iodide and N-1-phenyl-N-3-methyl-4-heptylimidazolium iodide (Figure 1.11) were synthesized based on an eight step synthetic route and the corresponding Ag-NHC complexes were synthesized by reacting these imidazolium salts with silver(I) oxide in DCM. The results of this study showed that increasing the length and steric hindrance of the side chain is directly related to the observed cytotoxicity. The Ag-NHC bearing a heptyl side chain at the 4-position displayed four- to six-fold lower IC_{50} values than the corresponding complex bearing methyl groups at the same position on the imidazole.

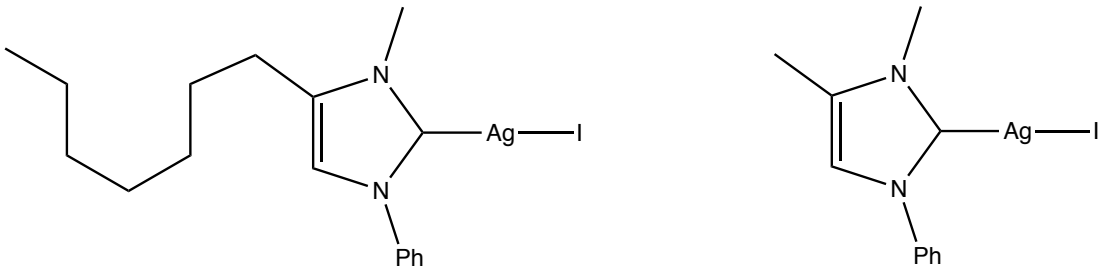

Figure 1.11. N-1-Phenyl-N-3-methyl-4-heptylimidazolium iodide (left) and N-1-phenyl-N-3-methyl-4-methylimidazolium iodide (right).[40]

Staying on the topic of substituents on the N-atoms, Chi-Ming Che *et al.* reported the use of N,N'-*p*-methoxyphenyl disubstituted imidazolidine-2-thiones with copper(I), silver(I), and gold(I) to create mononuclear homoleptic cationic complexes.[41]

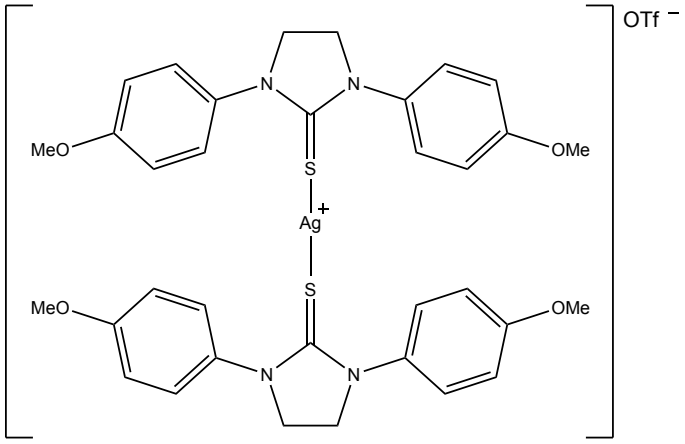

Figure 1.12. Mononuclear homoleptic Ag(I)-NHC complex synthesized by Che *et al.*[41]

The silver complex showed the greatest cytotoxicity with IC_{50} values for HeLa, HepG2, SUNEI, and NCI-H460 cells ranging from 4.0 to 8.9 μM (Figure 1.12). Also worth noting, this same Ag-NHC reportedly inhibited TrxR and glutathione peroxidase (GPx) at an IC_{50} of 100 nM and 1 μM, respectively, while also suppressing glucocorticoid receptor (GR) activities at a concentration of 50 μM. This paper was partially an influence to our

work, due to the similar nature of the thione ligand set bearing bulky aromatic substituents. Several attempts were made to synthesize the unsaturated imidazole analog of the ligands used in this study, but this came with little success as the imidazolium salt could not be isolated in pure form.

To compare the effects of mono- and dinuclear Ag-NHCs towards cancer cells, Haque *et al.* synthesized nitrile-functionalized NHC complexes to find that the binuclear complex afforded more promising results when compared to the mononuclear analog against HCT 116 cells with IC_{50} values of 1.7 ± 0.4 and 27.2 ± 1.1 μM, respectively (Figure 1.13).[42]

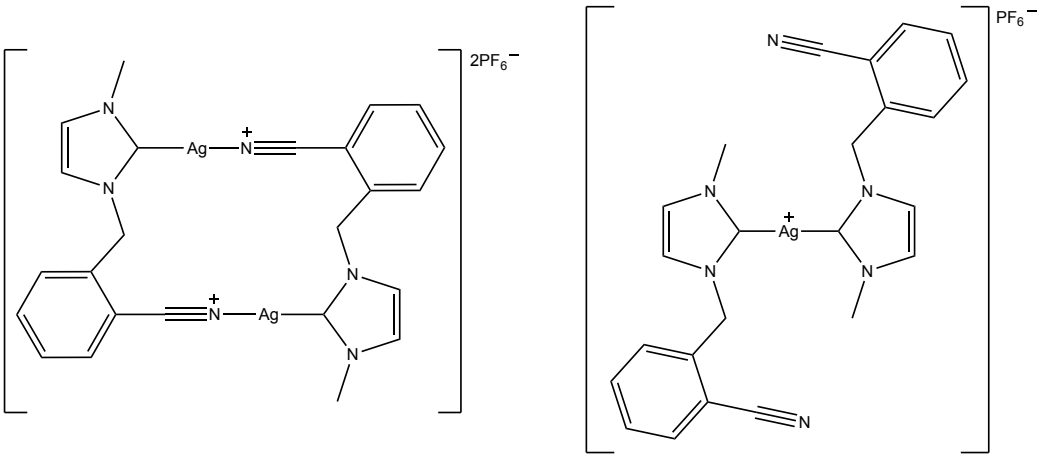

Figure 1.13. Di- and mononuclear nitrile-functinoalized Ag(I)-NHCs by Haque *et al.*[42]

On the topic of bis-NHC ligands, in a more recent article by Haque *et al*., propylene linked bis-benzimidazole complexes were tested against MCF-7 cells with all of the complexes showing significant and similar activity (IC_{50} = 7 ± 1 μM – 18 ± 3 μM) (Figure 1.14). The corresponding benzimidazolium salts were found to show no cytotoxic activity.[43]

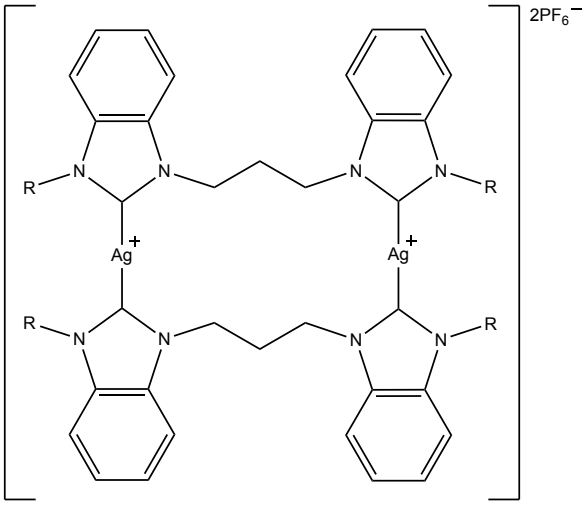

Figure 1.14. Dinuclear propylene-linked bis-benzimidazole Ag(I)-NHCs.[43]

As demonstrated, the diversity of Ag-NHC complexes is expansive and dizzying with appreciable progress being made in the last decade. It is safe to say that the scientific community is not yet able to make a claim that there is a "magic formula" when designing silver(I) complexes. It is apparent that Ag-NHC complexes benefit from a more synergistic effect, as the complexes repeatedly show higher cytotoxicity than the free metal and ligand individually. Several other studies have produced a large number of cytotoxic Ag(I)-NHC complexes with unique features.

Gandin *et al.* synthesized many water-soluble compounds and tested them against A549, HCT-15, MCF-7, A431, and A375 cells.[44] One of these compounds showed anticancer potential with an average IC_{50} value of 11.63 μM across all five cell lines, compared to cisplatin with an average of 8.50 μM (Figure 1.15).

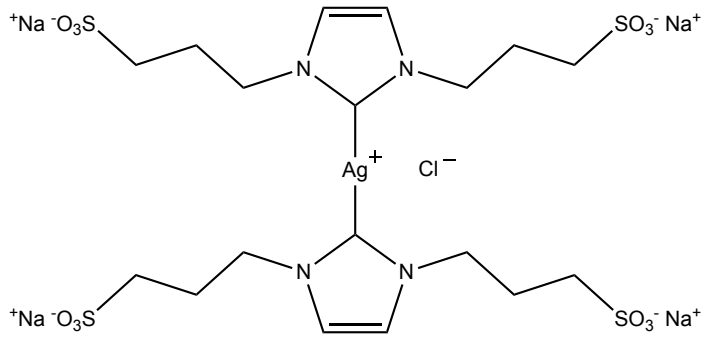

Figure 1.15. Example of an effective homoleptic water-soluble Ag(I)-NHC.[44]

Citta *et al.* synthesized a fluorescent Ag(I)-NHC bearing a anthracenyl moiety on the N1 position of the imidazole (Figure 1.16).[45] Against cisplatin sensitive (A2780S) and cisplatin resistant (A2780R) ovarian cancer cell lines and a human embryonic kidney cell line HEK-293T, the complex showed significant activity with IC_{50} values ranging from 3-7 μM. When observing the inhibitory effect on cytosolic (TrxR1) and mitochondrial (TrxR2) thioredoxin reductases, the silver analog was more effective here as well. Obviously, fluorescence studies were completed using fluorescence confocal microscopy to view the distribution of the cancer complexes within the cancer cells. As expected, the results showed that both complexes were able to penetrate the tumor cells and reach the nuclear compartment.

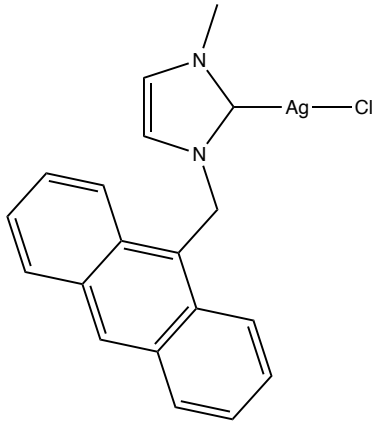

Figure 1.16. Fluorescent Ag(I)-NHC bearing an anthracenyl ligand.[45]

Lastly, many *p*-nitrobenzyl-substituted mono- and Ag(I)-bis-NHC complexes were synthesized and screened for their anticancer potential.[46] All complexes showed very potent effects with IC_{50} values in the nanomolar range against the human derived breast adenocarcinoma cell line (MCF 7). The Ag(I)-mono-NHC compounds demonstrated higher cytotoxicity than the bis-NHC variants, an important finding for the design of future silver anticancer drugs. However, one bis-NHC complex in particular outperformed all of the mono-NHC variants and was the best-performing complex tested in this study (IC_{50} = 10.39 nM) (Figure 1.17).

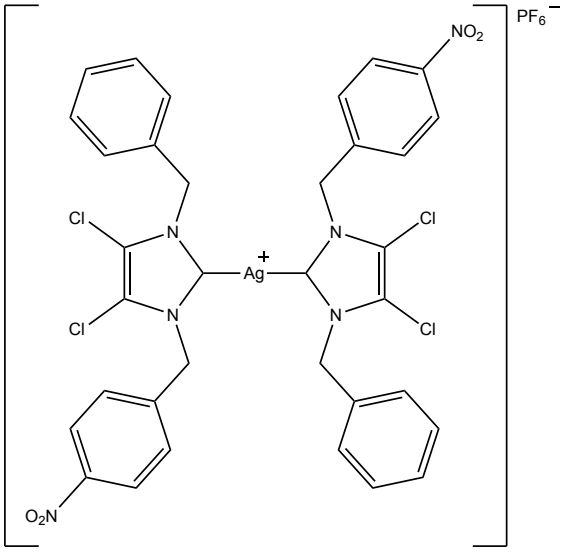

Figure 1.17. *p*-Nitrobenzyl-substituted mono- and bis-NHC-Ag(I) complex that showed substantial cytotoxic effects against MCF 7 breast cancer cell line.[46]

CHAPTER 2: RESULTS AND DISCUSSION

2.1. Synthesis of *N*-heterocyclic Thione and Selone Ligands

The ligands were synthesized according to a combination of procedures reported in literature (Scheme 2.1).[47-57] First, two equivalents of the corresponding aniline derivative is reacted with 40% w/w glyoxal in a warmed primary alcohol in the presence of micromolar amounts of acetic acid as an acid catalyst, resulting in the diimine or N,N'-bis(alkylphenyl)-1,4-diazabutadiene (DAD) product formation in as little as 5-10 minutes. It is important to note that this forms the backbone of the final ligand (C-C). A bright yellow fine powder is typically isolated easily after repeated washes with cold alcohol in a fritted funnel. It is likely that the conjugation across the entire system allows for the absorption in the visible region. This DAD intermediate is then dried under reduced pressure overnight.

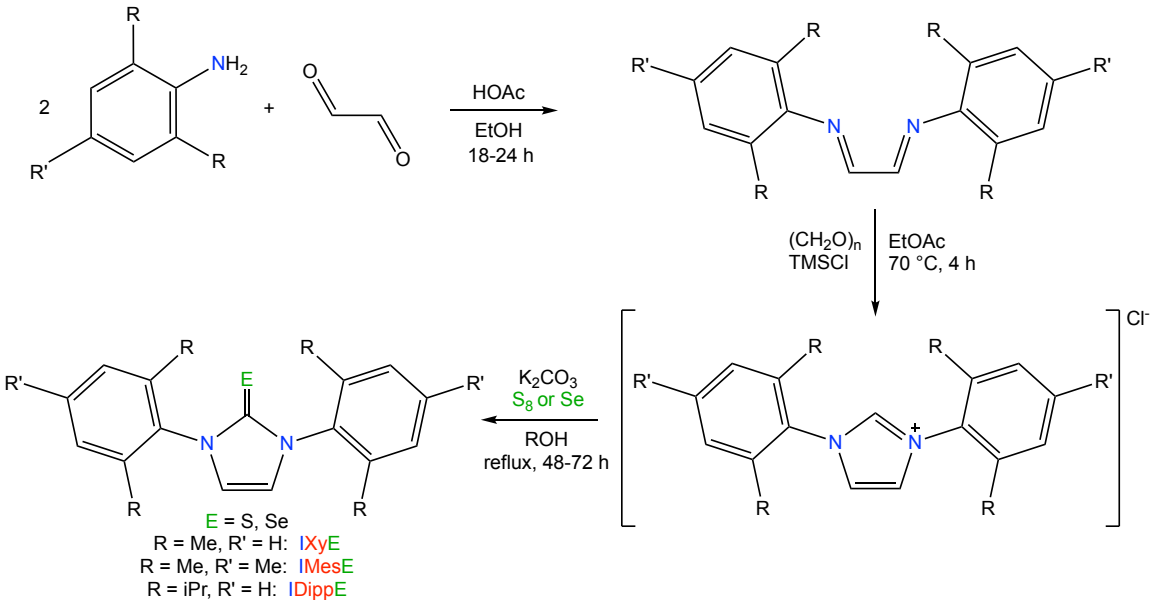

Scheme 2.1. Synthesis of NHT and NHSe ligands.

The DAD is then reacted with paraformaldehyde in warm anhydrous ethyl acetate to form the sp^2-hybridized N-C-N bond and form the heterocyclic ring. A solution of chlorotrimethylsilane in the same solvent is then added dropwise to the warmed suspension to assist in the formation of the imidazolium salt. The product is then isolated and washed extensively with cold ethyl acetate. The imidazolium salt is finally refluxed in a primary alcohol with K_2CO_3 to act as a powerful base to abstract the methine proton from the carbon atom located between the two nitrogen atoms on the imidazole ring. This generates the spin-paired singlet state carbene in solution that is then free to bond with either elemental sulfur or selenium. Potassium carbonate is believed to undergo multiple mechanisms to act as a base in this system. It is possible CO_3^{2-} is basic enough to deprotonate the primary alcohol in the presence of small amounts of water to produce a highly reactive alkoxide ion that is then free to deprotonate the C2 carbon of the imidazolium salt, regenerating the respective primary alcohol to form KCl as a byproduct. With the mildly basic carbonate/bicarbonate and alkoxide ions present in solution, the alkoxide ion will most likely abstract the methine proton through a S_N2 reaction due to it having lower steric hindrance. Potassium carbonate is insoluble in room temperature ethanol but upon refluxing with the imidazolium salt and elemental sulfur or selenium, it is observed to go into solution with a slight excess sometimes visible during the reaction and during workup, prior to extraction. This method seems to work best for IDipp and IMes imidazolium salts, with purity and yield issues arising when attempting to synthesize IXyE in any scale. It may be worthwhile to use the conjugate base of the primary alcohol to test the claim of an S_N2 mechanism occurring in the the chalcogenation reactions to generate the carbene in-situ. For example, using sodium

ethoxide in place of potassium carbonate when refluxing in ethanol may result in a more favorable deprotonation, also with less possible byproducts (only MCl where M = Li, Na, K). Potassium tert-butoxide, also could act as an inexpensive yet powerful base for the same outcome.

Upon synthesizing and isolating these six ligands, they appear as white or off-white powdery solids that have proven to be extremely air-stable and moisture resistant, dissimilar to traditional NHCs. This is a huge benefit that allows ease of handling and storage. It can be seen by ^{1}H NMR spectroscopy that minimal to no decomposition is observed in ligands synthesized 1-2 years previously.

2.2. Synthesis and Characterization of Copper(I) Complexes

A number of unusual copper(I) complexes supported by IArE ligands have been synthesized and fully characterized by a number of analytical and spectroscopic techniques. Copper(I) halide salts that are used to synthesize these complexes are air-sensitive and require the use of an inert atmosphere. A facile synthetic route that minimizes exposure to air in both the liquid and solid phases employs a glovebox. Once synthesized and dried *in vacuo* for at least 24 hours, the (IArE)CuX (X = Cl, Br, I) complexes were found to be stable in air, which demonstrates our ligands' ability to sterically protect the Cu(I) center and prevent oxidation and decomposition.

All complexes are synthesized by reacting one equivalent of the copper(I) halide salt with one equivalent of ligand in a 1:1 mixture of acetonitrile and tetrahydrafuran for 24-48 h to afford typically white or off-white powdery solids collected by vacuum

filtration and washed with pentane (Scheme 2.2).

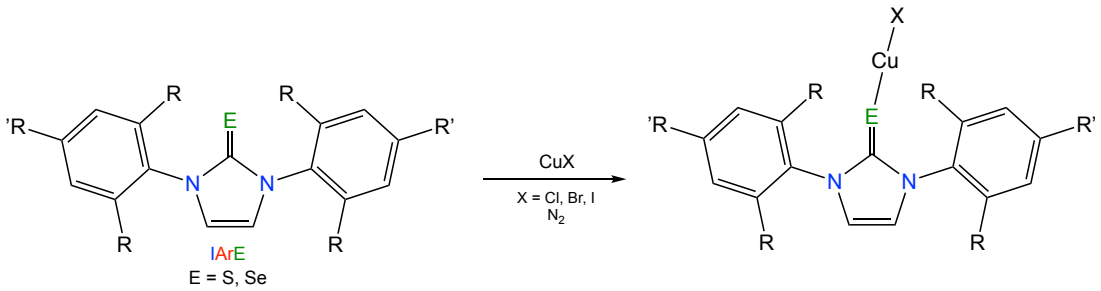

Scheme 2.2. Synthesis of copper(I) complexes supported by NHT or NHSe ligands.

Most of these complexes exhibit a linear heteroleptic two-coordinate geometry while $[Cu(IMesSe)_2]CuCl_2$ showed the formation of a linear homoleptic two-coordinate cationic copper(I) complex with a $CuCl_2^-$ counterion.[58] Complexes of this type bearing NHT or NHSe ligands are rare or unknown. Of these complexes, a few were used to grow crystals suitable for single-crystal x-ray diffraction using reaction filtrate or through dissolving a small amount in various organic solvents and allowing slow evaporation to occur. Reacting two equivalents of ligand is expected to increase the tendency to create these homoleptic cations but has not been fully pursued, due to the intention of using these species as an intermediate or synthon for further reactivity studies. These (IArE)CuX complexes were characterized further by ^1H and ^{13}C NMR spectroscopies (Figures 2.1-2.3), elemental analysis, melting point determination, and FT-IR spectroscopy.

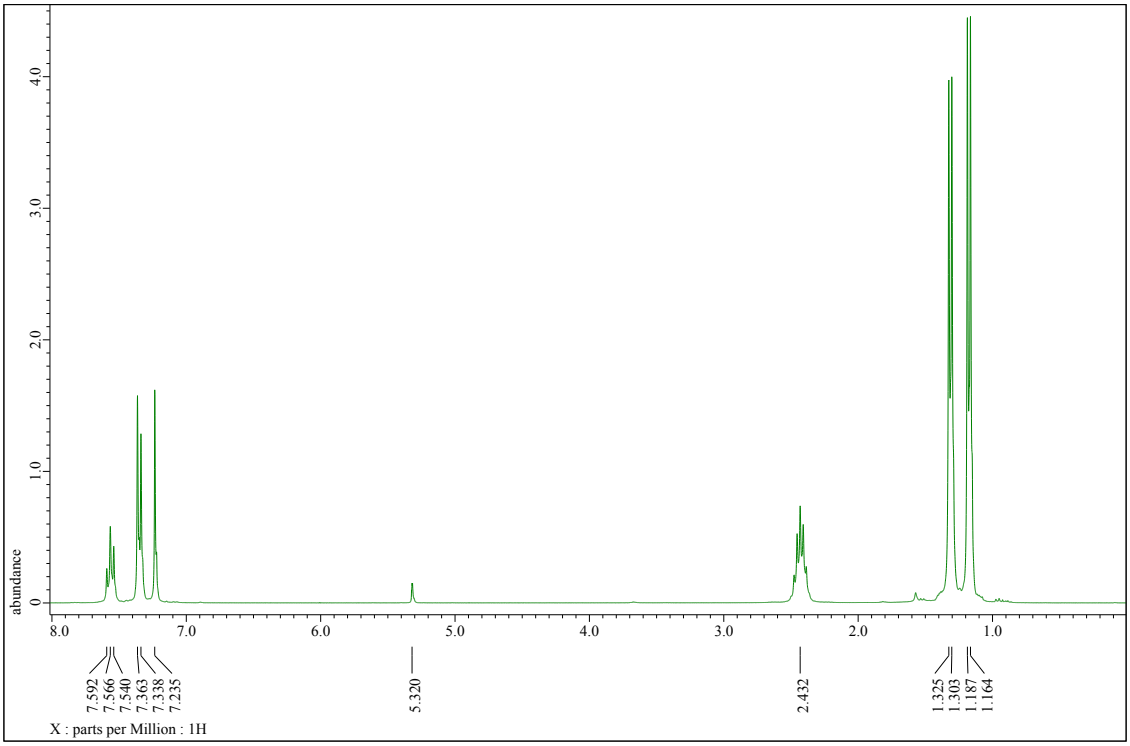

Figure 2.1. ^{1}H NMR spectrum of (IDippSe)CuBr in CD_2Cl_2.

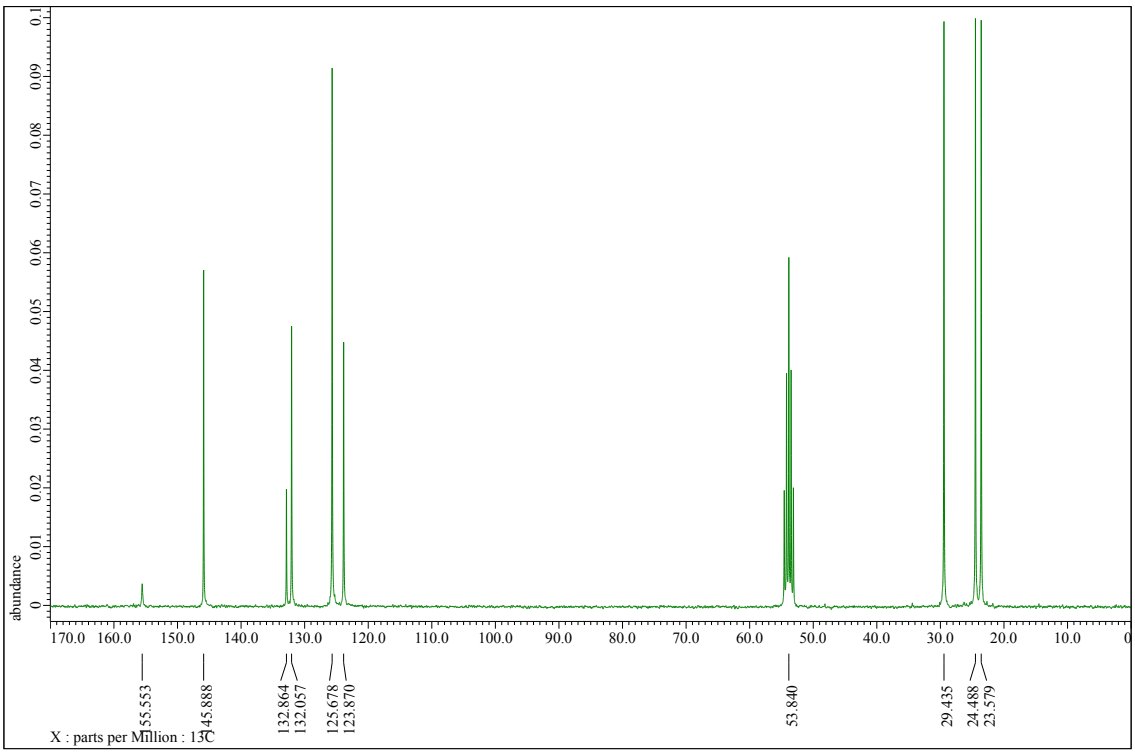

Figure 2.2. $^{13}C\{^{1}H\}$ NMR spectrum of (IDippSe)CuBr in CD_2Cl_2.

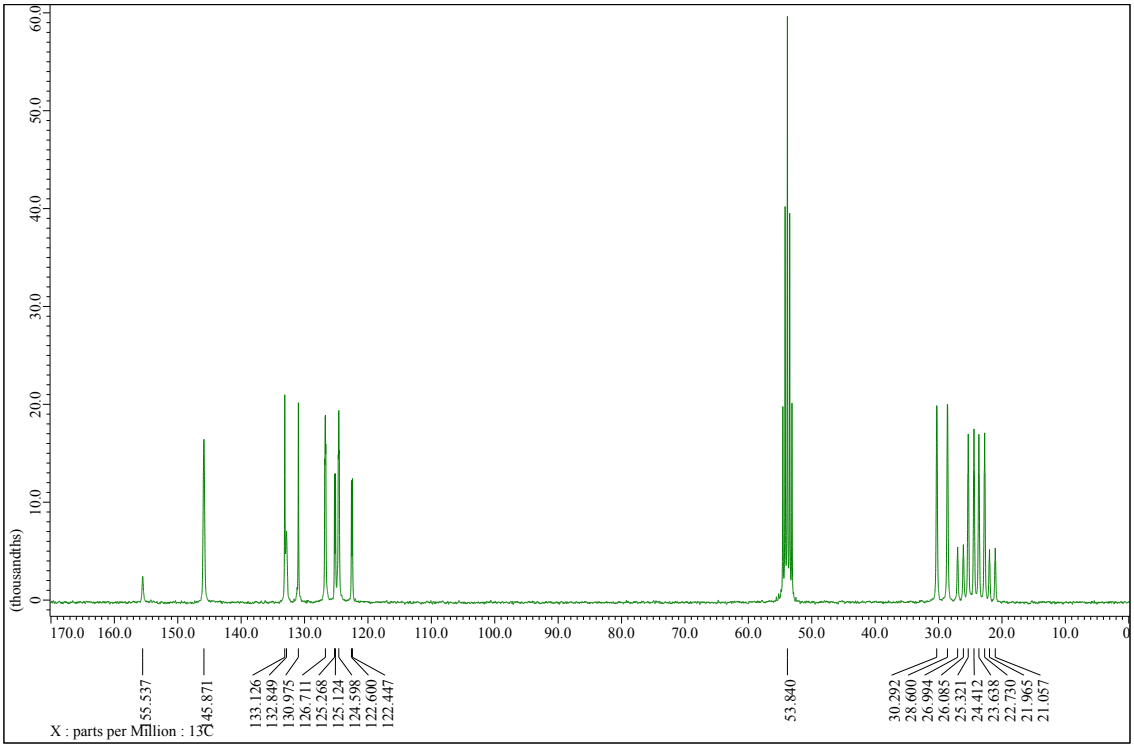

Figure 2.3. ^{13}C NMR spectrum of (IDippSe)CuBr in CD_2Cl_2.

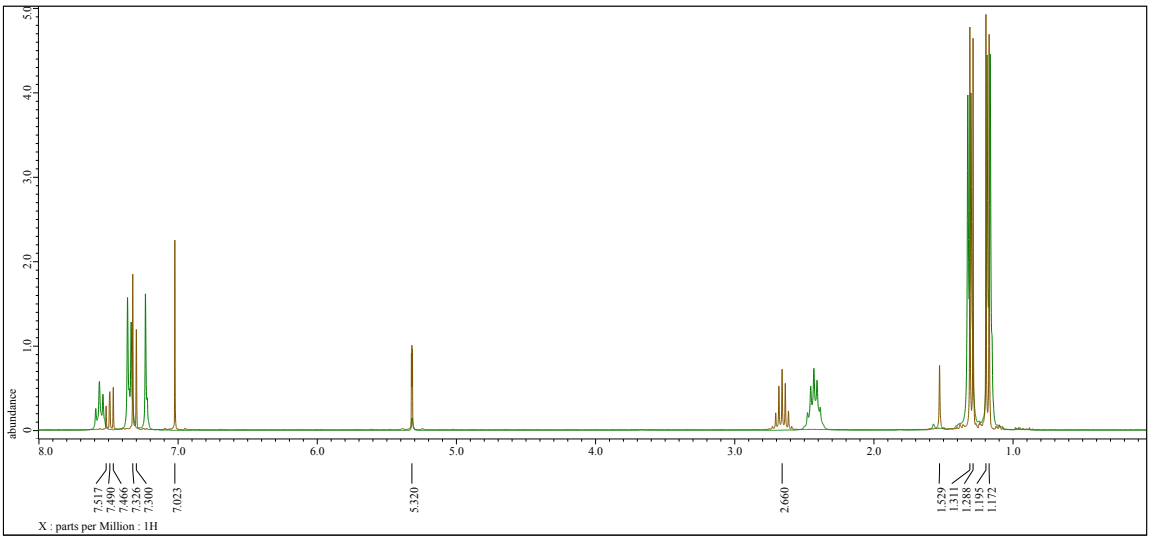

Figure 2.4. Overlaid ^{1}H NMR spectra of free IDippSe (brown) and (IDippSe)CuBr (green) in CD_2Cl_2.

There is a complex splitting pattern in the aromatic region of the ^{1}H NMR spectrum corresponding to the protons on the Xy- and Dipp-substituted aromatic rings. This second order effect is a result of the meta and para protons being in a nearly equivalent chemical environment. Upon coordination, the downfield shift of the singlet from hydrogens in the back of the imidazole ring is the most notable and varies (~0.1-0.2 ppm) (Figure 2.4).

Noticeable trends are also observed in ^{13}C NMR spectra that assist in understanding how the electronic characteristics are altered upon coordination to a copper center. There is an upfield chemical shift of the C=E (E = S, Se) carbon atom (~7-8 ppm) upon coordination. Upon complexation, the electron density around the chalcogen donor atom is shifted to copper. As a consequence, the electron density around the nitrogen atoms of the imidazole ring is also shifted to the carbon atom. When comparing the effect of the donor atom on the chemical shift of the C=E carbon atom, there is a moderate difference between the thiones and selones. Specifically, the complexes with NHSe ligands are observed to have a chemical shift of 5-7 ppm upfield when compared to those with NHT ligands. This can be explained by the differing electron donation properties of the chalcogen atoms, as selenium is a slightly better σ-donor than sulfur which will again result in increased electron density around the carbon atom.

2.3. Molecular Structures of Copper(I) Complexes

Several crystals that were suitable for XRD were obtained in various organic solvents such as Et_2O, CH_3CN, THF, acetone-d_6, pentane, and chloroform. Crystal structures of a few (IArSe)CuX complexes have been reported previously.[58] Molecular structures are shown in Figures 2.5-2.9, with selected bond lengths and angles included in Table 2.1.

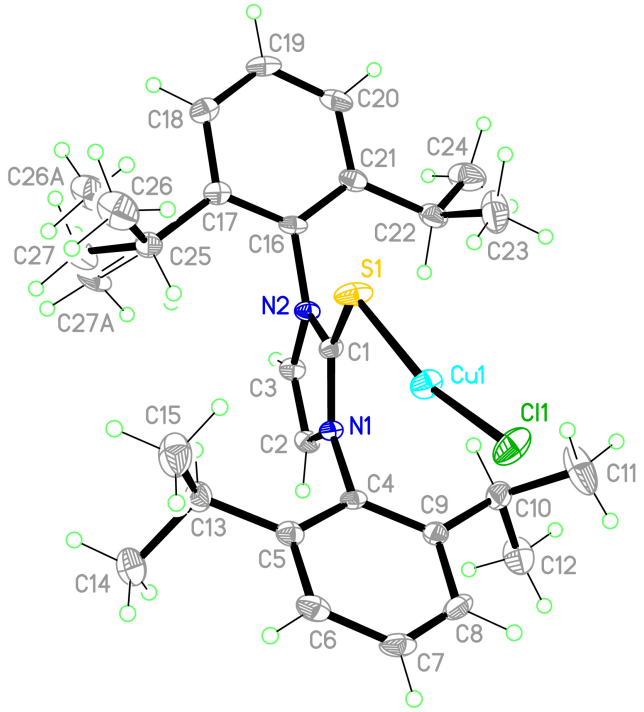

Figure 2.5. Molecular structure of (IDippS)CuCl.

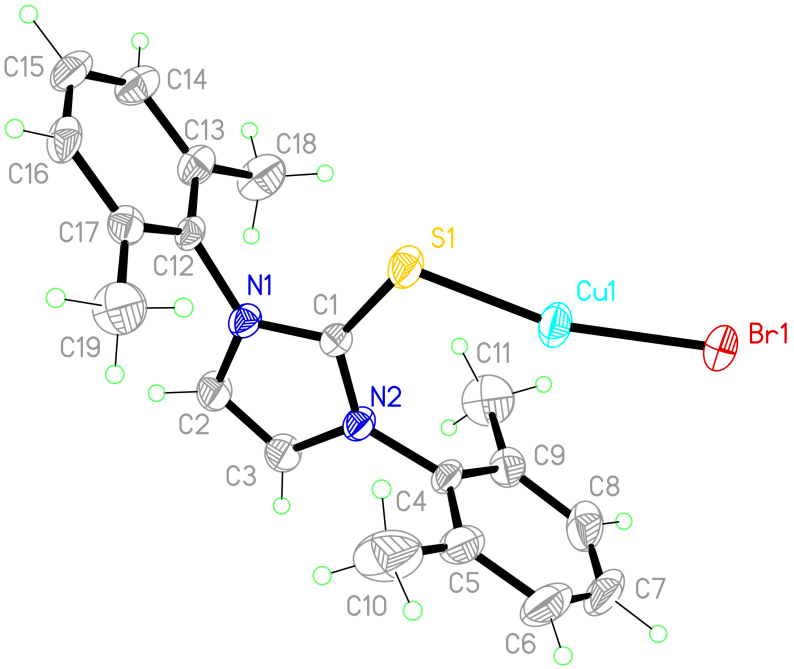

Figure 2.6. Molecular structure of (IXyS)CuBr.

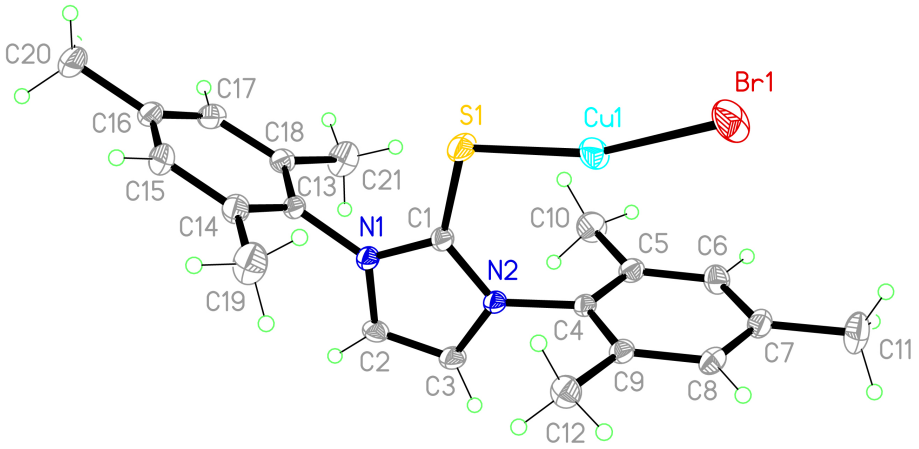

Figure 2.7. Molecular structure of (IMesS)CuBr.

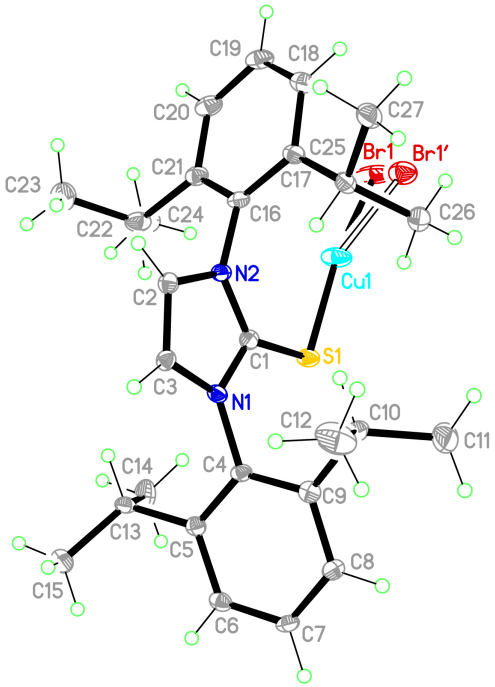

Figure 2.8. Molecular structure of (IDippS)CuBr.

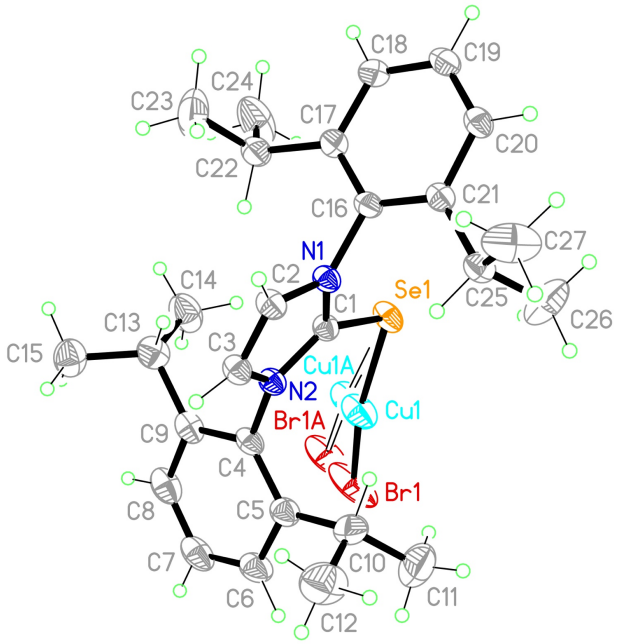

Figure 2.9. Molecular structure of (IDippSe)CuBr.

Table 2.1. Selected bond lengths (Å) and bond angles (°) for (IArE)CuX.

	C=E (Å)	Cu–E (Å)	Cu···Cent.‡ (Å)	C=E-Cu (°)	E=Cu–X (°)
(IMesSe)CuCl†	1.87	2.26	-	104.5	-
(IDippS)CuCl	1.71	2.15	-	107.4	164.3
(IDippSe)CuCl†	1.87	2.26	3.40	103.9	168.0
(IXyS)CuBr	1.71	2.15	3.24	106.2	166.7
(IXySe)CuBr†	1.85	2.25	3.24	102.9	164.9
(IMesS)CuBr	1.70	2.14	3.27	108.4	164.1
(IMesSe)CuBr†	1.86	2.26	-	105.1	163.5
(IDippS)CuBr	1.70	2.15	-	107.5	163.2*
(IDippSe)CuBr	1.86	2.26*	3.26	104.9	165.4*
(IMesSe)CuI†	1.85	2.26	-	104.5	159.9

* Average of two values
‡ Distance between copper atom and the centroid of the nearest aromatic ring
† Values from reference 58.

As previously discussed, with selenium having the larger atomic size, it was not surprising that the magnitude of the C=E bond length remained longer for the selones, regardless of coordination to a metal center. The length of the carbon-chalcogen bond is observed to decrease slightly (~0.01 Å) as the size of the halide increases down the group from chloride to iodide. This cannot be simply described by the size of the halide, but instead is a product of the trans influence of the opposing halide ligands. Chloride is the weaker σ-donor and π-acceptor due to its higher electronegativity, leading to an increased σ-donation from chalcogen donor atom of the IArE ligand, ultimately reducing the back bonding from the chalcogen to the carbon atom. This can also assist in explaining why the two-coordinate linear homoleptic cationic complex $[Cu(IMesSe)_2][CuCl_2]$ was observed as this isomer was also a kinetically favored product.[58] Interestingly, there was no notable deviation in the length of the Cu-E bond when keeping the ligand constant and substituting the halide ligand.

Due to the unshared pair of electrons on the chalcogen atom, these complexes form a bent molecular geometry across the C=E-Cu bonds. Basic atomic trends can assist in explaining the magnitude of this angle with selenium of course having the larger atomic size and thus a smaller angle. As a result, this places the copper atom at a close enough proximity to the π-electron-rich aromatic rings of the ligand. Transition metals have the ability to share some of their electron density with these π systems and is often viewed as a covalent-like interaction between the d orbitals of the metal and the p orbitals of the conjugated π system of the aromatic rings. The sterics of the aromatic groups (e.g. Dipp vs. Xy) are seen to have little influence of this interaction. Most importantly, this

interaction explains why there is a deviation from 180° in the E=Cu–X bond angle. The interaction between the neutral Cu(I) center and the center of the aromatic rings repels the halide atom, with the larger halide being repelled more intensely.

2.4. Synthesis and Characterization of Silver(I) Complexes

Literature suggested that Ag(I) prefers a linear homoleptic two-coordinate geometry when working with NHC ligands. Assuming similar reactivity, one equivalent of AgX (X = NO_3, BF_4, ClO_4, PF_6, or SbF_6) is dissolved in a few drops (<0.5 mL) of H_2O to allow for the complete dissolution of the silver salts before adding two equivalents of ligand in acetonitrile (Scheme 2.3). These reactions are performed in the absence of light to prevent the reduction of silver(I) to silver metal, as was noted in earlier attempts. To accomplish this, these reactions were allowed to stir in a reaction vessel wrapped in aluminum foil overnight, but minimal shielding from the light is used in the workup of these products, indicating their stability in the solution phase.

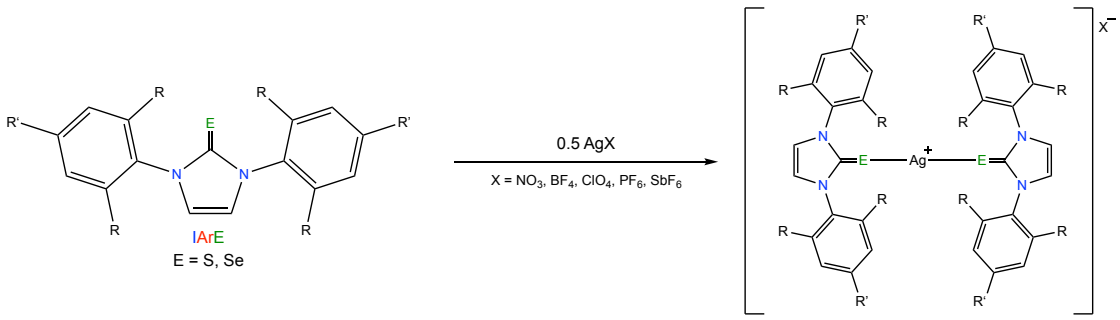

Scheme 2.3. Synthesis of silver(I) complexes supported by NHT or NHSe ligands.

Upon being dried, minimal decomposition is observed when storing these complexes in ambient conditions, although they continue to be kept in a vile free of light. These complexes also show high thermal stability and partial solubility in DMSO and high

solubility in acetone and chlorinated organic solvents such as chloroform and dichloromethane.

With the cations being symmetrical complexes, NMR spectroscopy was useful for determining the successful coordination to the silver center (Figures 2.10-2.12). The most notable chemical shift is observed for the hydrogen atoms on the imidazole rings in a ^{1}H NMR spectrum. Since the complexes are centrosymmetric, only one singlet arises from the backbone of the ring around 7 ppm which can be quantitatively compared to the chemical shift of the corresponding ligand in the same solvent (Figure 2.13). The downfield shift of the signal in the ^{1}H NMR spectrum by 0.1-0.3 ppm in CD_2Cl_2 was typical. Upon coordination, the electron density in the π system of the imidazole ring is shifted in the direction of the silver atom.

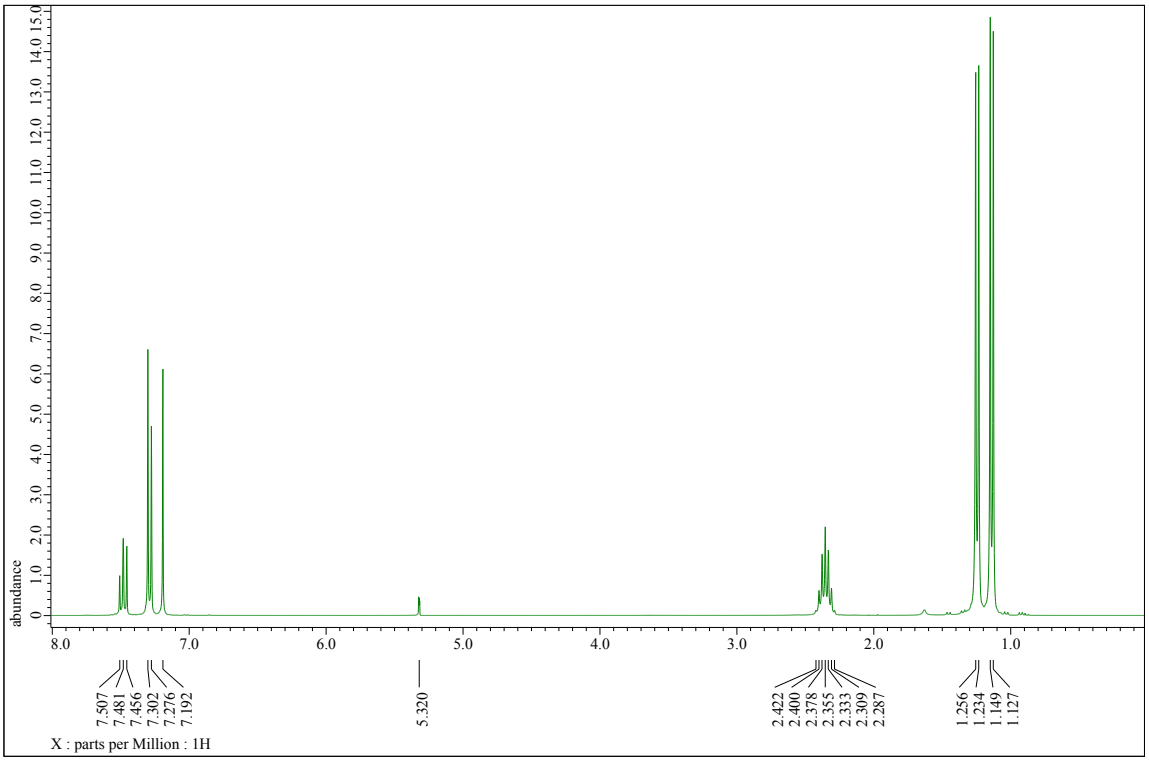

Figure 2.10. ^{1}H NMR spectrum of $[Ag(IDippSe)_2]BF_4$ in CD_2Cl_2.

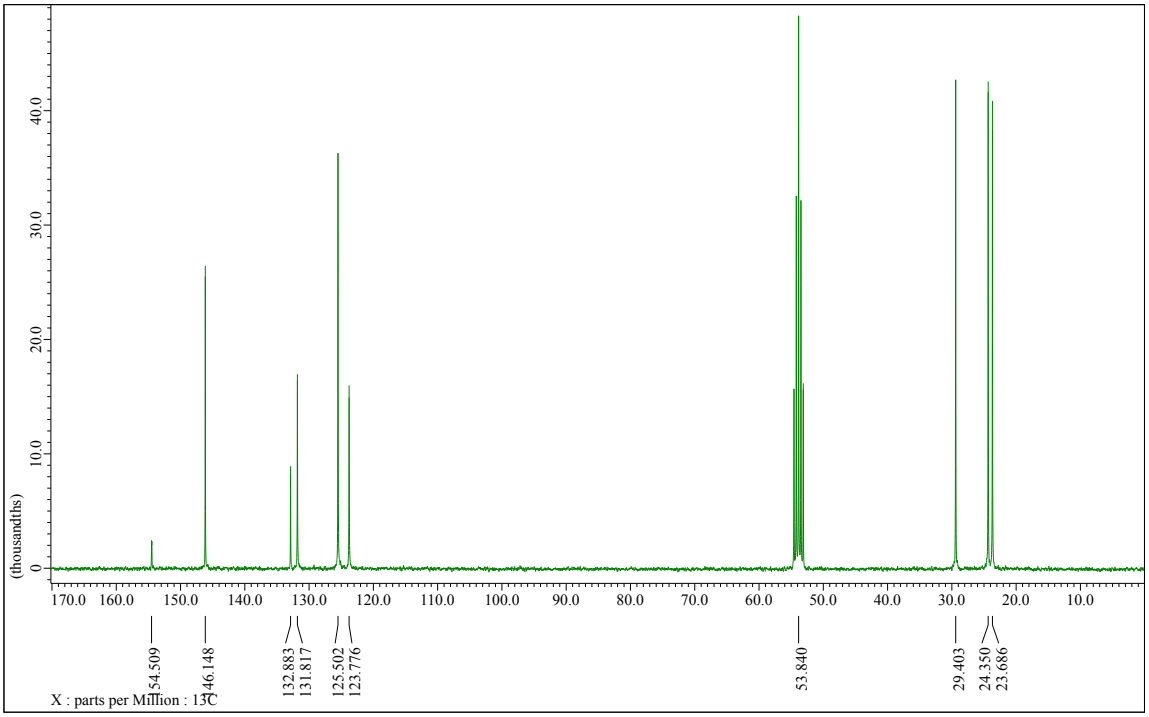

Figure 2.11. $^{13}C\{^{1}H\}$ NMR spectrum of $[Ag(IDippSe)_2]BF_4$ in CD_2Cl_2.

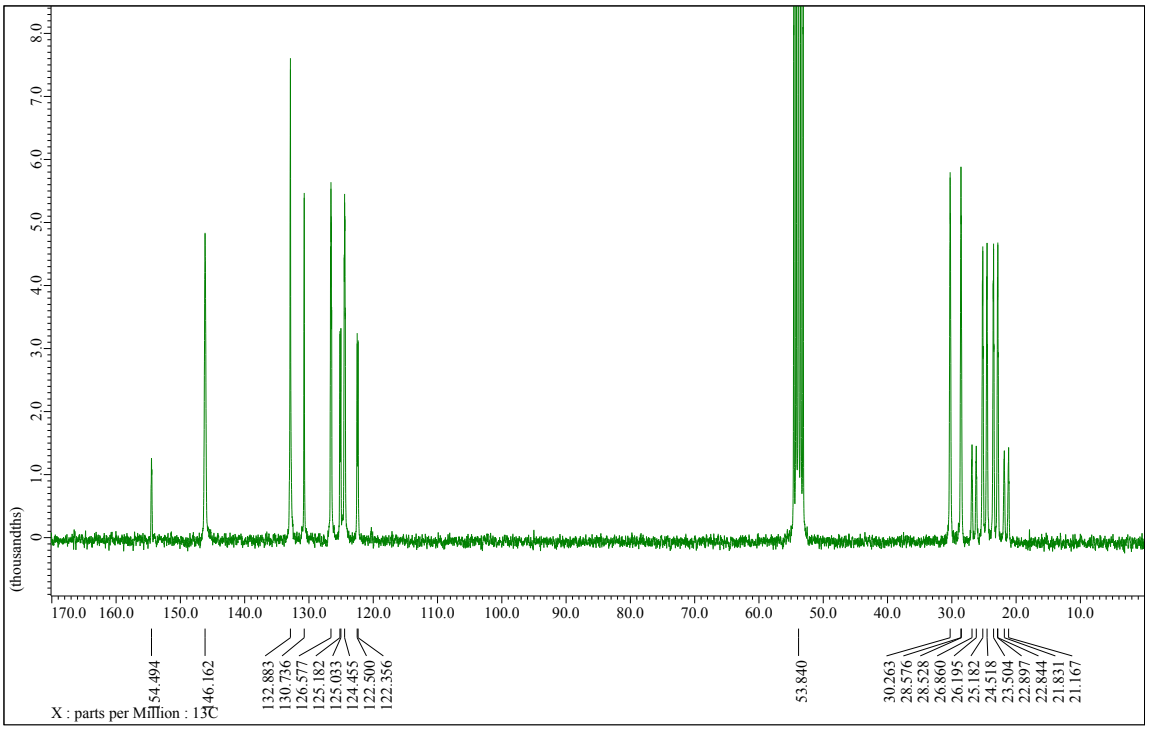

Figure 2.12. ^{13}C NMR spectrum of $[Ag(IDippSe)_2]BF_4$ in CD_2Cl_2.

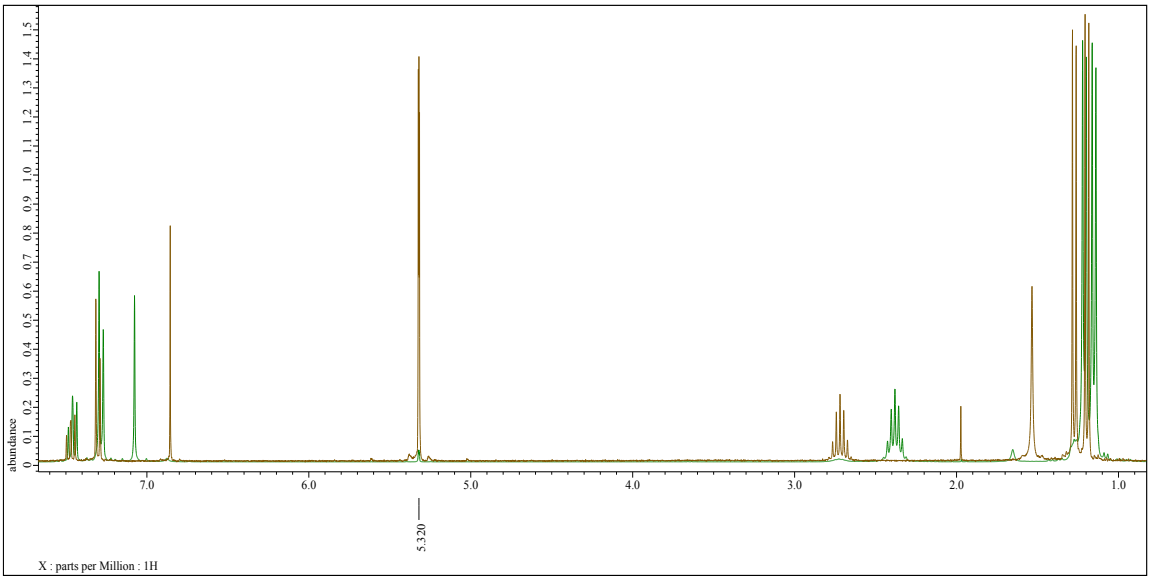

Figure 2.13. ^{1}H NMR spectra of free IDippS (brown) and $[Ag(IDippS)_2]ClO_4$ (green) in CD_2Cl_2.

The deshielding effect observed for imidazole hydrogen atoms can also be influenced by the anion. In the solution phase, it is possible for the counterion to have a significant effect on the electronic environment encountered by the ligands. This effect if most easily observed for $[Ag(IMesE)_2]X$ complexes due to the presence of only singlets in the aromatic region of the ^{1}H NMR spectrum (Figure 2.14). As the size of the anion increases, an increased shielding effect is observed for the imidazole hydrogen atoms. Most of these anions are weakly coordinating counterions that are inert with the only exception being NO_3^- that can act as a mono- or bidentate ligand. The others, BF_4^-, ClO_4^-, PF_6^-, and SbF_6^-, have their electron density distributed evenly across the bonded atoms rendering them unreactive. With the two tetrahedral and octahedral anions being similar electronically, a minimal difference in shielding effect is observed. The effects are the most notable in the thione complexes potentially due to decreased polarizability of the sulfur atom resulting in less σ donation to the silver center and reduced orbital overlap.

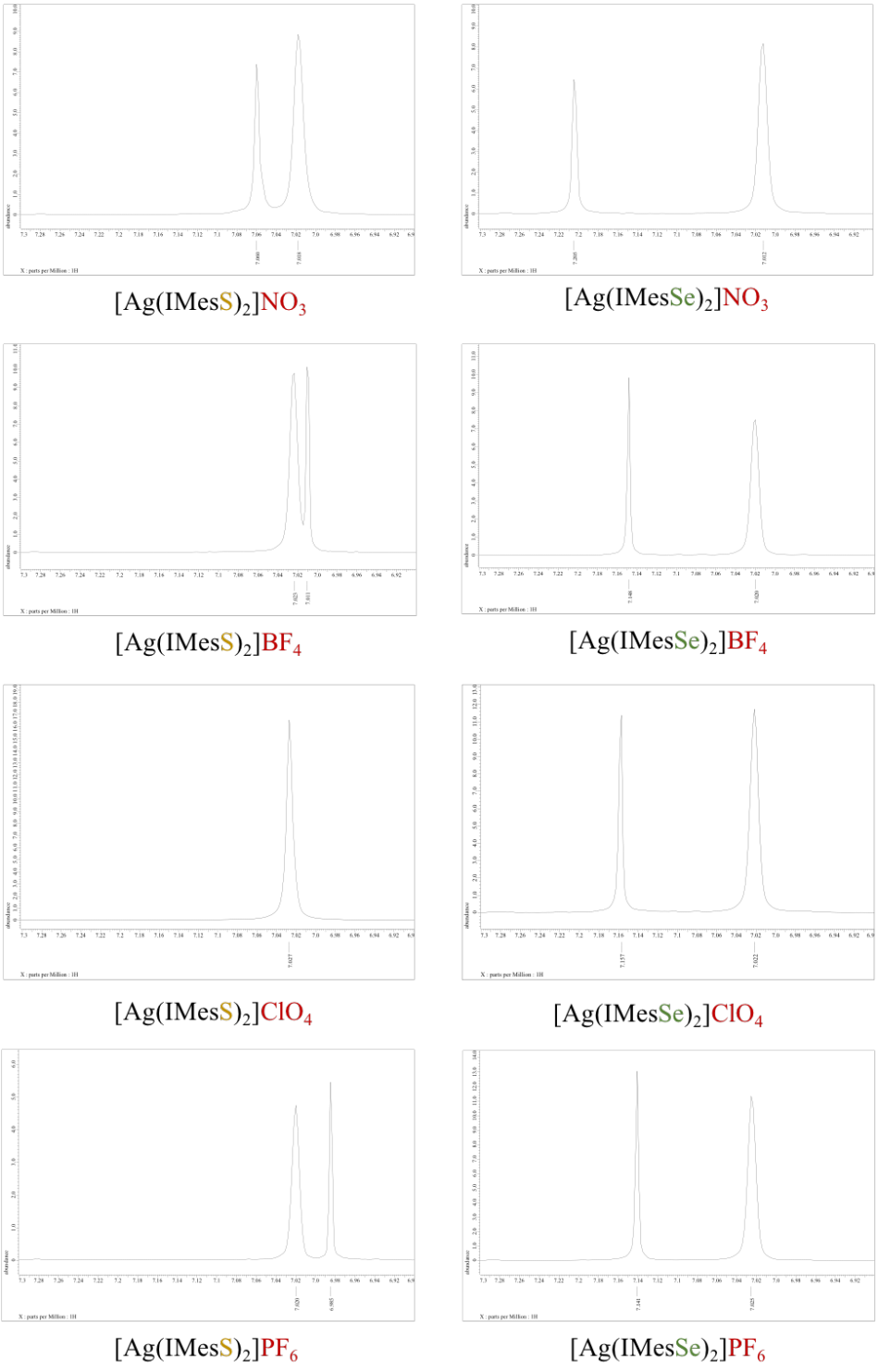

Figure 2.14. ^{1}H NMR shielding effect of the counterion in [Ag(IMesE)$_2$]X in CD_2Cl_2.

When viewing ^{13}C NMR spectra, similar observations are seen for the C=E chemical shift that occurs during complexation. When comparing the complexes bearing NHT or NHSe ligands, there is around a 6-7 ppm upfield shift for complexes with NHSe ligands. Being a d^{10} metal like copper(I), the same general effects can be rationalized similarly. Coordination to a Ag(I) center ultimately results in an overall shift in electron density from the nitrogen atoms of the imidazole ring towards the direction of the chalcogen, resulting in a localized increase in electron density around the carbon atom. Interestingly, there is also a trend observed for the aromatic substituents on the chemical shift of the C=E signal. Complexes with IDippE ligands tend to display a 3-4 ppm shift downfield relative to the IXyE and IMesE ligands.

Additionally, ESI-MS was useful for determining that these complexes maintained their linear homoleptic geometry in solution as was observed in the solid state from the structures below. Dilute acetonitrile solutions of the cationic complexes show strong peaks that correspond to the $[Ag(IArE)_2]^+$ fragments in each case, matching the theoretical isotopic distriubutions (Figure 2.15). This is evidence that the loss of the anion is the most common ionization pathway for these metal complexes.

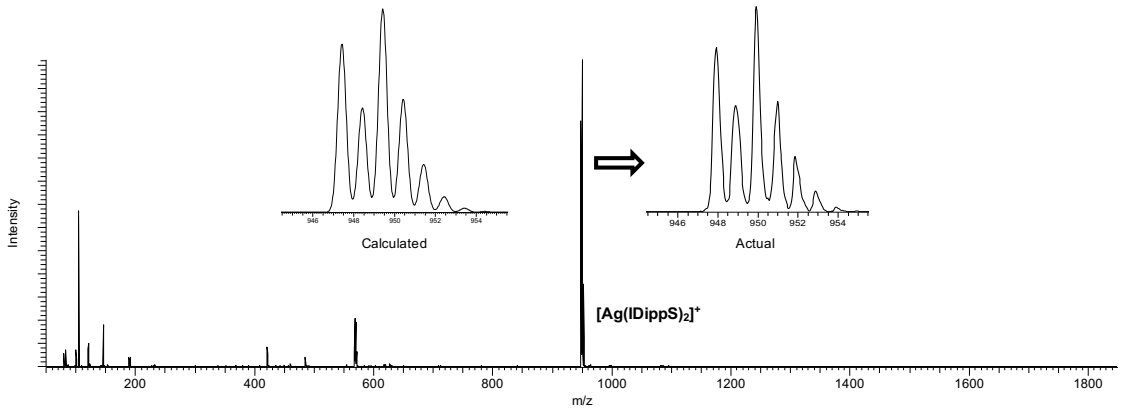

Figure 2.15. ESI-MS of $[Ag(DippS)_2]^+$ with calculated and observed isotopic distributions.

2.5. Molecular Structures of Silver(I) Complexes

Crystals suitable for X-ray diffraction studies have been obtained for several $[Ag(IArE)_2]X$ complexes by utilizing a variety of crystallization techniques including solvent evaporation or vapor layer diffusion. It is also worth noting that crystals were obtained in both the absence and presence of light with little influence. Molecular structures are shown in Figures 2.16-2.33, with selected bond lengths and angles included in Table 2.2.

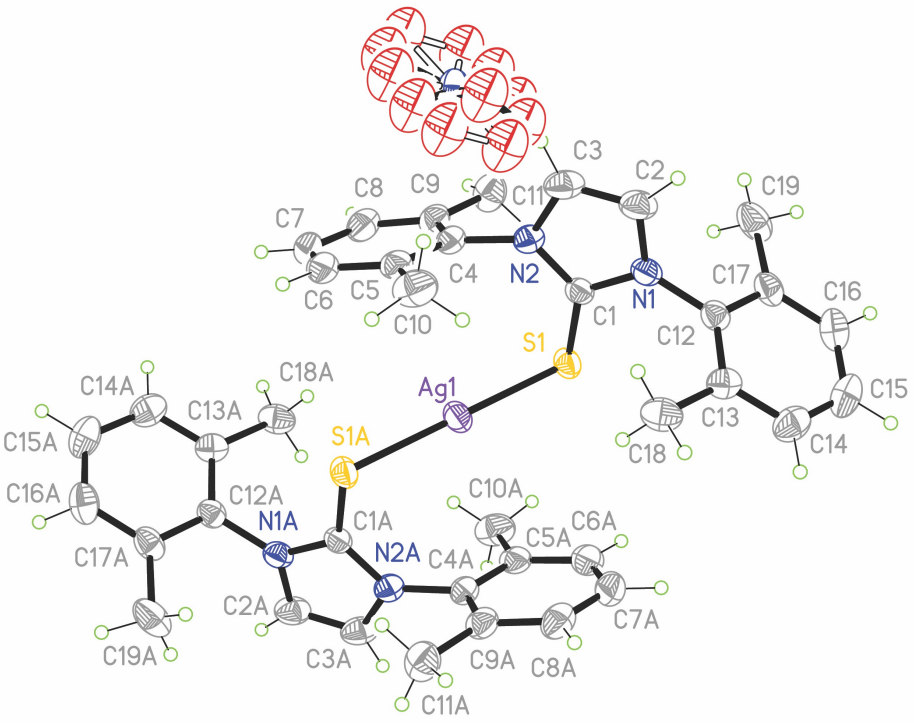

Figure 2.16. Molecular structure of $[Ag(IXyS)_2]NO_3$.

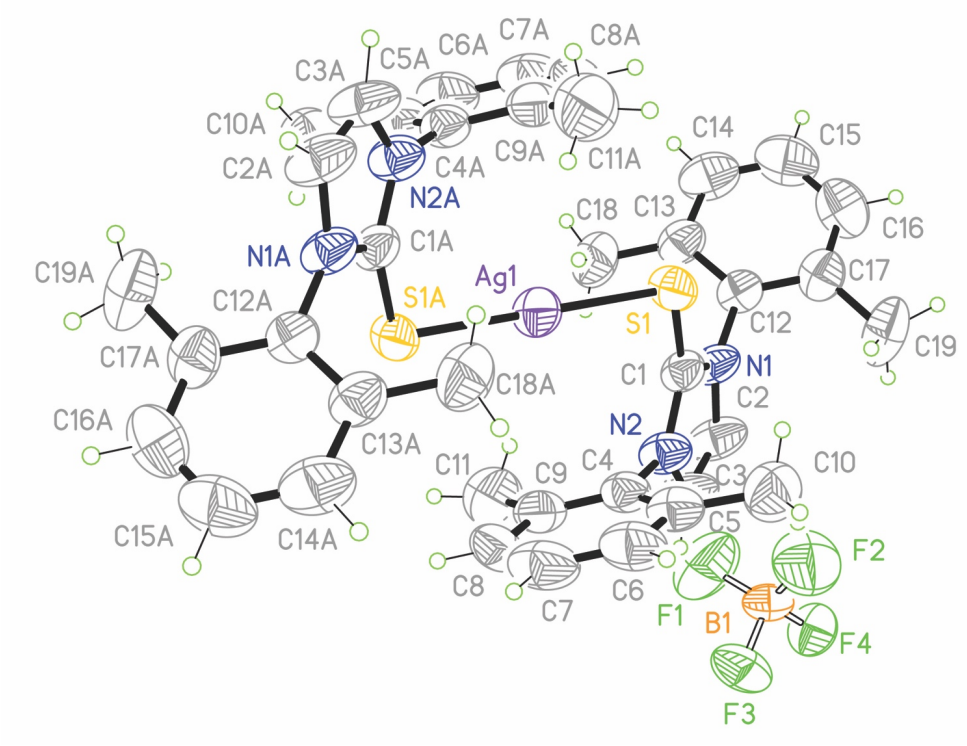

Figure 2.17. Molecular structure of $[Ag(IXyS)_2]BF_4$.

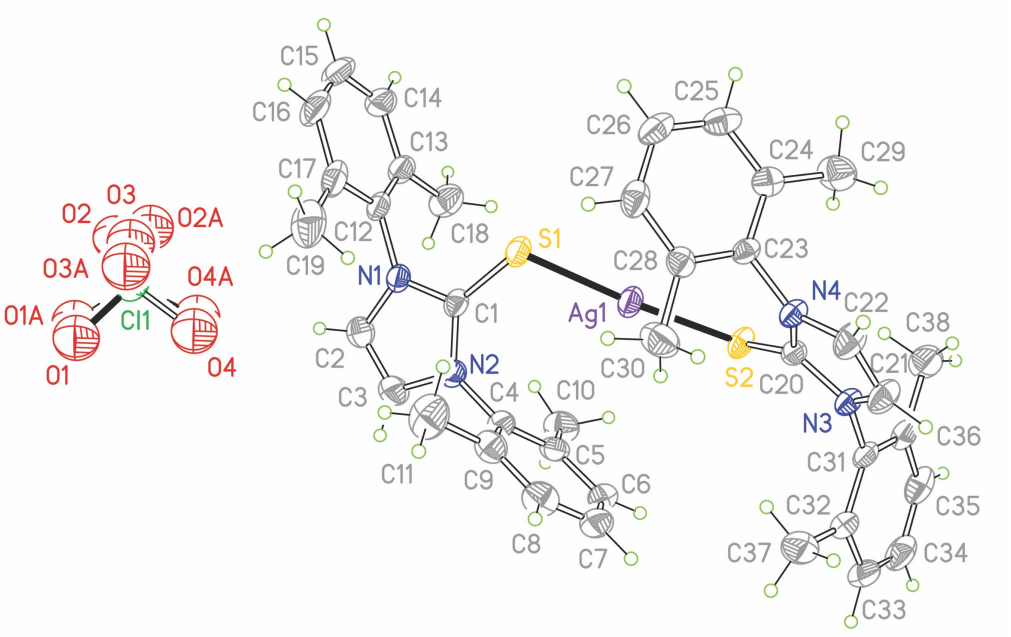

Figure 2.18. Molecular structure of $[Ag(IXyS)_2]ClO_4$.

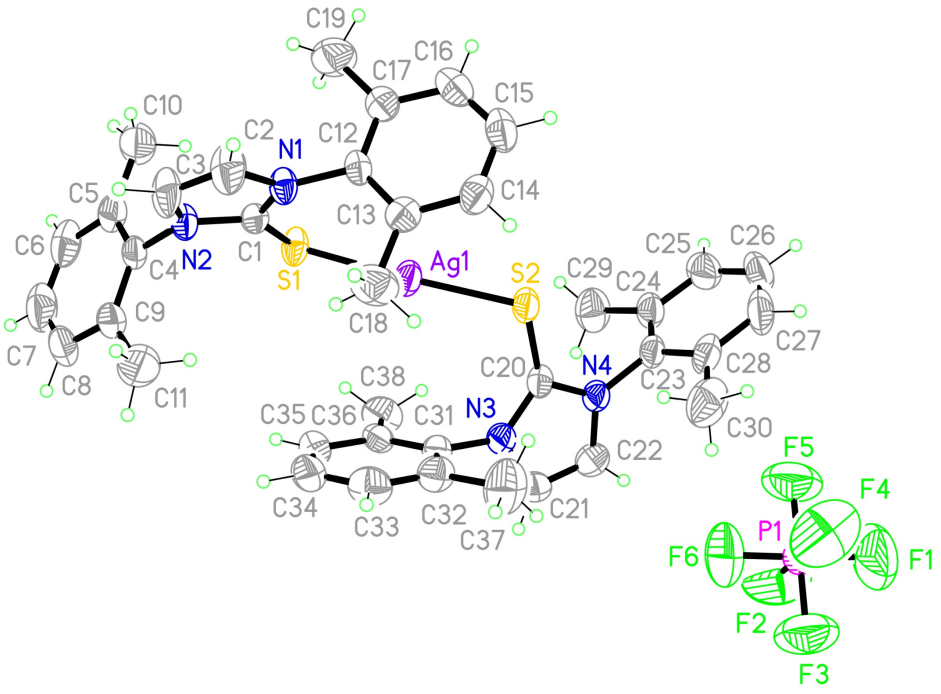

Figure 2.19. Molecular structure of $[Ag(IXyS)_2]PF_6$.

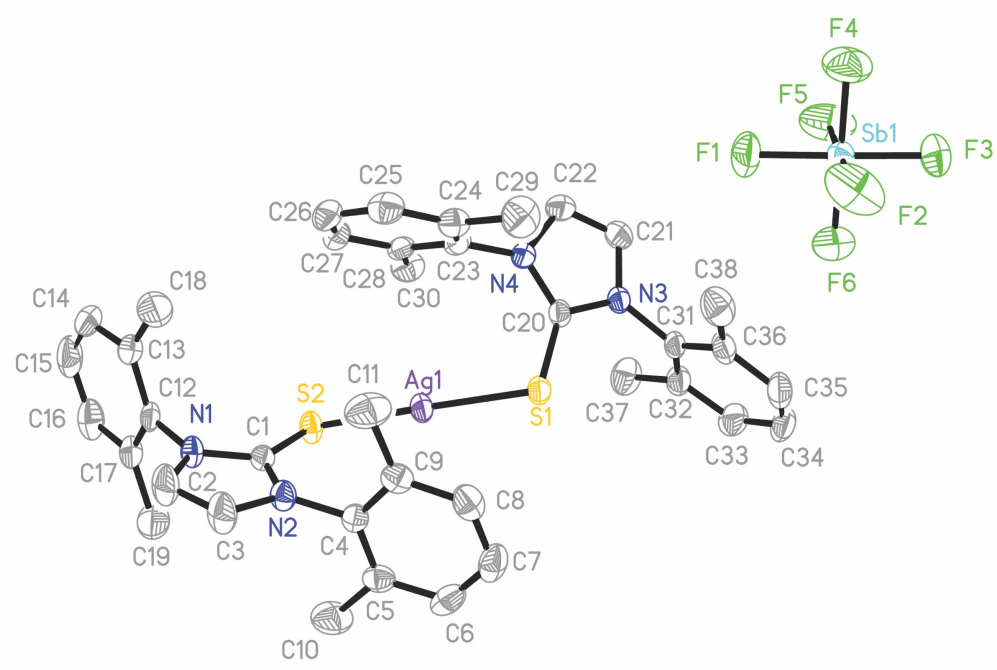

Figure 2.20. Molecular structure of $[Ag(IXyS)_2]SbF_6$

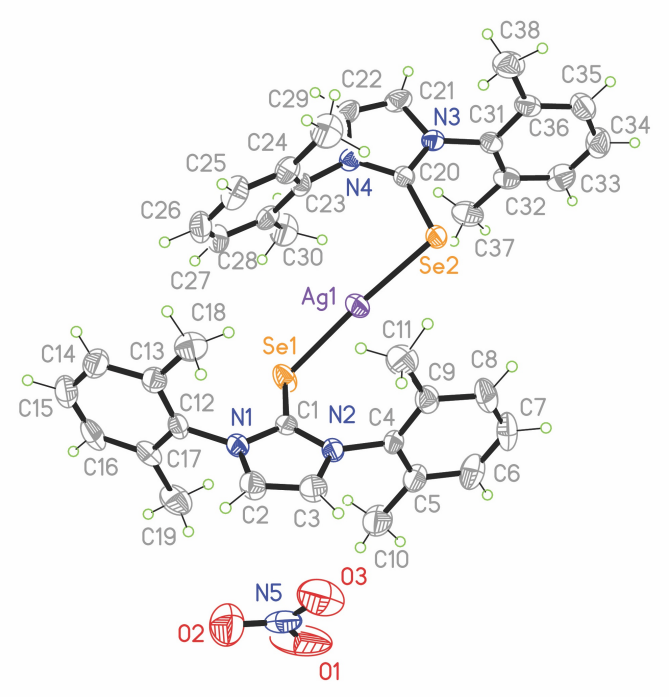

Figure 2.21. Molecular structure of $[Ag(IXySe)_2]NO_3$.

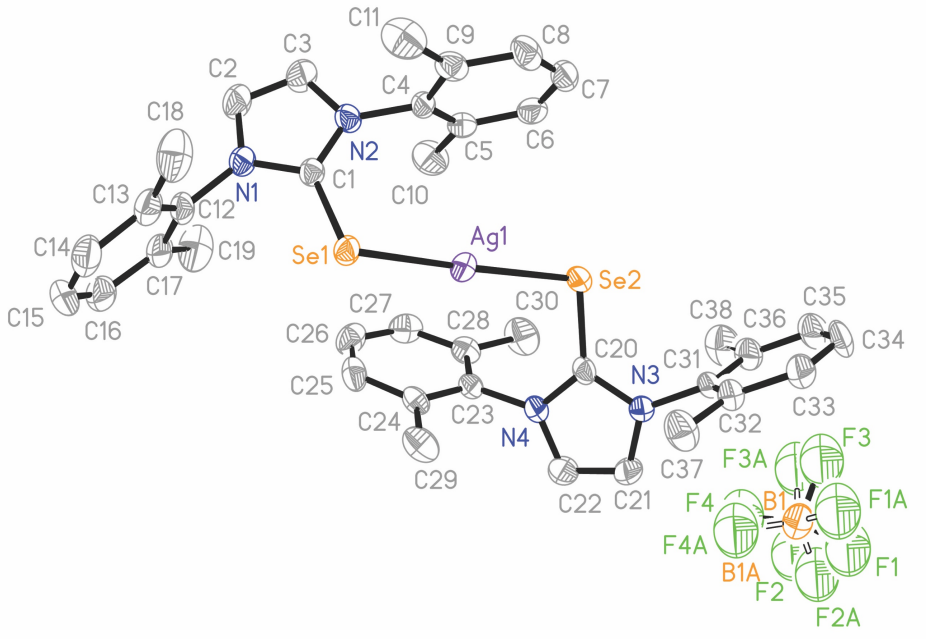

Figure 2.22. Molecular structure of $[Ag(IXySe)_2]BF_4$.

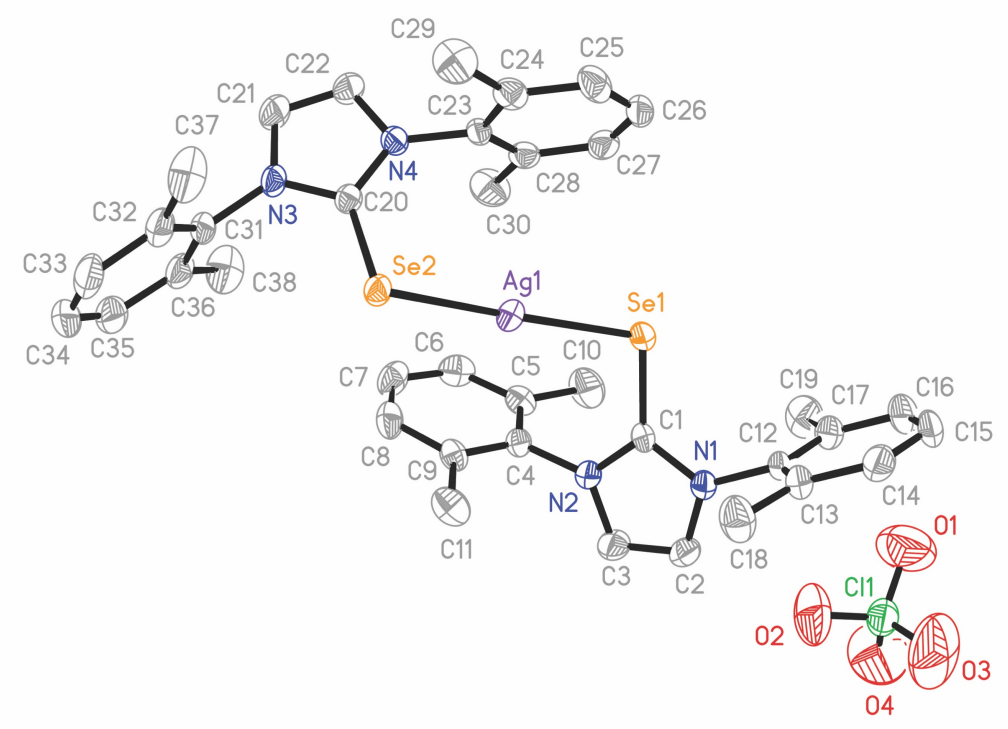

Figure 2.23. Molecular structure of $[Ag(IXySe)_2]ClO_4$.

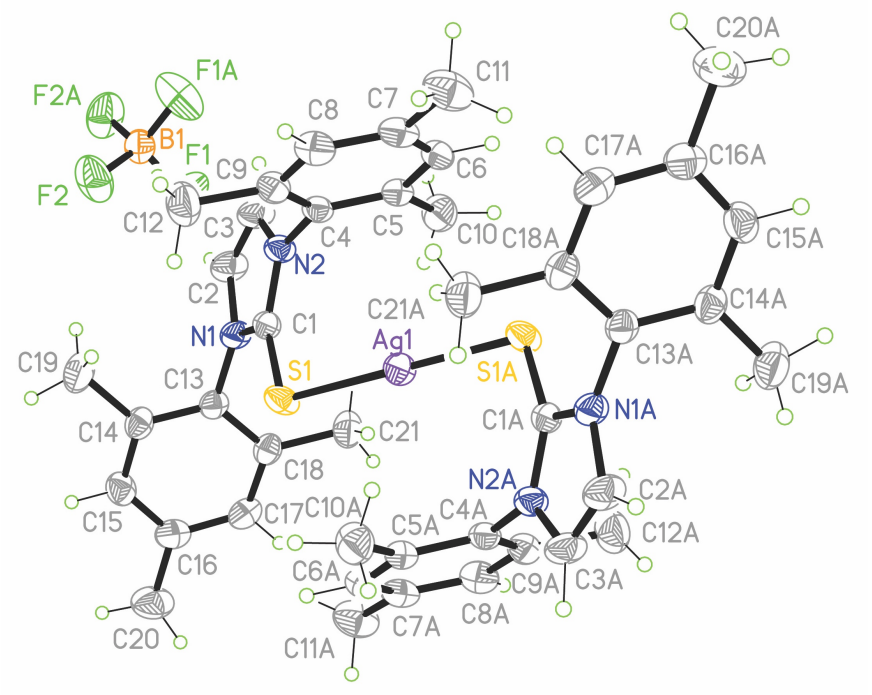

Figure 2.24. Molecular structure of $[Ag(IMesS)_2]BF_4$.

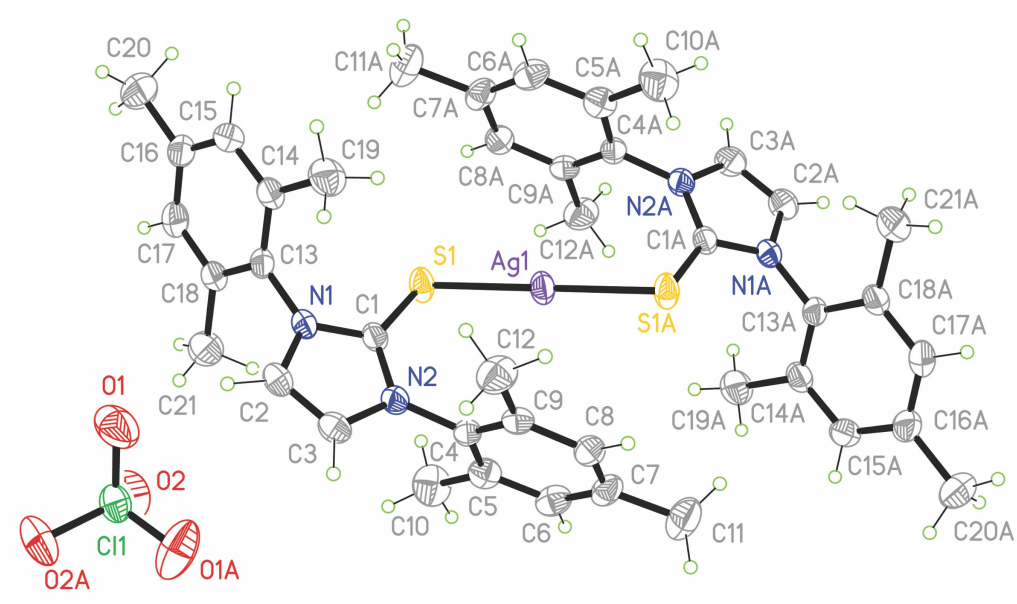

Figure 2.25. Molecular structure of $[Ag(IMesS)_2]ClO_4$.

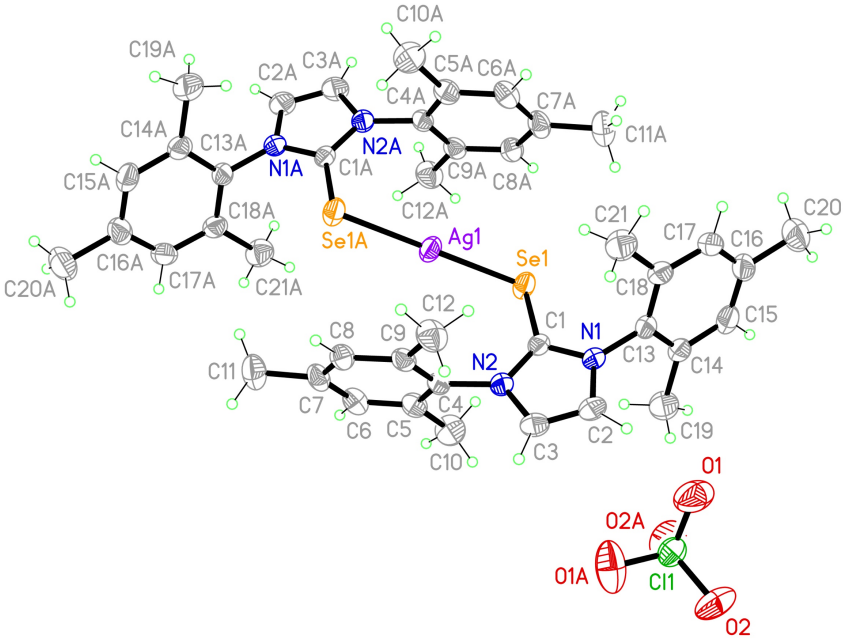

Figure 2.26. Molecular structure of $[Ag(IMesSe)_2]ClO_4$.

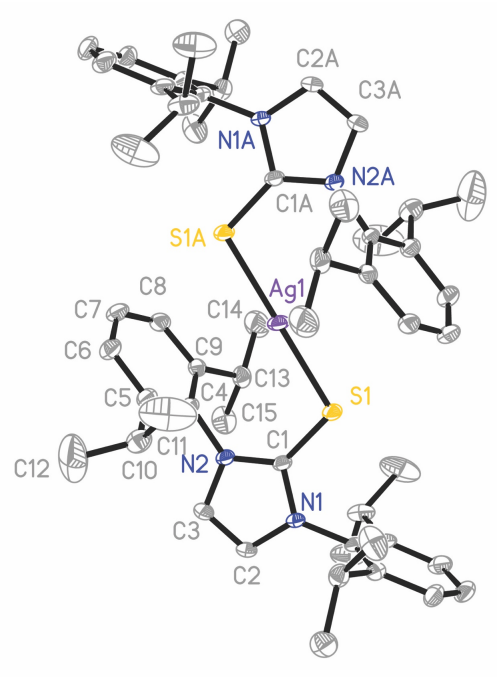

Figure 2.27. Molecular structure of the cation in $[Ag(IDippS)_2]BF_4$.

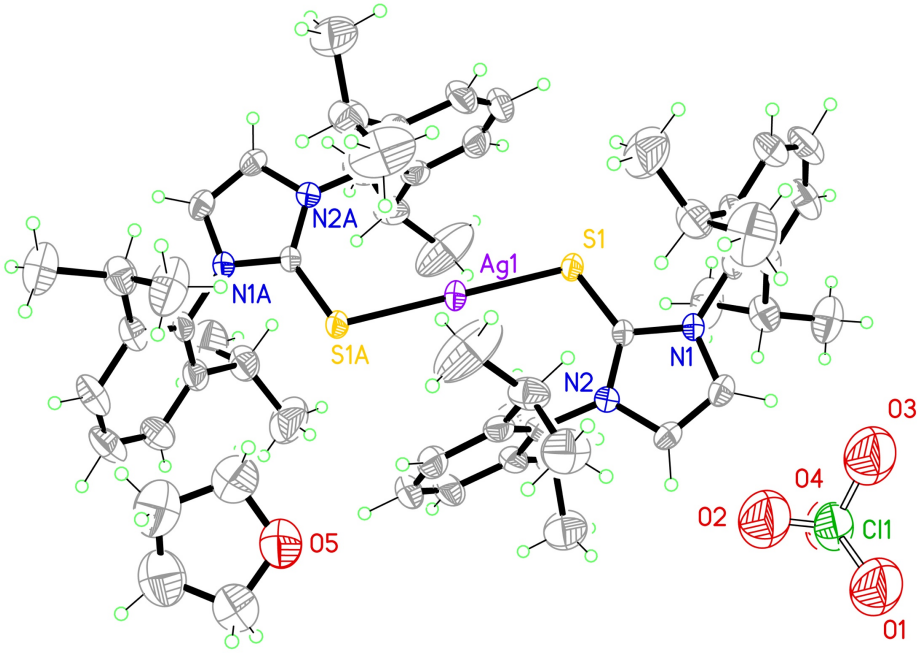

Figure 2.28. Molecular structure of $[Ag(IDippS)_2]ClO_4$.

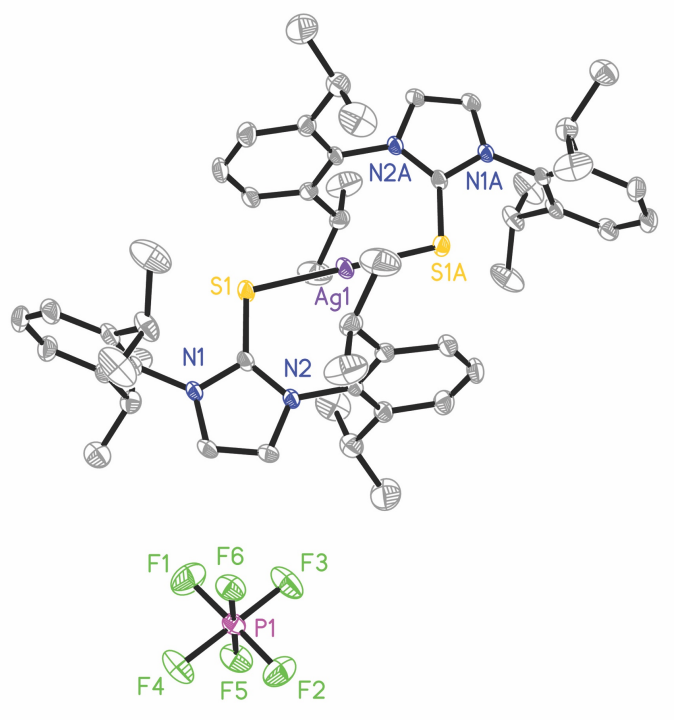

Figure 2.29. Molecular structure of $[Ag(IDippS)_2]PF_6$.

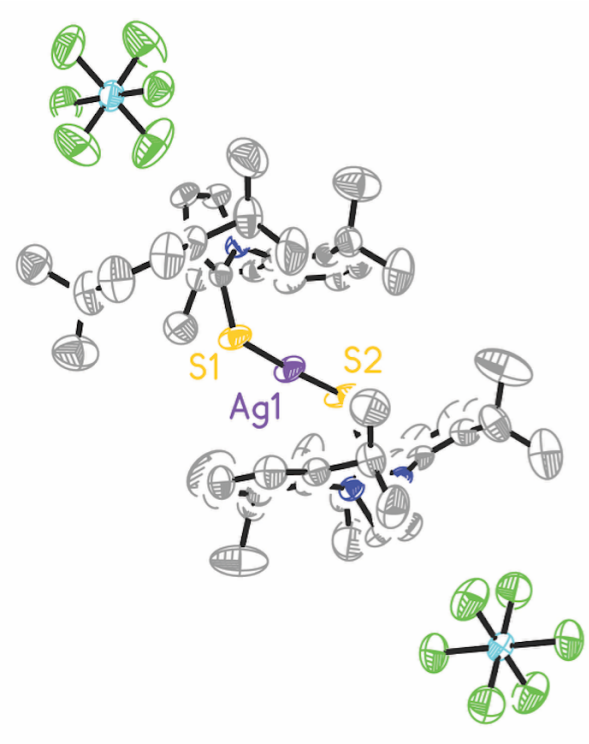

Figure 2.30. Molecular structure of $[Ag(IDippS)_2]SbF_6$.

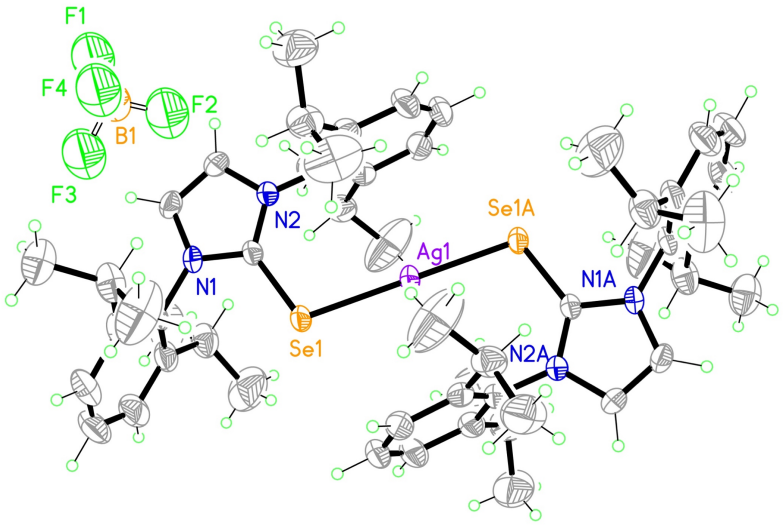

Figure 2.31. Molecular structure of $[Ag(IDippSe)_2]BF_4$.

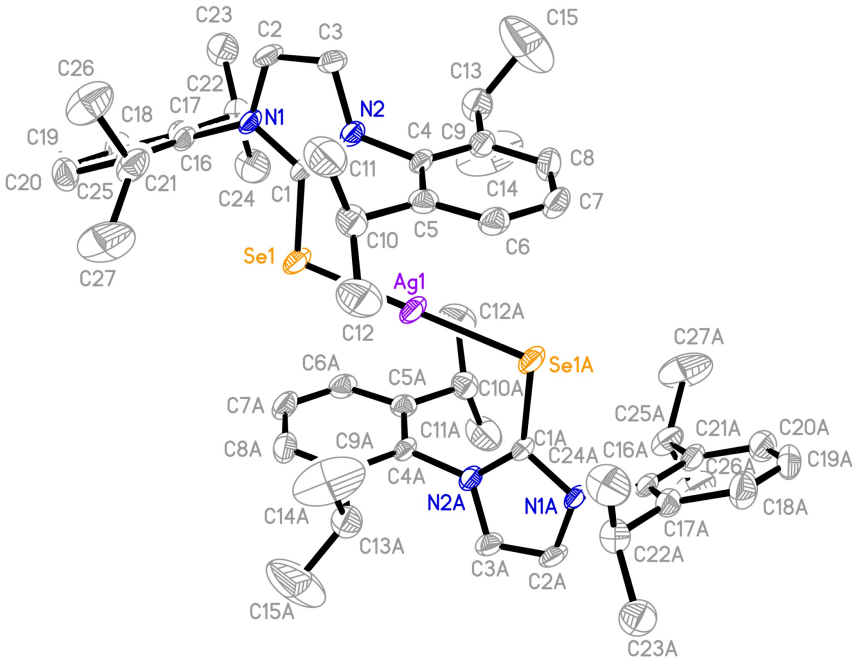

Figure 2.32. Molecular structure of the cation in $[Ag(IDippSe)_2]ClO_4$.

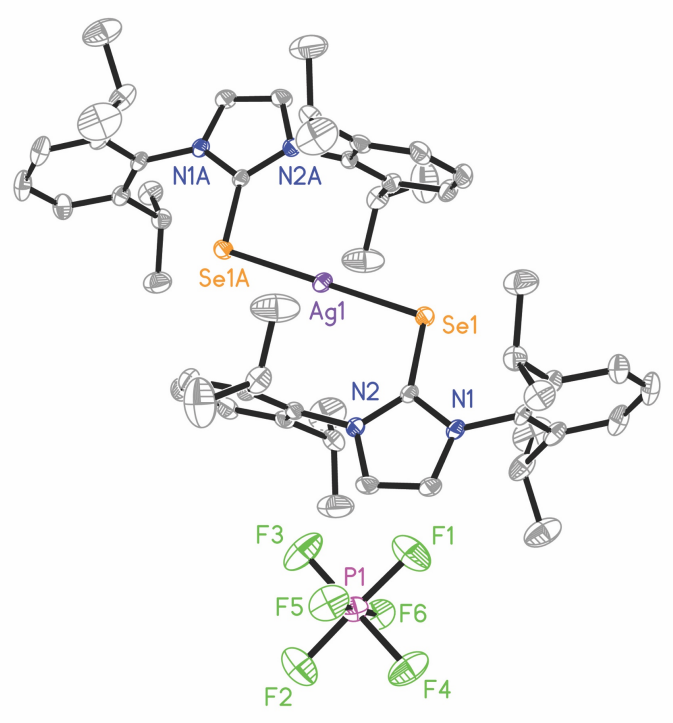

Figure 2.33. Molecular structure of $[Ag(IDippSe)_2]PF_6$.

Of the synthesized complexes, they all exhibit a linear geometry in the solid state. The selection of counterion was to tune the solubility of these cationic complexes in different solvents for subsequent biological studies. Complexes containing a SbF_6^- counterion were deemed less desirable due to similar solubility and nucleophilicity as PF_6^-, in combination with the high cost of $AgSbF_6$. The anion is observed to have little influence on the overall molecular structure of the cation in the solid state and the anion is considered to be chemically inert.

Table 2.2. Selected bond lengths (Å) and bond angles (°) for $[Ag(IArE)_2]X$.

	C=E (Å)	Ag-E (Å)	Ag···Cent.‡ (Å)	Ag-E-C (°)	E-Ag-E (°)
$[Ag(IXyS)_2]NO_3$	1.71	2.36	3.42	100.9	180.0
$[Ag(IXyS)_2]BF_4$	1.70	2.35	3.40	103.4	180.0
$[Ag(IXyS)_2]ClO_4$	1.71*	2.37*	3.35	106.1*	174.6
$[Ag(IXyS)_2]PF_6$	1.71	2.37	3.31	108.1	174.3
$[Ag(IXyS)_2]SbF_6$	1.71*	2.38*	3.22	105.4*	174.0
$[Ag(IXySe)_2]NO_3$	1.86*	2.46*	3.42	102.5*	172.6
$[Ag(IXySe)_2]BF_4$	1.86*	2.47*	3.42	102.7*	174.3
$[Ag(IXySe)_2]ClO_4$	1.87*	2.47*	3.40	102.6*	174.0
$[Ag(IMesS)_2]BF_4$	1.70	2.35	3.35	106.5	180.0
$[Ag(IMesS)_2]ClO_4$	1.71	2.36	3.33	105.9	180.0
$[Ag(IMesSe)_2]ClO_4$	1.86*	2.48*	3.12	100.6*	172.2
$[Ag(IDippS)_2]BF_4$	1.71	2.38	3.18	108.0	180.0
$[Ag(IDippS)_2]ClO_4$	1.71	2.37	3.24	108.3	180.0
$[Ag(IDippS)_2]PF_6$	1.70	2.38	3.19	107.7	180.0
$[Ag(IDippS)_2]SbF_6$	1.70	2.38	3.23	108.1	180.0
$[Ag(IDippSe)_2]BF_4$	1.87	2.48*	3.20	105.6	180.0
$[Ag(IDippSe)_2]ClO_4$	1.86	2.47	3.20	102.9	180.0
$[Ag(IDippSe)_2]PF_6$	1.86	2.48	3.22	104.2	180.0

‡: Distance between silver atom and the centroid of the nearest aromatic ring
*: Average of two values

The length of the C=E and Ag-E bonds is evidently influenced by the size of the chalcogen. Selenium has a larger atomic radius and is a better σ-donor than sulfur. This also has an effect on the Ag-E-C angle for the same reasons noted for the (IArE)CuX complexes as Cu(I) and Ag(I) display similar reactivity. It would be expected that the

steric hindrance from the aromatic substituents (Xy, Mes, Dipp) would result in an increased Ag-E-C angle but this is not the case. With no noticeable trend, it is likely that the deviation in this parameter is most likely due to how these structures pack in the crystal lattice. The counterions do not appear to have a significant influence of the structure of these complexes either. As the molecular weight and size of the counterions increase, the E-Cu-E bond angle fluctuates without explanation. This is also theorized to be a factor of how these complexes pack in the crystal lattice. This claim could be tested by measuring the lattice energy to quantify the attraction between the cationic silver center and counter anion.

Several of the complexes were observed to have metal-arene interactions of varying magnitude (3.12-3.42 Å). When comparing this distance of the Ag(I) atom to the centroid of the nearest aromatic ring, the steric hindrance of the groups on the ring seem to have little significance. Noting that the distance between the Ag(I) atom and the centroid of the nearest ring is often dissimilar, it can be concluded that this is most likely an effect of the steric hindrance encountered by the aromatic groups on the opposing ligand. Due to this, electron density is shared disproportionately with only one of the two close-by electronically-equivalent π-systems. The π-electron donation to the electron deficient Ag(I) atom should provide an additional stabilizing effect for the complex.

When referencing literature, similar bond lengths are observed for two- and three-coordinate Ag(I) complexes bearing other NHT ligands. More specifically, there are only three known two-coordinate complexes bearing at least one NHT ligand in literature to date (Figure 2.34).[59,60,41]

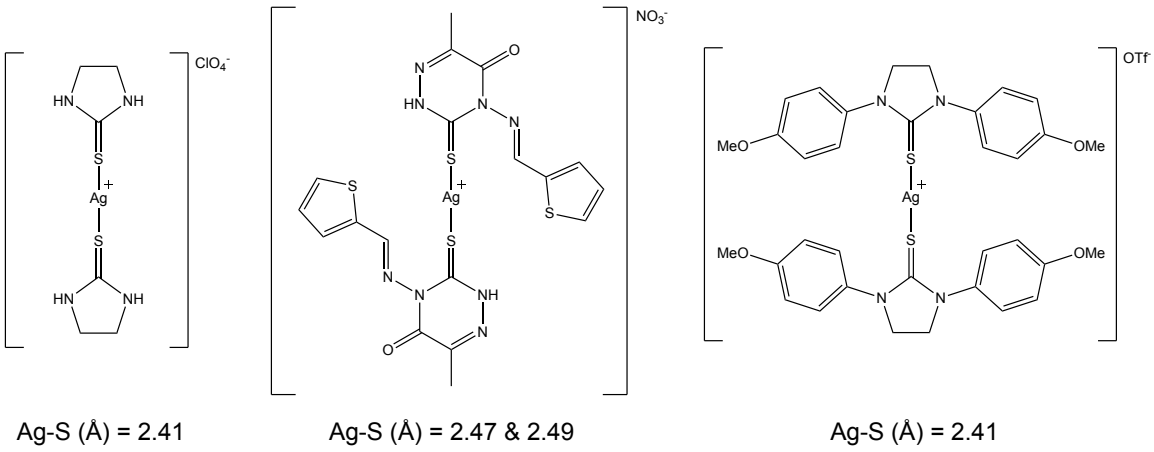

Figure 2.34. Molecular structures of mononuclear two-coordinate Ag(I) complexes with NHT ligands.

There are several known examples of mononuclear three-coordinate silver complexes with monodentate NHTs, which are typically in the range of 2.41-2.57 Å. The increased length of the Ag-S bond is most likely a result of increased steric hindrance around the silver atom for the three-coordinate complexes. When comparing these values with our $[Ag(IArS)_2]X$ complexes, slightly shorter bond lengths are observed (2.35-2.38 Å).[61-72] Significantly, there are currently no two- or three-coordinate Ag(I) complexes supported by monodentate NHSe ligands reported in literature at this time.

CHAPTER 3: BIOLOGICAL ACTIVITY OF SILVER COMPLEXES

3.1. Cytotoxicity Studies

Based on these recent findings, it was of interest to investigate the anticancer potential using our NHT and NHSe ligands. Upon the generation of a series of $[Ag(IArE)_2]X$ (Ar = Xy, Mes, Dipp; E = S, Se; X = NO_3, BF_4, ClO_4, PF_6, or SbF_6) complexes as previously discussed, the cytotoxicity of this set of compounds has been investigated in a study involving HeLa (cervical), MDA-MD-231 (breast), and PC3 (prostate) cancer cell lines. Several compounds have displayed cytotoxic capabilities of varying degree, all discussed herein.

3.2. Experimental Background

The first efficacy of our Ag(I)-IArE compounds against the three cancer cell lines (HeLa, MDA-MD-231, PC3) was assessed via MTT assay. An MTT assay is used for the quantitative determination of cell metabolic activity, used primarily to measure cell viability. MTT (3-(4,5-dimethylthiazol-2-yl)-2,5-diphenyltetrazolium bromide) is converted to a purple formazan dye compound by living cells exhibiting NAD(P)H-dependent cellular oxidoreductase enzymes (Scheme 3.1).

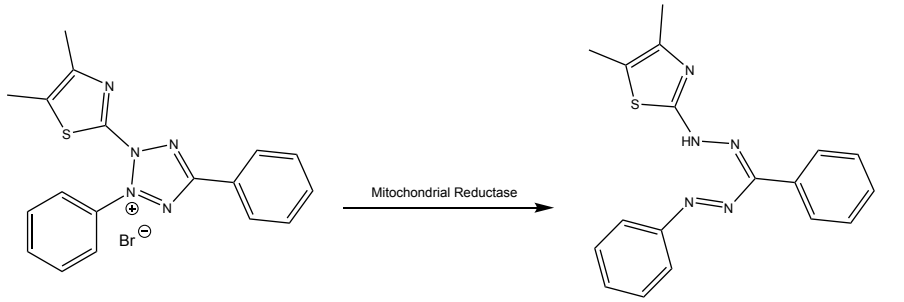

Scheme 3.1. Conversion of MTT to formazan via a mitochondrial reductase route only possible in living cells.

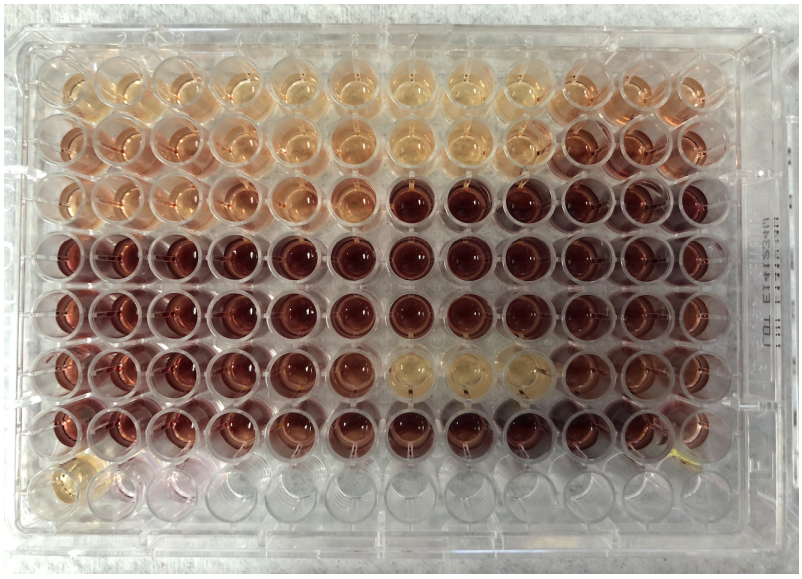

Figure 3.1. 96-Well culture plate containing samples treated with MTT. The wells containing the purple solutions indicate the presence of living cells and the yellow wells indicate the absence of living cells.

3.3. Materials and Methods

A total of ten $[Ag(IArE)_2]X$ complexes were chosen for this study that aimed to observe the effects of varying the chalcogen donor atom, aromatic substituents, and counter ion through a set of *in vitro* cell viability assays: $[Ag(IXyS)_2]BF_4$ (**1**), $[Ag(IXySe)_2]BF_4$ (**2**), $[Ag(IMesS)_2]BF_4$ (**3**), $[Ag(IMesSe)_2]BF_4$ (**4**), $[Ag(IDippS)_2]BF_4$ (**5**), $[Ag(IDippSe)_2]BF_4$ (**6**), $[Ag(IDippS)_2]NO_3$ (**7**), $[Ag(IDippS)_2]ClO_4$ (**8**), $[Ag(IDippS)_2]PF_6$ (**9**), $[Ag(IDippS)_2]SbF_6$ (**10**). Additionally, the controls IXyS (**11**), IXySe (**12**), IMesS (**13**), IMesSe (**14**), IDippS (**15**), IDippSe (**16**), $AgNO_3$ (**17**), $AgClO_4$ (**18**), $AgBF_4$ (**19**), $AgPF_6$ (**20**), $AgSbF_6$ (**21**) were used to assess the synergistic effect of the generated homoleptic complexes compared to their individual components. The water solubility of all of the $[Ag(IArE)_2]X$ complexes are inconsistent, so all samples were diluted to a final concentration of 1% DMSO in cell media for cell inoculation. Due to

DMSO being cytotoxic towards cells, a DMSO control was also included in the study as a control. The procedure for these studies is outlined below (Figure 3.2).

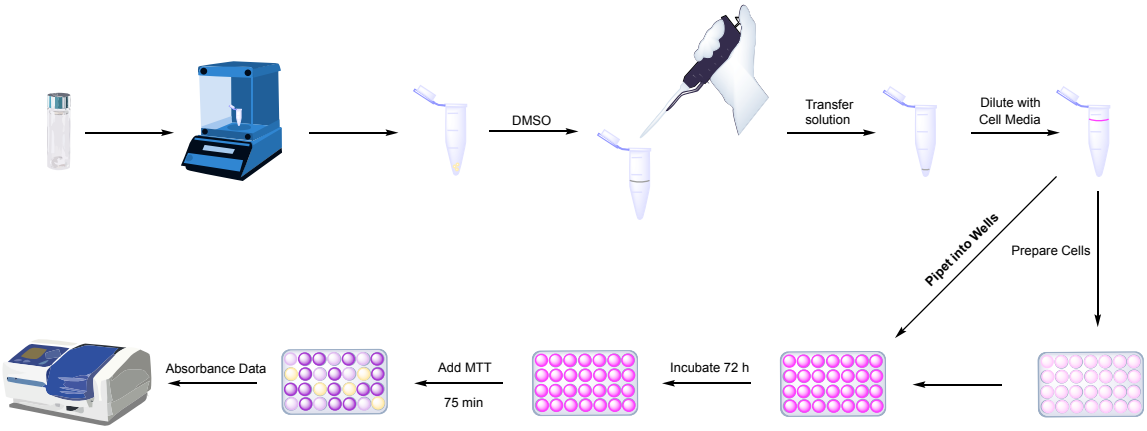

Figure 3.2. General procedure for completing cell viability assays.

MDA-MB-231 and HeLa cells were maintained in DMEM (Gibco), 10% FBS (Corning), and 1% Pen-strep (VWR), while PC3 cells were maintained in RPMI, 10% FBS, and 1% Pen-strep. Cells were plated in 96-well plates, 10000 cells per well. To prepare the samples, small amounts of the solids were massed on a semi microbalance into 1.5 mL Eppendorf Safe-Lock tubes and labeled. The individual samples were further diluted with calculated volumetric amounts of 99.8% anhydrous DMSO and vortexed to insure solvation and homogenous distribution. Microliter amounts of this sample solution are then transferred to an additional Eppendorf Safe-Lock tube and centrifuged. The samples were inoculated onto cells at 10 µM with 1% DMSO and left to incubate for 72 hours. Following 72 hours, 20 µL of Celltiter solution (Promega) was added to the cells. The solution was incubated for 75 minutes and absorbance data was obtained via a microplate photometer (515 nm) and the data was normalized to the average values for the untreated cells to determine relative cell viability across the series. Care was taken

throughout this process to limit exposure to external light sources by storing light-sensitive materials in foil-lined containers when necessary.

3.4. Results of Cell Viability Assays

Early results indicate several complexes possess anticancer activity across all three cell lines (Figures 3.3 and 3.4). HeLa cells seemed to be the most resilient against the silver complexes with few complexes showing any negative effects in terms of cell viability. Most notably, the free ligands and silver salts showed virtually no biological activity which further reinforces the hypothesis that the synergistic effect the complexes themselves are a major factor in the effectiveness in these *in vitro* studies. The ligands are observed to be crucial to the mobility of the complexes in a cellular environment. Microscope images were obtained for qualitative observation of cellular death (Figure 3.5).

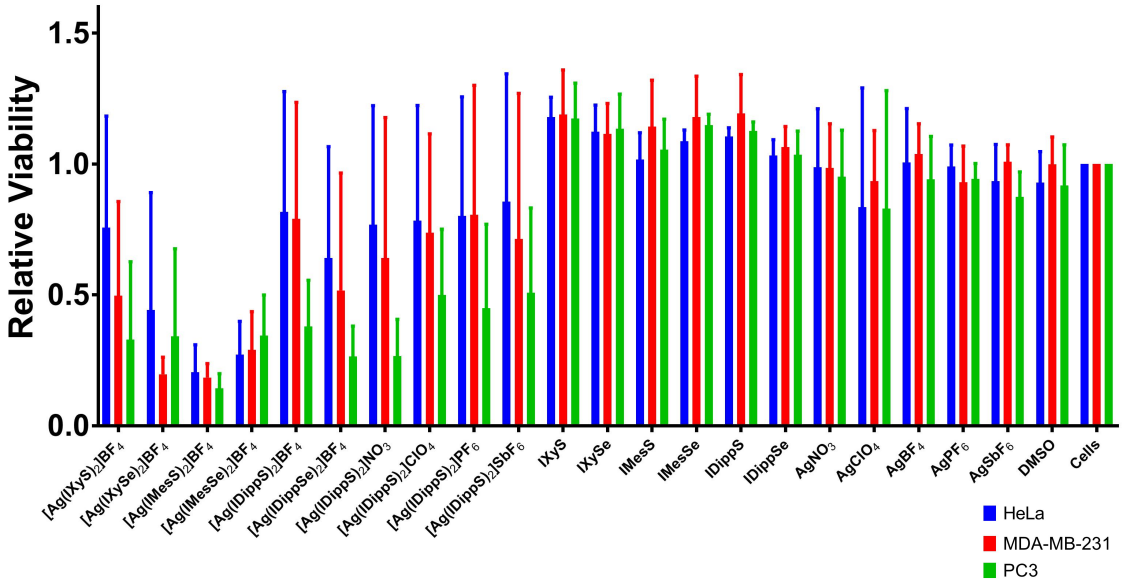

Figure 3.3. Relative cell viabilities of HeLa (blue), MDA-MB-231 (red), and PC3 (green) cell lines following treatment.

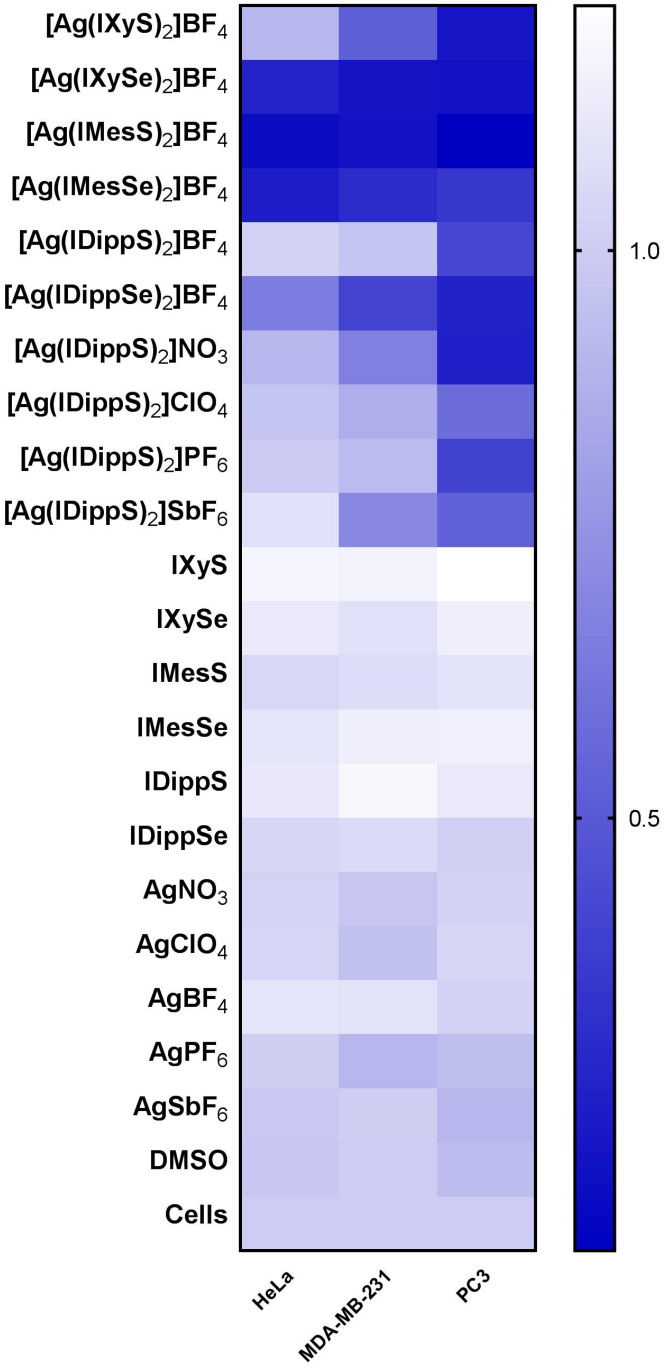

Figure 3.4. Heat map showing the efficacy of the samples and controls used in this study where the dark blue indicates a high level of cell death normalized to healthy, untreated cells.

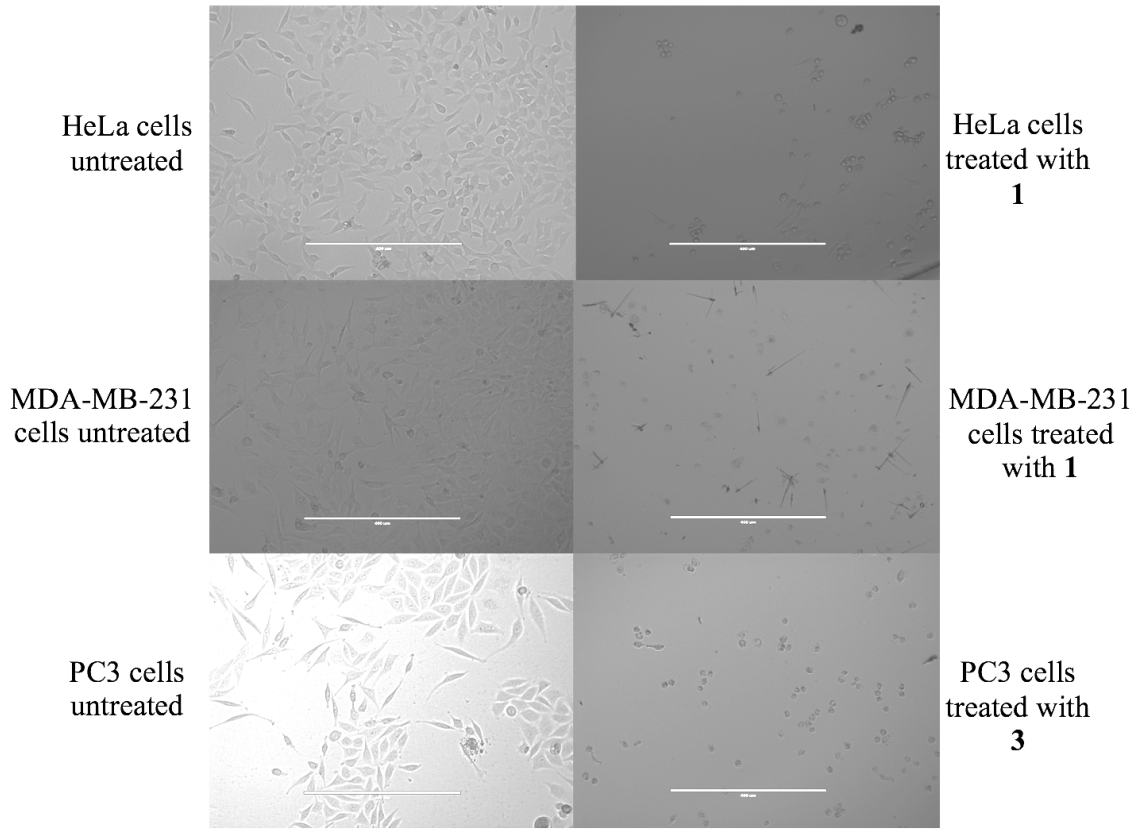

Figure 3.5. Microscope images comparing untreated HeLa, MDA-MB-231, and PC3 cells with the same cells that have been treated with $[Ag(IArE)_2]X$ complexes at 10 μM.

The counterion of these complexes also seems to have an effect, and can most likely be attributed to being the leading factor for the solubility of these compounds in the both the cell media and in the lipophilic environment of the cells. Lipophilic materials are essential when designing chemotherapeutic drugs to pass through the lipid bilayer of the cellular membrane. The counterions were all chosen carefully for this precise reason. Typically, the solubility of ionic compounds depends directly on both the cation and anion. In this case, the cation is the species of interest, containing the cytotoxic Ag^+ ion and alterations can be made to the ligands to increase or decrease lipophilicity in a specific medium. However, the anion can also obviously be altered and usually increases solubility in organic solvents when the anion is lipophilic. Typically, quaternary salts are

more lipophilic due to their tetrahedral character leading to an even distribution of its charge density across four highly electronegative fluoride atoms, making it relatively inert in terms of its reactivity. For this reason, the tetrafluoroborate (BF_4^-) anion is nonpolar and lipophilic, moreso than nitrates (which can also act as a coordinating ligand) or halides that tend to be more labile. Perchlorate (ClO_4^-) is isoelectronic to BF_4^- and shares very similar properties although the potential explosiveness of perchlorate salts has led to a decrease in their use. The other counterions, hexafluorophosphate (PF_6^-) and hexafluoroanimonate (SbF_6^-) used in this study were chosen due to their suspected increased lipophilicity when compared to the tetrahedral anions due to a higher degree of charge distribution, inertness, and larger size which should contribute to its lability. It was observed that the complexes bearing a BF_4^- counterion performed the best in the preliminary trials.

The effect of the chalcogen donor atom was observed to have little significance towards the cytotoxicity of the complex. The aromatic substituents seemed to have a small effect as the Dipp-substituted ligands didn't perform as well as the complexes with the Xy or Mes aromatic substituents. However, against the PC3 cancer cell line, several complexes regardless of the aromatic substituent showed significant activity. This could be an indicator that the substituents are able to fine tune the the properties of the complex to be effective towards various cancers.

3.5. Results of Dose Dependence Studies

Many compounds provided promising results against the MDA-MD-231 and PC3 cell lines. Of these [Ag(IArE)2]X complexes, the three most cytotoxic complexes were chosen for dose-dependence studies: $[Ag(IXySe)_2]BF_4$ **(2)**, $[Ag(IMesS)_2]BF_4$ **(3)**, and

$[Ag(IMesSe)_2]BF_4$ **(4)**. The ligands IXySe **(12)**, IMesS **(13)**, and IMesSe **(14)** as well as the silver salt $AgBF_4$ **(19)** were also included in this study as controls even though they show little to no activity. Noting that the inoculation of cells with compounds **2-4** in the preliminary cell viability assays resulted in relative cell viabilities below 0.5, it was assumed that their IC_{50} values would be below 10 μM. For this reason, the range of concentrations for the dose-dependent studies were chosen to be 1, 2.5, 5, 7.5, 10, and 25 μM. The preparation of the HeLa, MDA-MB-231, and PC3 cells was identical to the method utilized for the cell viability assays. The incubation time also remained constant at 72 h and MTT was used to quantitatively measure the absorbance of the solutions to determine the cell populations (Figure 3.6). At this time, only preliminary data has been obtained and replicate trials are ongoing, which will lower the standard deviations observed for all samples. Currently, the IC_{50} values for the three selected $[Ag(IArE)_2]X$ complexes are between 2-7 μM across all cell lines.

The three $[Ag(IArE)_2]X$ complexes were observed to be significantly more cytotoxic than the ligands that showed little to no activity at any concentration. $AgBF_4$ possesses some cytotoxic activity at higher concentrations for MDA-MB-231 and HeLa cells as it is still a source of Ag^+ ions to the cells. Even at various concentrations, there is no clear trend to indicate a preferential donor atom or aromatic substituent in terms to the overall cytotoxicity. The aromatic substituents only play a small role in the relative stability of these complexes through sterics as there were no Dipp-substituted ligands in these dose-dependence studies. However, the Dipp-substituted complexes did show some cytotoxic activity in the preliminary cell viability assays.

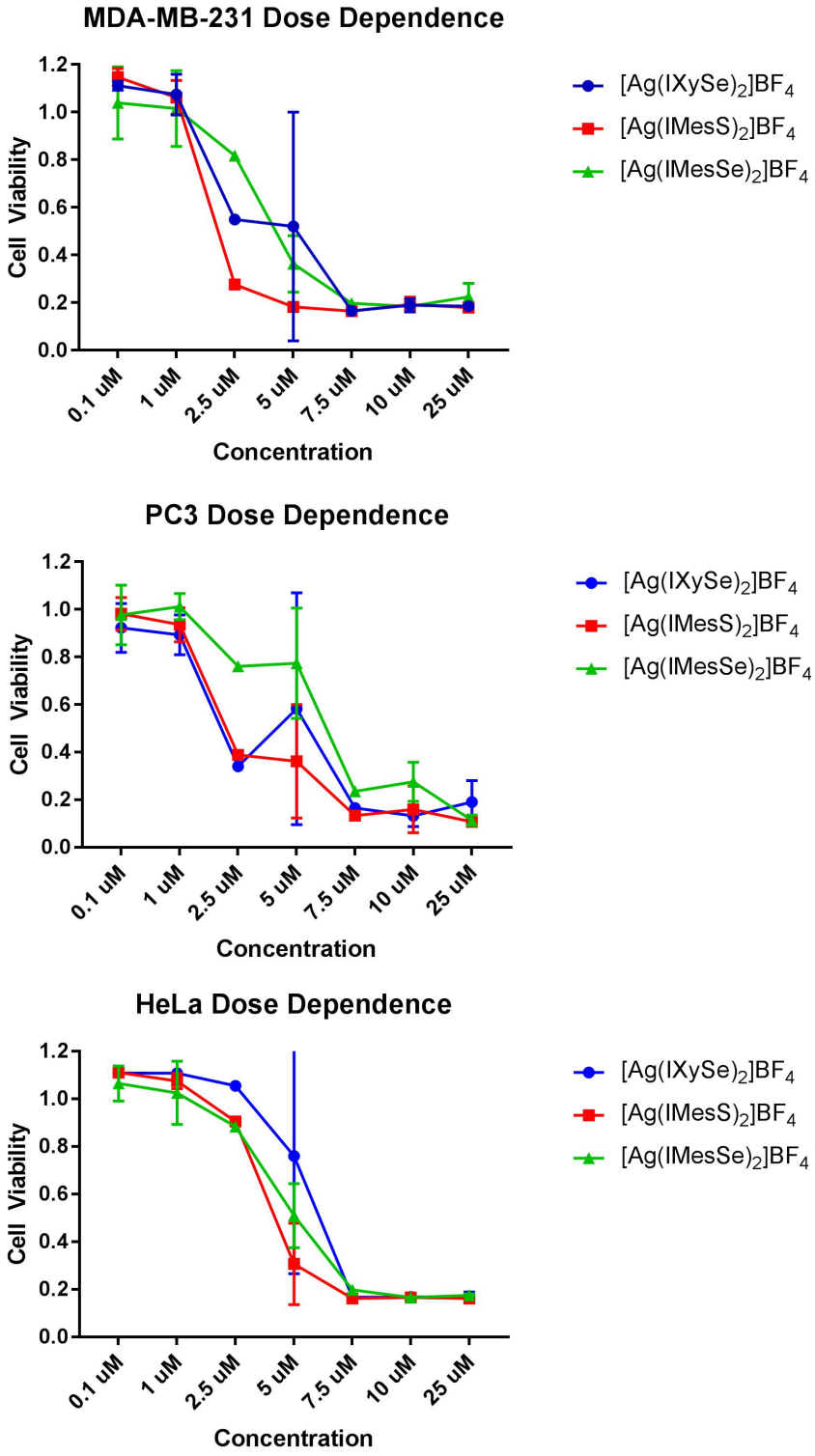

Figure 3.6. Dose dependence plots showing relative cell viability at varying μM doses.

CHAPTER 4: EXPERIMENTALS

4.1. General Considerations

All reactions were performed under aerobic conditions or under dry oxygen-free nitrogen in an Innovative Technology System One-M-DC glove box where indicated. Solvents were purified and degassed by standard procedures and all commercially available reagents were used as received. The 1,3-diaryl-imidazolium chlorides (aryl = 2,6-Xy, Mes, Dipp) ([IArEH]Cl) and their corresponding diazabutadiene precursors were prepared as reported.[73] The purity of the [IArEH]Cl intermediates was confirmed spectroscopically prior to their use in subsequent reactions. The three IArS ligands were synthesized using a combination of literature procedures, as described below.[47-57] The synthesis of the three IArSe ligands has also been described elsewhere.[58] Silver(I) salts and complexes thereof were handled under normal atmospheric conditions while limiting exposure to light by using glassware wrapped in aluminum foil. ^{1}H and ^{13}C NMR spectra were obtained on a JEOL ECX-300 (300 MHz) or a JEOL ECX-500 (500 MHz). NMR chemical shifts reported in ppm relative to TMS (δ = 0 ppm) for ^{1}H and ^{13}C NMR spectra and were referenced internally with respect to the residual protio solvent peaks (^{1}H: δ 1.94 ppm for $CD_2\mathit{H}CN$, 2.05 ppm for d_5-acetone, 2.50 ppm for d_5-DMSO, 5.32 ppm for $CD\mathit{H}Cl_2$, 7.26 ppm for $C\mathit{H}Cl_3$; ^{13}C: 1.32 ppm for CD_3CN, 29.84 ppm for d_6-acetone, 39.52 ppm for d_6-DMSO, 53.84 ppm for CD_2Cl_2, 77.16 ppm for $CDCl_3$).[74] FT-IR spectra data obtained using a Perkin-Elmer Spectrum 100 FT-IR spectrometer with relative intensities of the absorptions indicated in parentheses (vs = very strong, s = strong, m = medium, w = weak). Electrospray ionization mass spectrometry (ESI-MS) was performed

on a Thermo Scientific MSQ Plus in a 50/50 acetonitrile:water solvent mixture at a flow rate of 10 mL/min. Elemental analyses were performed by Atlantic Microlab, Inc. (Norcross, GA).

4.2. Synthesis of IArS Ligands

4.2.1. Synthesis of IXyS

Under an argon atmosphere, a stirred mixture of 1,3-bis(2,6-dimethylphenyl)imidazolium chloride (4.002 g, 12.79 mmol), potassium carbonate (1.947 g, 14.09 mmol), and elemental sulfur (0.491 g, 15.32 mmol) in ethanol (120 mL) was heated to reflux for 23 h. The resulting brownish-yellow suspension was allowed to cool to room temperature, concentrated under reduced pressure to *ca.* 20 mL, and the beige solid was separated by filtration, washed with ethanol (2 x 10 mL), and dried *in vacuo* for 22 h. The crude product was extracted into dichloromethane (60 mL) and the pale yellow organic phase was washed with DI water (2 x 20 mL). Concentration of the solution under vacuum to *ca.* 2 mL and addition of pentane (12 mL) led to the separation of the off-white product, which was isolated by filtration and dried *in vacuo* for 22 h (1.924 g, 49%). Mp = 313-316 °C (dec.). NMR data (in CD_2Cl_2): ^{1}H δ 2.17 (s, 12 H, C*H*$_3$), 6.84 (s, 2 H, imidazole *H*), 7.21-7.32 (AB$_2$ pattern, 6 H, C$_6$*H*$_3$); ^{13}C δ 18.1 (qd, $^{1}J_{C\text{-}H}$ = 128, $^{3}J_{C\text{-}H}$ = 5, 4 C, *C*H$_3$), 118.4 (dd, $^{1}J_{C\text{-}H}$ = 198, $^{2}J_{C\text{-}H}$ = 11, 2 C, imidazole *C*), 128.8 (d, $^{1}J_{C\text{-}H}$ = 160, 4 C, *C*$_6$H$_3$), 129.6 (d, $^{1}J_{C\text{-}H}$ = 160, 2 C, *C*$_6$H$_3$), 136.8 (s, 2 C, *C*$_6$H$_3$), 136.9 (s, 4 C, *C*$_6$H$_3$), 163.8 (s, 1 C, *C*=S). IR data: 3175 (w), 3149 (w), 2948 (w), 2919 (w), 2859 (w), 1640 (w), 1602 (w), 1565 (w), 1536 (w), 1472 (m), 1444 (w), 1401 (w), 1357 (s), 1339 (w), 1274 (m), 1255 (w), 1218 (m), 1149 (w), 1114 (w), 1078 (w), 1036 (w), 973 (w), 934 (m) 820

(w), 783 (s), 717 (m), 677 (s). Anal. Calc. for $C_{19}H_{20}N_2S$: C, 74.0; H, 6.5; N, 9.1. Found: C, 73.9; H, 6.4; N, 8.9%.

4.2.2. Synthesis of IMesS

A stirred mixture of 1,3-bis(2,4,6-trimethylphenyl)imidazolium chloride (5.842 g, 17.137 mmol), potassium carbonate (2.454 g, 17.756 mmol), and elemental sulfur (0.529 g, 16.495 mmol) in ethanol (150 mL) was heated to reflux for 19 h. The resulting brownish-yellow suspension was cooled to room temperature and the beige product was separated by filtration, washed with ethanol (2 x 10 mL), and dried *in vacuo* for 22 h (3.963 g, 71%). Mp = 290-291 °C (dec.). NMR data (in d_6-acetone) : ^{1}H δ 2.13 (s, 12 H, C*H*$_3$), 2.32 (s, 6 H, C*H*$_3$), 7.07 (s, 4 H, aryl *H*), 7.48 (s, 2 H, imidazole *H*); ^{13}C δ 17.6 (q, $^1J_{C\text{-}H}$ = 126, 4 C, *C*H$_3$), 20.4 (q, $^1J_{C\text{-}H}$ = 124, 2 C, *C*H$_3$), 120.8 (dd, $^1J_{C\text{-}H}$ = 202, $^2J_{C\text{-}H}$ = 11, 2 C, imidazole *C*), 129.8 (d, $^1J_{C\text{-}H}$ = 158, 4 C, *C*$_6$H$_2$), 132.9 (s, 2 C, *C*$_6$H$_2$), 135.5 (s, 4 C, *C*$_6$H$_2$), 140.0 (s, 2 C, *C*$_6$H$_2$), 158.0 (s, 1 C, *C*=S). IR data: 3168 (w), 3143 (w), 3031 (w), 2971 (w), 2951 (w), 2917 (w), 2857 (w), 2731 (w), 1748 (w), 1706 (w), 1639 (w), 1609 (w), 1560 (w), 1537 (w), 1486 (m), 1437 (m), 1403 (m), 1358 (vs), 1346 (s), 1297 (w), 1265 (w), 1225 (w), 1165 (w), 1148 (w), 1138 (w), 1094 (w), 1084 (w), 1035 (w), 1016 (w), 982 (w), 959 (w), 943 (w), 923 (m), 897 (w), 853 (s), 820 (w), 743 (w), 718 (s), 681 (vs), 652 (w). Anal. Calc. for $C_{21}H_{24}N_2S$: C, 75.0; H, 7.2; N, 8.3. Found: C, 75.0; H, 7.2; N, 8.2%.

4.2.3. Synthesis of IDippS

Under an argon atmosphere, a stirred mixture of 1,3-bis(2,6-diisopropylphenyl)imidazolium chloride (8.900 g, 20.94 mmol), potassium

carbonate (4.106 g, 29.71 mmol), and elemental sulfur (0.890 g, 27.75 mmol) in ethanol (250 mL) was heated to reflux for 24 h. The resulting brownish yellow suspension was cooled to room temperature and the off-white solids were separated by filtration. The product was extracted into dichloromethane (150 mL) and the pale brown extract was washed with deionized water (3 x 100 mL). Concentration of the extract under reduced pressure to *ca.* 10 mL and addition of diethyl ether (50 mL) led to the separation of the fluffy white product, which was isolated by filtration and dried *in vacuo* for 24 h (3.891 g, 44%). Mp = 315-317 °C. NMR data (in CD_2Cl_2): ^{1}H δ 1.23 [d, $^3J_{H-H}$ = 7.2, 12 H, CH(C*H*$_3$)$_2$], 1.31 [d, $^3J_{H-H}$ = 6.9, 12 H, CH(C*H*$_3$)$_2$], 2.75 [septet, $^3J_{H-H}$ = 6.9, 4 H, C*H*(CH$_3$)$_2$], 6.88 (s, 2 H, imidazole *H*), 7.29-7.53 (AB$_2$ pattern, 6 H, C$_6$*H*$_3$); ^{13}C δ 23.5 [q, $^1J_{C-H}$ = 126, 4 C, CH(*C*H$_3$)$_2$], 24.2 [q, $^1J_{C-H}$ = 126, 4 C, CH(*C*H$_3$)$_2$], 29.3 [d, $^1J_{C-H}$ = 129, 4 C, *C*H(CH$_3$)$_2$], 119.6 (dd, $^1J_{C-H}$ = 198, $^2J_{C-H}$ = 11, 2 C, imidazole *C*), 124.5 (d, $^1J_{C-H}$ = 157, 4 C, *C*$_6$H$_3$), 130.3 (d, $^1J_{C-H}$ = 160, 2 C, *C*$_6$H$_3$), 134.4 (s, 2 C, *C*$_6$H$_3$), 147.1 (s, 4 C, *C*$_6$H$_3$), 167.2 (s, 1 C, *C*=S). IR data: 3159 (w), 3112 (w), 3063 (m), 2958 (m), 2927 (w), 2866 (m), 1708 (w), 1591 (w), 1561 (w), 1466 (m), 1412 (m), 1381 (w), 1369 (sh), 1355 (s), 1329 (m), 1273 (m) 1257 (w), 1213 (w), 1165 (w), 1145 (w), 1122 (w), 1104 (w), 1061 (m), 985 (w), 934 (m), 856 (w), 803 (m), 771 (m), 757 (m), 729 (m), 689 (m). Anal. Calc. for $C_{27}H_{36}N_2S$: C, 77.1; H, 8.6; N, 6.7. Found: C, 77.1; H, 8.7; N, 6.6%.

4.3. Synthesis of (IArE)CuX

Copper(I) halides were used as received and handled under an inert nitrogen atmosphere. The purity of the ligands was confirmed spectroscopically by ^{1}H NMR spectroscopy prior to their use. All other reagents were used as received.

4.3.1. Synthesis of (IXyS)CuCl

A stirred suspension of CuCl (0.082 g, 0.828 mmol) in THF (8 mL) was treated with a suspension of IXyS (0.254 g, 0.823 mmol) in the same solvent (8 mL), resulting in the formation of a beige solid and a colorless solution. The suspension was stirred for 24 h, concentrated under reduced pressure to *ca.* 1 mL, treated with diethyl ether (4 mL), and the product was isolated by filtration and dried *in vacuo* for 24 h (0.224 g, 67%). Mp = 265-268 °C (dec.). NMR data (in CD_2Cl_2): ^{1}H δ 2.08 (s, 12 H, C*H*$_3$), 7.24-7.33 (AB_2 pattern, 6 H, C_6H_3), 7.48 (s, 2 H, imidazole *H*); ^{13}C δ 18.2 (q, $^1J_{C\text{-}H}$ = 128, 4 C, *C*H_3), 121.3 (d, $^1J_{C\text{-}H}$ = 202, 2 C, imidazole *C*), 130.0 (d, $^1J_{C\text{-}H}$ = 162, 4 C, C_6H_3), 131.3 (d, $^1J_{C\text{-}H}$ = 162, 2 C, C_6H_3), 134.8 (s, 2 C, C_6H_3), 136.2 (s, 4 C, C_6H_3), 157.6 (s, 1 C, *C*=S). IR data: 3147 (w), 3115 (w), 3089 (w), 2945 (w), 2911 (w), 2851 (w), 1714 (w), 1605 (w), 1560 (w), 1538 (w), 1472 (m), 1445 (w), 1416 (w), 1389 (sh), 1379 (s), 1337 (w), 1325 (w), 1291 (w), 1264 (w), 1223 (m), 1169 (w), 1141 (w), 1122 (w), 1077 (w), 1034 (w), 988 (w), 977 (w), 940 (w), 919 (w), 885 (w), 858 (w), 796 (w), 780 (vs), 766 (m), 751 (s), 692 (m). Anal. Calc. for $C_{19}H_{20}ClCuN_2S$: C, 56.0; H, 5.0; N, 6.9. Found: C, 55.5; H, 5.0; N, 6.7%.

4.3.2. Synthesis of (IXyS)CuBr

A stirred suspension of CuBr (0.046 g, 0.321 mmol) in THF (8 mL) was treated with a suspension of IXyS (0.109 g, 0.353 mmol) in the same solvent (8 mL), resulting in the formation of a light brown solid and a colorless solution. The suspension was stirred for 48 h, concentrated under reduced pressure to *ca.* 1 mL, treated with diethyl ether (4 mL), and the product was isolated by filtration and dried *in vacuo* for 24 h (0.108 g, 74%). Mp

= 246-249 °C (dec.). NMR data (in d_6-DMSO): ^{1}H δ 2.06 (s, 12 H, C*H*$_3$), 7.27-7.40 (AB$_2$ pattern, 6 H, C$_6$*H*$_3$), 7.67 (s, 2 H, imidazole *H*); ^{13}C δ 17.2 (q, $^1J_{C\text{-}H}$ = 127, 4 C, *C*H$_3$), 120.8 (d, $^1J_{C\text{-}H}$ = 200, 2 C, imidazole *C*), 128.6 (d, $^1J_{C\text{-}H}$ = 160, 4 C, *C*$_6$H$_3$), 129.7 (d, $^1J_{C\text{-}H}$ = 160, 2 C, *C*$_6$H$_3$), 134.8 (s, 2 C, *C*$_6$H$_3$), 135.1 (s, 4 C, *C*$_6$H$_3$), 156.7 (s, 1 C, *C*=S). IR data: 3147 (w), 3116 (w), 3090 (w), 2946 (w), 2915 (w), 1709 (w), 1603 (w), 1560 (w), 1504 (w), 1472 (s), 1445 (m), 1416 (w), 1389 (sh), 1378 (s), 1337 (w), 1291 (m), 1222 (s), 1168 (m), 1140 (m), 1121 (m), 1033 (w), 987 (w), 976 (w), 939 (m), 921 (w), 855 (w), 794 (m), 778 (vs), 765 (s), 751 (s), 692 (s). Anal. Calc. for $C_{19}H_{20}BrCuN_2S$: C, 50.5; H, 4.5; N, 6.2. Found: C, 50.3; H, 4.4; N, 6.2%.

4.3.3. Synthesis of (IXyS)CuI

A stirred suspension of CuI (0.057 g, 0.299 mmol) in acetonitrile (5 mL) was treated with a suspension of IXyS (0.102 g, 0.331 mmol) in THF (5 mL), resulting in the formation of a light brown solid and a colorless solution. The suspension was stirred for 24 h, concentrated under reduced pressure to *ca.* 1 mL, treated with diethyl ether (4 mL), and the product was isolated by filtration and dried *in vacuo* for 24 h (0.088 g, 59%). Mp = 208-211 °C (dec.). NMR data (in CD_2Cl_2): ^{1}H δ 2.06 (s, 12 H, C*H*$_3$), 7.23-7.38 (AB$_2$ pattern, 6 H, C$_6$*H*$_3$), 7.58 (s, 2 H, imidazole *H*); ^{13}C δ 17.4 (q, $^1J_{C\text{-}H}$ = 128, 4 C, *C*H$_3$), 120.4 (d, $^1J_{C\text{-}H}$ = 202, 2 C, imidazole *C*), 128.5 (d, $^1J_{C\text{-}H}$ = 162, 4 C, *C*$_6$H$_3$), 129.5 (d, $^1J_{C\text{-}H}$ = 161, 2 C, *C*$_6$H$_3$), 135.2 (s, 2 C, *C*$_6$H$_3$), 135.3 (s, 4 C, *C*$_6$H$_3$), 157.7 (s, 1 C, *C*=S). IR data: 3389 (w), 3352 (w), 3174 (w), 3145 (w), 3105 (w), 2947 (w), 2919 (w), 2858 (w), 1639 (w), 1603 (w), 1591 (w), 1565 (w), 1535 (w), 1510 (w), 1471 (m), 1444 (m), 1401 (m), 1341 (vs), 1274 (m), 1254 (m), 1217 (m), 1159 (w), 1149 (m), 1126 (w), 1114 (m),

1078 (w), 1030 (m), 1012 (w), 990 (w), 973 (m), 934 (m), 871 (w), 859 (w), 835 (w), 819 (w), 804 (w), 781 (vs), 741 (w), 717 (vs), 677 (s). Anal. Calc. for $C_{19}H_{20}CuIN_2S$: C, 45.7; H, 4.0; N, 5.6. Found: C, 45.7; H, 4.0; N, 5.7%.

4.3.4. Synthesis of (IXySe)CuI

A stirred suspension of CuI (0.147 g, 0.772 mmol) in THF (5 mL) was treated with a suspension of IXySe (0.274 g, 0.771 mmol) in the same solvent (5 mL), resulting in the formation of a beige solid and a pale brown solution. The suspension was stirred for 48 h, concentrated under reduced pressure to *ca.* 1 mL, treated with diethyl ether (4 mL), and the product was isolated by filtration and dried *in vacuo* for 24 h (0.323 g, 77%). Mp = 226-229 °C (dec.). NMR data (in CD_2Cl_2): ^{1}H δ 2.05 (s, 12 H, C*H*$_3$), 7.25-7.39 (AB_2 pattern, 6 H, C_6H_3), 7.80 (s, 2 H, imidazole *H*); ^{13}C δ 17.5 (q, $^1J_{C-H}$ = 129, 4 C, *C*H$_3$), 122.7 (d, $^1J_{C-H}$ = 203, 2 C, imidazole *C*), 128.5 (d, $^1J_{C-H}$ = 162, 4 C, C_6H_3), 129.6 (d, $^1J_{C-H}$ = 161, 2 C, C_6H_3), 134.9 (s, 2 C, C_6H_3), 135.6 (s, 4 C, C_6H_3), 149.3 (s, 1 C, *C*=Se). IR data: 3168 (w), 3144 (w), 3038 (w), 2970 (w), 2943 (w), 2918 (w), 2857 (w), 1646 (w), 1601 (w), 1560 (w), 1540 (w), 1479 (m), 1471 (m), 1443 (w), 1403 (w), 1372 (w), 1343 (vs), 1280 (m), 1256 (w), 1221 (m), 1169 (w), 1158 (w), 1132 (w), 1113 (m), 1078 (m), 1036 (w), 991 (w), 969 (m), 938 (m), 919 (w), 849 (w), 823 (w), 787 (vs), 743 (w), 719 (vs), 674 (s). Anal. Calc. for $C_{19}H_{20}CuIN_2Se$: C, 41.8; H, 3.7; N, 5.1. Found: C, 41.5; H, 3.7; N, 5.1%.

4.3.5. Synthesis of (IMesS)CuCl

A stirred suspension of CuCl (0.042 g, 0.424 mmol) in acetonitrile (5 mL) was treated with a suspension of IMesS (0.156 g, 0.464 mmol) in THF (8 mL), resulting in the

formation of a white solid and a colorless solution. The suspension was stirred for 24 h, concentrated under reduced pressure to *ca.* 1 mL, treated with diethyl ether (4 mL), and the product was isolated by filtration and dried *in vacuo* for 6 h (0.147 g, 80%). Mp = 229-232 °C (dec.). NMR data (in d_6-DMSO): ^{1}H δ 1.97 (s, 12 H, C*H*$_3$), 2.28 (s, 6 H, C*H*$_3$), 7.09 (s, 4 H, C$_6$*H*$_2$), 7.68 (s, 2 H, imidazole *H*); ^{13}C δ 17.0 (q, $^{1}J_{C\text{-}H}$ = 128, 4 C, *C*H$_3$), 20.6 (q, $^{1}J_{C\text{-}H}$ = 127, 2 C, *C*H$_3$), 121.6 (dd, $^{1}J_{C\text{-}H}$ = 204, $^{2}J_{C\text{-}H}$ = 12, 2 C, imidazole *C*), 129.6 (d, $^{1}J_{C\text{-}H}$ = 159, 4 C, *C*$_6$H$_2$), 131.8 (s, 2 C, *C*$_6$H$_2$), 134.6 (d, $^{2}J_{C\text{-}H}$ = 6, 4 C, *C*$_6$H$_2$), 140.0 (d, $^{2}J_{C\text{-}H}$ = 6, 2 C, *C*$_6$H$_2$), 155.6 (s, 1 C, *C*=S). IR data: 3149 (m), 3113 (m), 3083 (m), 2949 (w), 2919 (w), 2856 (w), 2734 (w), 1808 (w), 1771 (w), 1733 (w), 1711 (w), 1608 (m), 1559 (m), 1483 (s), 1451 (s), 1417 (w), 1394 (sh), 1389 (vs), 1347 (m), 1293 (m), 1237 (s), 1168 (w), 1142 (w), 1107 (w), 1035 (m), 1012 (w), 984 (w), 961 (w), 942 (w), 925 (m), 888 (w), 867 (m), 853 (s), 752 (vs), 695 (vs). Anal. Calc. for $C_{19}H_{24}ClCuN_2S$: C, 57.9; H, 5.6; N, 6.4. Found: C, 58.0; H, 5.6; N, 6.3%.

4.3.6. Synthesis of (IMesS)CuBr

A stirred suspension of CuBr (0.056 g, 0.390 mmol) in acetonitrile (5 mL) was treated with a suspension of IMesS (0.145 g, 0.431 mmol) in THF (8 mL), resulting in the formation of a white solid and a pale green solution. The suspension was stirred for 24 h, concentrated under reduced pressure to *ca.* 1 mL, treated with diethyl ether (4 mL), and the product was isolated by filtration and dried *in vacuo* for 6 h (0.103 g, 55%). Mp = 244-246 °C (dec.). NMR data (in d_6-DMSO): ^{1}H δ 1.98 (s, 12 H, C*H*$_3$), 2.28 (s, 6 H, C*H*$_3$), 7.08 (s, 4 H, C$_6$*H*$_2$), 7.64 (s, 2 H, imidazole *H*); ^{13}C δ 17.1 (q, $^{1}J_{C\text{-}H}$ = 127, 4 C, *C*H$_3$), 20.6 (q, $^{1}J_{C\text{-}H}$ = 126, 2 C, *C*H$_3$), 121.2 (dd, $^{1}J_{C\text{-}H}$ = 203, $^{2}J_{C\text{-}H}$ = 11, 2 C, imidazole

C), 129.4 (d, $^{1}J_{C\text{-}H}$ = 158, 4 C, C_6H_2), 132.1 (s, 2 C, C_6H_2), 134.7 (d, $^{2}J_{C\text{-}H}$ = 6, 4 C, C_6H_2), 139.7 (d, $^{2}J_{C\text{-}H}$ = 5, 2 C, C_6H_2), 156.5 (s, 1 C, *C*=S). IR data: 3149 (m), 3114 (m), 3085 (m), 1607 (m), 1559 (m), 1483 (s), 1450 (m), 1385 (vs), 1346 (m), 1292 (m), 1236 (s), 1168 (m), 1142 (m), 1032 (w), 983 (w), 961 (w), 926 (m), 867 (m), 852 (s), 750 (vs), 695 (vs). Anal. Calc. for $C_{21}H_{24}BrCuN_2S$: C, 52.6; H, 5.0; N, 5.8. Found: C, 52.5; H, 5.1; N, 6.0%.

4.3.7. Synthesis of (IMesS)CuI

A stirred suspension of CuI (0.095 g, 0.499 mmol) in acetonitrile (5 mL) was treated with a suspension of IMesS (0.184 g, 0.547 mmol) in THF (8 mL), resulting in the formation of a white solid and a colorless solution. The suspension was stirred for 24 h, concentrated under reduced pressure to *ca.* 1 mL, treated with diethyl ether (4 mL), and the product was isolated by filtration and dried *in vacuo* for 6 h (0.175 g, 67%). Mp = 252-255 °C (dec.). NMR data (in d_6-DMSO): ^{1}H δ 1.97 (s, 12 H, CH_3), 2.28 (s, 6 H, CH_3), 7.08 (s, 4 H, C_6H_2), 7.60 (s, 2 H, imidazole *H*); ^{13}C δ 17.3 (q, $^{1}J_{C\text{-}H}$ = 131, 4 C, *C*H_3), 20.7 (q, $^{1}J_{C\text{-}H}$ = 131, 2 C, *C*H_3), 121.2 (dd, $^{1}J_{C\text{-}H}$ = 203, $^{2}J_{C\text{-}H}$ = 11, 2 C, imidazole *C*), 129.5 (d, $^{1}J_{C\text{-}H}$ = 158, 4 C, C_6H_2), 132.3 (s, 2 C, C_6H_2), 134.8 (d, $^{2}J_{C\text{-}H}$ = 5, 4 C, C_6H_2), 139.7 (d, $^{2}J_{C\text{-}H}$ = 6, 2 C, C_6H_2), 156.8 (s, 1 C, *C*=S). IR data: 3149 (w), 3115 (m), 3086 (w), 2969 (w), 2918 (w), 2851 (w), 1607 (w), 1594 (w), 1559 (w), 1481 (m), 1449 (m), 1415 (w), 1392 (sh), 1384 (vs), 1345 (w), 1290 (w), 1234 (s), 1167 (w), 1141 (w), 1105 (w), 1032 (w), 1012 (w), 925 (w), 868 (m), 851 (s), 747 (vs), 694 (vs). Anal. Calc. for $C_{21}H_{24}CuIN_2S$: C, 47.9; H, 4.6; N, 5.3. Found: C, 48.3; H, 4.6; N, 5.4%.

4.3.8. Synthesis of (IDippS)CuCl

A stirred suspension of CuCl (0.138 g, 1.394 mmol) in diethyl ether (5 mL) was treated with a suspension of IDippS (0.616 g, 1.464 mmol) in the same solvent (8 mL). After stirring for 23 h, the suspension and concentrated under reduced pressure to *ca.* 1 mL, treated with pentane (6 mL), and the white product was isolated by filtration and dried *in vacuo* for 3 h (0.613 g, 85%). Mp = 220-223 °C (dec.). NMR data (in d_6-DMSO): ^{1}H δ 1.16 [d, $^{3}J_{H-H}$ = 6.9, 12 H, CH(C*H*$_3$)$_2$], 1.23 [d, $^{3}J_{H-H}$ = 6.6, 12 H, CH(C*H*$_3$)$_2$], 2.38 [septet, $^{3}J_{H-H}$ = 6.8, 4 H, C*H*(CH$_3$)$_2$], 7.35-7.56 (AB$_2$ pattern, 6 H, C$_6$*H*$_3$), 7.89 (s, 2 H, imidazole *H*); ^{13}C δ 22.9 [q, $^{1}J_{C-H}$ = 126, 4 C, CH(*C*H$_3$)$_2$], 23.7 [q, $^{1}J_{C-H}$ = 125, 4 C, CH(*C*H$_3$)$_2$], 28.5 [d, $^{1}J_{C-H}$ = 129, 4 C, *C*H(CH$_3$)$_2$], 122.6 (dd, $^{1}J_{C-H}$ = 203, $^{2}J_{C-H}$ = 12, 2 C, imidazole *C*), 124.7 (d, $^{1}J_{C-H}$ = 160, 4 C, *C*$_6$H$_3$), 130.9 (d, $^{1}J_{C-H}$ = 161, 2 C, *C*$_6$H$_3$), 131.9 (s, 2 C, *C*$_6$H$_3$), 145.2 (s, 4 C, *C*$_6$H$_3$), 159.6 (s, 1 C, *C*=S). IR data: 3168 (w), 3139 (w), 3076 (w), 2964 (m), 2926 (w), 2868 (w), 1566 (w), 1555 (w), 1455 (m), 1422 (m), 1377 (s), 1362 (s), 1326 (m), 1253 (w), 1210 (w), 1178 (w), 1121 (w), 1101 (w), 1058 (w), 1041 (w), 980 (w), 936 (w), 802 (s), 766 (m), 757 (s), 729 (s), 691 (s). Anal. Calc. for $C_{27}H_{36}ClCuN_2S$: C, 62.4; H, 7.0; N, 5.4. Found: C, 61.9; H, 6.9; N, 5.4%.

4.3.9. Synthesis of (IDippS)CuBr

A stirred suspension of CuBr (0.073 g, 0.509 mmol) in THF (8 mL) was treated with a solution of IDippS (0.214 g, 0.509 mmol) in the same solvent (8 mL). The resulting colorless solution was stirred for 48 h, concentrated under reduced pressure to *ca.* 1 mL, and treated with pentane (6 mL), leading to the separation of the white product, which was isolated by filtration and dried *in vacuo* for 3 h (0.208 g, 72%). Mp = 217-219 °C

(dec.). ^{1}H NMR data (in CD_2Cl_2): δ 1.20 [d, $^{3}J_{H-H}$ = 6.9, 12 H, CH(CH_3)$_2$], 1.34 [d, $^{3}J_{H-H}$ = 6.9, 12 H, CH(CH_3)$_2$], 2.52 [septet, $^{3}J_{H-H}$ = 6.8, 4 H, CH(CH$_3$)$_2$], 7.09 (s, 2 H, imidazole *H*), 7.39 (d, $^{3}J_{H-H}$ = 7.8, 4 H, C$_6H_3$), 7.61 (d, $^{3}J_{H-H}$ = 7.8, 2 H, C$_6H_3$); ^{13}C NMR data (in d_6-DMSO): δ 22.7 [q, $^{1}J_{C-H}$ = 125, 4 C, CH(*C*H$_3$)$_2$], 23.5 [q, $^{1}J_{C-H}$ = 126, 4 C, CH(*C*H$_3$)$_2$], 28.2 [d, $^{1}J_{C-H}$ = 128, 4 C, *C*H(CH$_3$)$_2$], 121.9 (dd, $^{1}J_{C-H}$ = 203, $^{2}J_{C-H}$ = 12, 2 C, imidazole *C*), 124.4 (d, $^{1}J_{C-H}$ = 160, 4 C, *C*$_6$H$_3$), 130.5 (d, $^{1}J_{C-H}$ = 161, 2 C, *C*$_6$H$_3$), 132.0 (s, 2 C, *C*$_6$H$_3$), 145.1 (s, 4 C, *C*$_6$H$_3$), 160.6 (s, 1 C, *C*=S). IR data: 3168 (w), 3140 (w), 3088 (w), 2962 (s), 2924 (m), 2867 (m), 1669 (w), 1591 (w), 1557 (m), 1457 (s), 1422 (m), 1377 (vs), 1362 (vs), 1325 (m), 1301 (w), 1255 (w), 1209 (m), 1179 (m), 1121 (m), 1101 (w), 1076 (w), 1058 (m), 1042 (w), 979 (m), 935 (m), 802 (vs), 767 (m), 756 (s), 727 (vs), 689 (vs). Anal. Calc. for $C_{27}H_{36}BrCuN_2S$: C, 57.5; H, 6.4; N, 5.0. Found: C, 57.2; H, 6.3; N, 5.0%.

4.3.10. Synthesis of (IDippSe)CuBr

A stirred suspension of CuBr (0.091 g, 0.634 mmol) in THF (5 mL) was treated with a suspension of IDippSe (0.298 g, 0.637 mmol) in the same solvent (5 mL), resulting in the formation of a white solid and a colorless solution. The suspension was stirred for 48 h, concentrated under reduced pressure to ca. 1 mL, treated with diethyl ether (4 mL), and the product was isolated by filtration and dried *in vacuo* for 24 h (0.234 g, 60%). Mp = 231-234 °C (dec.). NMR data (in CD_2Cl_2): ^{1}H δ 1.18 [d, $^{3}J_{H-H}$ = 6.9, 12 H, CH(CH_3)$_2$], 1.31 [d, $^{3}J_{H-H}$ = 6.6, 12 H, CH(CH_3)$_2$], 2.43 [septet, $^{3}J_{H-H}$ = 6.9, 4 H, CH(CH$_3$)$_2$], 7.24 (s, 2 H, imidazole *H*), 7.35 (d, $^{3}J_{H-H}$ = 7.7, 4 H, C$_6H_3$), 7.57 (t, $^{3}J_{H-H}$ = 7.8, 2 H, C$_6H_3$); ^{13}C δ 23.6 [q, $^{1}J_{C-H}$ = 127, 4 C, CH(*C*H$_3$)$_2$], 24.5 [q, $^{1}J_{C-H}$ = 127, 4 C, CH(*C*H$_3$)$_2$], 29.4 [d, $^{1}J_{C-H}$

= 128, 4 C, *C*H(CH_3)$_2$], 123.9 (dd, $^1J_{C-H}$ = 202, $^2J_{C-H}$ = 12, 2 C, imidazole *C*), 125.7 (d, $^1J_{C-H}$ = 160, 4 C, C_6H_3), 132.1 (d, $^1J_{C-H}$ = 163, 2 C, C_6H_3), 132.9 (s, 2 C, C_6H_3), 145.9 (s, 4 C, C_6H_3), 155.6 (s, 1 C, *C*=Se). IR data: 3147 (w), 3115 (w), 3084 (w), 2961 (s), 2928 (w), 2869 (w), 1713 (w), 1611 (w), 1593 (w), 1557 (w), 1516 (w), 1459 (s), 1424 (w), 1383 (m), 1363 (m), 1351 (m), 1328 (m), 1310 (w), 1290 (w), 1273 (w), 1256 (w), 1213 (m), 1181 (w), 1166 (w), 1149 (w), 1123 (w), 1106 (w), 1062 (m), 1044 (w), 976 (w), 937 (w), 901 (w), 859 (w), 810 (m), 798 (vs), 770 (w), 752 (vs), 730 (w), 689 (m). Anal. Calc. for $C_{27}H_{36}BrCuN_2Se$: C, 53.1; H, 5.9; N, 4.6. Found: C, 52.8; H, 5.8; N, 4.6%.

4.4. Synthesis of [Ag(IArE)$_2$]X

4.4.1. Synthesis of [Ag(IXyS)$_2$]NO_3

A stirred suspension of IXyS (0.288 g, 0.932 mmol) in acetonitrile (5 mL) was treated dropwise with a solution of $AgNO_3$ (0.079 g, 0.466 mmol) in the same solvent (5 mL). After stirring the resulting solution for 24 h, the solvent was removed under reduced pressure to give a white solid, which was washed with pentane (10 mL), separated by filtration, and dried *in vacuo* for 24 h (0.284 g, 77%). Mp = 278-281 °C (dec.). NMR data (in CD_2Cl_2): ^{1}H δ 2.05 (s, 24 H, C*H*$_3$), 7.11 (s, 4 H, imidazole *H*), 7.20-7.39 (m, 12 H, C$_6$*H*$_3$); ^{13}C δ 18.0 [q, $^1J_{C-H}$ = 129, 8 C, *C*H$_3$], 121.2 (dd, $^1J_{C-H}$ = 202, $^2J_{C-H}$ = 11, 4 C, imidazole *C*), 129.7 (d, $^1J_{C-H}$ = 164, 8 C, C_6H_3), 131.1 (d, $^1J_{C-H}$ = 162, 4 C, C_6H_3), 134.7 (s, 4 C, C_6H_3), 136.0 (s, 8 C, C_6H_3), 157.0 (s, 2 C, *C*=S). IR data: 3167 (w), 3125 (w), 3083 (w), 2976 (w), 2915 (w), 2857 (w), 1600 (w), 1557 (w), 1472 (m), 1444 (w), 1414 (w), 1360 (m), 1338 (s), 1296 (w), 1227 (m) 1164 (m), 1145 (w), 1123 (w), 1085 (w), 1031 (w), 988 (w), 979 (w), 942 (w), 830 (w), 807 (w), 784 (s), 743 (w), 729 (m), 692

(s), 642 (w), 620 (w). ESI-MS (in MeCN): *m/z* = 725.41, $[Ag(IXyS)_2]^+$. Anal. Calc. for $C_{38}H_{40}AgN_5O_3S_2$: C, 58.0; H, 5.1, N, 8.9. Found: C, 58.0; H, 5.2; N, 8.9%.

4.4.2. Synthesis of $[Ag(IXyS)_2]BF_4$

A stirred suspension of IXyS (0.145 g, 0.471 mmol) in acetonitrile (5 mL) was treated with a solution of $AgBF_4$ (0.046 g, 0.235 mmol) in deionized H_2O (2 mL). After stirring the resulting solution for 24 h, the solvent was removed under reduced pressure to give an off-white solid, which was washed with pentane (10 mL), isolated by filtration and dried *in vacuo* for 24 h (0.094 g, 49%). Mp = 299-302 °C (dec.). NMR data (in CD_2Cl_2): ^{1}H δ 2.06 (s, 24 H, C*H*$_3$), 7.06 (s, 4 H, imidazole *H*), 7.19-7.40 (m, 12 H, C_6H_3); ^{13}C δ 18.0 [q, $^1J_{C\text{-}H}$ = 128, 8 C, *C*H$_3$],121.1 (dd, $^1J_{C\text{-}H}$ = 202, $^2J_{C\text{-}H}$ = 11, 4 C, imidazole *C*), 129.7 (d, $^1J_{C\text{-}H}$ = 161, 8 C, C_6H_3), 131.1 (d, $^1J_{C\text{-}H}$ = 162, 4 C, C_6H_3),134.7 (s, 4 C, C_6H_3),136.0 (s, 8 C, C_6H_3), 157.3 (s, 2 C, *C*=S). IR data: 3191 (w), 3165 (w), 2979 (w), 2950 (w), 2919 (w), 2860 (w), 1683 (w), 1602 (w), 1560 (w), 1536 (w), 1472 (m), 1445 (m), 1412 (w), 1369 (s) 1295 (w), 1285 (w), 1225 (m), 1165 (w), 1146 (w), 1083 (sh), 1050 (vs), 1035 (vs), 990 (w), 976 (w), 941 (m), 920 (w), 783 (vs), 732 (m), 693 (m), 678 (w), 619 (w). Anal. Calc. for $C_{38}H_{40}N_4AgBF_4S_2$: C, 56.2; H, 5.0, N, 6.9. Found: C, 56.5; H, 5.0; N, 7.0%.

4.4.3. Synthesis of $[Ag(IXyS)_2]ClO_4$

A stirred suspension of IXyS (0.153 g, 0.473 mmol) in acetonitrile (5 mL) was treated dropwise with a solution of $AgClO_4$ (0.053 g, 0.236 mmol) in deionized water (2 mL) resulting in the immediate formation of a colorless solution. After stirring for 24 h, the solvent was removed under reduced pressure to give a white solid, which was washed

with pentane (10 mL) and dried *in vacuo* for 24 h (0.129 g, 59%). Mp = 303-305 °C (dec.). NMR data (in CD_2Cl_2): ^{1}H δ 2.06 (s, 24 H, CH_3), 7.05 (s, 4 H, imidazole *H*), 7.20-7.39 (m, 12 H, C_6H_3); ^{13}C δ 18.0 (q, $^1J_{C\text{-}H}$ = 128, 8 C, *C*H_3), 120.8 (dd, $^1J_{C\text{-}H}$ = 202, $^2J_{C\text{-}H}$ = 11, 4 C, imidazole *C*), 129.6 (d, $^1J_{C\text{-}H}$ = 161, 8 C, C_6H_3), 131.0 (d, $^1J_{C\text{-}H}$ = 162, 4 C, C_6H_3),134.8 (s, 4 C, C_6H_3),136.0 (s, 8 C, C_6H_3), 157.6 (s, 2 C, *C*=S). IR data: 3176 (w), 3140 (w), 3103 (w), 2978 (w), 2921 (w), 2859 (w), 1562 (w), 1473 (m), 1443 (w), 1372 (s), 1338 (w), 1295 (w), 1227 (w), 1167 (w), 1147 (w), 1080 (vs), 1037 (m), 992 (w), 976 (w), 942 (w), 833 (w), 779 (s), 727 (m), 686 (s), 620 (s). Anal. Calc. for $C_{38}H_{40}N_4AgClO_4S_2$: C, 55.4; H, 4.9, N, 6.8. Found: C, 56.0; H, 4.9; N, 6.8%.

4.4.4. Synthesis of $[Ag(IXyS)_2]PF_6$

A stirred suspension of IXyS (0.147 g, 0.477 mmol) in acetonitrile (6 mL) was treated dropwise with a solution of $AgPF_6$ (0.060 g, 0.237 mmol) in deionized water (~0.5 mL), resulting in the immediate formation of a colorless solution. After stirring for 23 h, the solvent was removed under reduced pressure to give a white solid, which was washed with diethyl ether (10 mL), and dried *in vacuo* for 2 days (0.153 g, 74%). Mp = 304-307 °C (dec.). NMR data (in CD_2Cl_2): ^{1}H δ 2.05 (s, 24 H, CH_3), 7.04 (s, 4 H, imidazole *H*), 7.20-7.40 (m, 12 H, C_6H_3); ^{13}C δ 17.9 (q, $^1J_{C\text{-}H}$ = 128, 8 C, *C*H_3), 121.0 (dd, $^1J_{C\text{-}H}$ = 202, $^2J_{C\text{-}H}$ = 11, 4 C, imidazole *C*), 129.7 (d, $^1J_{C\text{-}H}$ = 162, 8 C, C_6H_3), 131.1 (d, $^1J_{C\text{-}H}$ = 161, 4 C, C_6H_3), 134.6 (s, 4 C, C_6H_3),136.0 (s, 8 C, C_6H_3), 157.1 (s, 2 C, *C*=S). IR data: 3175 (w), 3147 (w), 3100 (w), 2981 (w), 2922 (w), 2863 (w), 1561 (w), 1473 (m), 1445 (w), 1374 (m), 1338 (w), 1322 (w), 1295 (w), 1227 (m), 1167 (w), 1145 (w), 1122 (w), 1080 (w), 978 (w), 942 (w), 876 (w), 840 (vs), 826 (vs), 779 (s), 766 (sh), 727 (m), 687 (m),

620 (w). Anal. Calc. for $C_{38}H_{40}AgF_6N_4PS_2$: C, 52.5; H, 4.6, N, 6.4. Found: C, 52.8; H, 4.8; N, 6.6%.

4.4.5. Synthesis of $[Ag(IXyS)_2]SbF_6$

A stirred suspension of IXyS (0.149 g, 0.483 mmol) in acetonitrile (5 mL) was treated dropwise with a solution of $AgSbF_6$ (0.061 g, 0.241 mmol) in deionized water (~0.5 mL), resulting in the formation of a fine off-white solid and a colorless solution. After stirring the suspension for 24 h, the solvent was removed under reduced pressure to give an off-white solid, which was washed with diethyl ether (10 mL), and dried *in vacuo* for 24 h (0.162 g, 77%). Mp = 273-276 °C (dec.). NMR data (in CD_2Cl_2): ^{1}H δ 2.06 (s, 24 H, C*H*$_3$), 7.05 (s, 4 H, imidazole *H*), 7.20-7.40 (m, 12 H, C$_6$*H*$_3$); ^{13}C δ 18.0 (q, $^1J_{C\text{-}H}$ = 128, 8 C, *C*H$_3$), 120.9 (dd, $^1J_{C\text{-}H}$ = 202, $^2J_{C\text{-}H}$ = 11, 4 C, imidazole *C*), 129.6 (d, $^1J_{C\text{-}H}$ = 161, 8 C, *C*$_6$H$_3$), 131.0 (d, $^1J_{C\text{-}H}$ = 161, 4 C, *C*$_6$H$_3$), 134.8 (s, 4 C, *C*$_6$H$_3$), 136.0 (s, 8 C, *C*$_6$H$_3$), 157.4 (s, 2 C, *C*=S). IR data: 3172 (w), 3146 (w), 3097 (w), 2977 (w), 2920 (w), 2862 (w), 1560 (w), 1473 (m), 1444 (w), 1413 (w), 1373 (s), 1339 (w), 1294 (w), 1227 (m), 1171 (w), 1145 (w), 1121 (w), 1079 (w), 1035 (w), 977 (w), 941 (w), 784 (sh), 779 (s), 735 (w), 725 (w), 685 (m), 662 (s), 628 (vs). Anal. Calc. for $C_{38}H_{40}AgF_6N_4S_2Sb$: C, 47.5; H, 4.2, N, 5.8. Found: C, 48.3; H, 4.4; N, 6.0.

4.4.6. Synthesis of $[Ag(IXySe)_2]NO_3$

A stirred suspension of IXySe (0.174 g, 0.490 mmol) in acetonitrile (5 mL) was added to a solution of $AgNO_3$ (0.042 g, 0.247 mmol) in deionized water (~0.5 mL), resulting in the immediate formation of a colorless solution. After stirring for 24 h, the solvent was removed under reduced pressure from the solution to give a white solid, which was

washed with diethyl ether (10 mL), and dried *in vacuo* for 24 h (0.151 g, 70%). Mp = 250-252 °C (dec.). NMR data (in CD_2Cl_2): ^{1}H δ 2.04 (s, 24 H, C*H*$_3$), 7.27 (s, 4 H, imidazole *H*), 7.18-7.40 (m, 12 H, C$_6$*H*$_3$); ^{13}C δ 18.1 (q, $^1J_{C\text{-}H}$ = 128, 8 C, *C*H$_3$), 123.1 (dd, $^1J_{C\text{-}H}$ = 203, $^2J_{C\text{-}H}$ = 11, 4 C, imidazole *C*), 129.7 (d, $^1J_{C\text{-}H}$ = 162, 8 C, *C*$_6$H$_3$), 131.1 (d, $^1J_{C\text{-}H}$ = 162, 4 C, *C*$_6$H$_3$), 135.5 (s, 4 C, *C*$_6$H$_3$), 135.8 (s, 8 C, *C*$_6$H$_3$), 149.8 (s, 2 C, *C*=Se). IR data: 3170 (w), 3129 (w), 3088 (w), 2976 (w), 2944 (w), 2915 (w), 2859 (w), 1558 (w), 1474 (m), 1446 (w), 1415 (w), 1340 (vs), 1302 (m), 1226 (m), 1168 (w), 1116 (w), 1081 (w), 1038 (w), 973 (w), 943 (w), 831 (w), 817 (m), 779 (s), 736 (s), 686 (m). Anal. Calc. for $C_{38}H_{40}AgN_5O_3Se_2$: C, 51.8; H, 4.6, N, 8.0. Found: C, 51.5; H, 4.5; N, 8.1%.

4.4.7. Synthesis of [Ag(IXySe)$_2$]BF$_4$

A solution of $AgBF_4$ (0.036 g, 0.185 mmol) in deionized water (~0.5 mL) was treated with a stirred suspension of IXySe (0.131 g, 0.369 mmol) in acetonitrile (6 mL), resulting in the immediate formation of a colorless solution. After stirring for 24 h, the solvent was removed under reduced pressure from the solution to give a white solid, which was washed with diethyl ether (10 mL), and dried *in vacuo* for 25 h (0.139 g, 83%). Mp = 280-283 °C (dec.). NMR data (in CD_2Cl_2): ^{1}H δ 2.05 (s, 24 H, C*H*$_3$), 7.19 (s, 4 H, imidazole *H*), 7.20-7.39 (m, 12 H, C$_6$*H*$_3$); ^{13}C δ 18.1 (q, $^1J_{C\text{-}H}$ = 128, 8 C, *C*H$_3$), 122.8 (dd, $^1J_{C\text{-}H}$ = 202, $^2J_{C\text{-}H}$ = 11, 4 C, imidazole *C*), 129.7 (d, $^1J_{C\text{-}H}$ = 162, 8 C, *C*$_6$H$_3$), 131.1 (d, $^1J_{C\text{-}H}$ = 161, 4 C, *C*$_6$H$_3$), 135.7 (s, 4 C, *C*$_6$H$_3$), 135.9 (s, 8 C, *C*$_6$H$_3$), 150.5 (s, 2 C, *C*=Se). IR data: 3172 (w), 3138 (w), 2915 (w), 2860 (w), 1558 (w), 1477 (m), 1447 (w), 1416 (w), 1363 (m), 1334 (w), 1299 (w), 1225 (w), 1168 (w), 1050 (vs), 1032 (vs), 972 (w),

924 (m), 779 (s), 749 (w), 689 (m), 614 (w). Anal. Calc. for $C_{38}H_{40}AgBF_4N_4Se_2$: C, 50.4; H, 4.5, N, 6.2. Found: C, 50.9; H, 4.6; N, 6.3%.

4.4.8. Synthesis of $[Ag(IXySe)_2]ClO_4$

A stirred suspension of IXySe (0.168 g, 0.473 mmol) in acetonitrile (6 mL) was treated dropwise with a solution of $AgClO_4$ (0.049 g, 0.236 mmol) in deionized water (2 mL), resulting in the immediate formation of a white solid suspended in a colorless solution. After stirring for 24 h, the solvent was removed under reduced pressure from the suspension to give a white solid, which was washed with pentane (10 mL), and dried *in vacuo* for 24 h (0.129 g, 60%). Mp = 297-300 °C (dec.). NMR data (in CD_2Cl_2): ^{1}H δ 2.04 (s, 24 H, C*H*$_3$), 7.20 (s, 4 H, imidazole *H*), 7.15-7.38 (m, 12 H, C$_6$*H*$_3$); ^{13}C δ 18.1 (q, $^1J_{C\text{-}H}$ = 128, 8 C, *C*H$_3$), 122.9 (dd, $^1J_{C\text{-}H}$ = 202, $^2J_{C\text{-}H}$ = 11, 4 C, imidazole *C*), 129.7 (d, $^1J_{C\text{-}H}$ = 161, 8 C, *C*$_6$H$_3$), 131.1 (d, $^1J_{C\text{-}H}$ = 162, 4 C, *C*$_6$H$_3$), 135.6 (s, 4 C, *C*$_6$H$_3$), 135.8 (s, 8 C, *C*$_6$H$_3$), 150.2 (s, 2 C, *C*=Se). IR data: 3172 (w), 3137 (w), 2976 (w), 2920 (w), 2861 (w), 1559 (w), 1473 (m), 1442 (w), 1360 (m), 1330 (w), 1299 (w), 1281 (w), 1224 (w), 1166 (w), 1083 (vs), 1037 (m), 998 (w), 971 (w), 943 (w), 837 (w), 794 (w), 778 (s), 765 (w), 726 (m), 684 (m), 620 (s). Anal. Calc. for $C_{38}H_{40}N_4AgClO_4Se_2$: C, 49.7; H, 4.4, N, 6.1. Found: C, 49.3; H, 4.4; N, 6.3%.

4.4.9. Synthesis of $[Ag(IXySe)_2]PF_6$

A solution of $AgPF_6$ (0.041 g, 0.162 mmol) in deionized water (~0.5 mL) was treated with a stirred suspension of IXySe (0.115 g, 0.324 mmol) in acetonitrile (5 mL), resulting in the immediate formation of a colorless solution. After stirring for 24 h, the solvent was removed under reduced pressure from the solution to give a white solid, which was

washed with diethyl ether (10 mL), and dried *in vacuo* for 27 h (0.085 g, 54%). Mp = 285-288 °C (dec.). NMR data (in CD_2Cl_2): ^{1}H δ 2.05 (s, 24 H, C*H*$_3$), 7.18 (s, 4 H, imidazole *H*), 7.20-7.39 (m, 12 H, C$_6$*H*$_3$); ^{13}C δ 18.1 (q, $^1J_{C-H}$ = 128, 8 C, *C*H$_3$), 122.8 (dd, $^1J_{C-H}$ = 202, $^2J_{C-H}$ = 11, 4 C, imidazole *C*), 129.7 (d, $^1J_{C-H}$ = 162, 8 C, *C*$_6$H$_3$), 131.1 (d, $^1J_{C-H}$ = 162, 4 C, *C*$_6$H$_3$), 135.6 (s, 4 C, *C*$_6$H$_3$), 135.8 (s, 8 C, *C*$_6$H$_3$), 150.4 (s, 2 C, *C*=Se). IR data: 3172 (w), 3143 (w), 2979 (w), 2922 (w), 2858 (w), 1558 (w), 1477 (w), 1444 (w), 1413 (w), 1361 (w), 1322 (w), 1298 (w), 1282 (w), 1226 (w), 1168 (w), 1131 (w), 1119 (w), 1080 (w), 1032 (w), 972 (w), 944 (w), 875 (w), 835 (vs), 827 (vs), 799 (m), 777 (s), 766 (m), 726 (m), 685 (m), 614 (w). ESI-MS (in MeCN): *m/z* = 819.39, $[Ag(IXySe)_2]^+$. Anal. Calc. for $C_{38}H_{40}AgF_6N_4PSe_2$: C, 47.4; H, 4.2, N, 5.8. Found: C, 48.0; H, 4.2; N, 5.9%.

4.4.10. Synthesis of $[Ag(IMesS)_2]NO_3$

A stirred suspension of IMesS (0.167 g, 0.496 mmol) in acetonitrile (5 mL) was treated with a solution of $AgNO_3$ (0.042 g, 0.247 mmol) in deionized water (1 mL), resulting in the immediate formation of a colorless solution. After stirring for 24 h, the solvent was removed under reduced pressure from the solution to give a white solid, which was washed with ether (10 mL) and dried *in vacuo* for 24 h (0.121 g, 58%). Mp = 325-327 °C (dec.). NMR data (in CD_2Cl_2): ^{1}H δ 1.99 (s, 24 H, C*H*$_3$), 2.31 (s, 12 H, C*H*$_3$), 7.02 (s, 8 H, C$_6$*H*$_2$), 7.06 (s, 4 H, imidazole *H*); ^{13}C δ 17.8 (q, $^1J_{C-H}$ = 128, 8 C, *C*H$_3$), 21.3 (q, $^1J_{C-H}$ = 127, 4 C, *C*H$_3$), 121.1 (dd, $^1J_{C-H}$ = 202, $^2J_{C-H}$ = 11, 4 C, imidazole *C*), 130.3 (d, $^1J_{C-H}$ = 159, 8 C, *C*$_6$H$_2$), 132.1 (s, 4 C, *C*$_6$H$_2$), 135.5 (q, $^2J_{C-H}$ = 6, 8 C, *C*$_6$H$_2$), 141.5 (q, $^2J_{C-H}$ = 6, 4 C, *C*$_6$H$_2$), 157.1 (s, 2 C, *C*=S). IR data: 3170 (w), 3119 (w), 3084 (w), 2972

(w), 2947 (w), 2917 (w), 2856 (w), 1629 (w), 1607 (w), 1558 (w), 1484 (m), 1441 (w), 1414 (w), 1375 (s), 1339 (vs), 1290 (w), 1253 (w), 1234 (m), 1168 (w), 1141 (w), 1100 (w), 1037 (w), 1016 (w), 983 (w), 926 (w), 856 (m), 828 (w), 745 (w), 738 (w), 698 (m), 645 (w), 608 (m). Anal. Calc. for $C_{42}H_{48}AgN_5O_3S_2$: C, 59.9; H, 5.7; N, 8.3. Found: C, 59.6; H, 5.8; N, 8.3%.

4.4.11. Synthesis of $[Ag(IMesS)_2]BF_4$

A stirred suspension of IMesS (0.142 g, 0.422 mmol) in acetonitrile (5 mL) was added to a solution of $AgBF_4$ (0.041 g, 0.211 mmol) in deionized water (0.5 mL), resulting in the immediate formation of a colorless solution. After stirring for 22 h, the solvent was removed under reduced pressure to give a white solid, which was washed with diethyl ether (10 mL), separated by filtration, and dried *in vacuo* for 24 h (0.129 g, 70%). Mp = 348-350 °C (dec.). NMR data (in CD_2Cl_2): ^{1}H δ 1.99 (s, 24 H, C*H*$_3$), 2.31 (s, 12 H, C*H*$_3$), 7.01 (s, 4 H, imidazole *H*), 7.02 (s, 8 H, C_6H_2); ^{13}C δ 17.8 (q, $^1J_{C\text{-}H}$ = 128, 8 C, *C*H$_3$), 21.4 (q, $^1J_{C\text{-}H}$ = 127, 4 C, *C*H$_3$), 121.0 (dd, $^1J_{C\text{-}H}$ = 202, $^2J_{C\text{-}H}$ = 11, 4 C, imidazole *C*), 130.4 (d, $^1J_{C\text{-}H}$ = 159, 8 C, *C*$_6$H$_2$), 132.1 (s, 4 C, *C*$_6$H$_2$), 135.5 (q, $^2J_{C\text{-}H}$ = 6, 8 C, *C*$_6$H$_2$), 141.5 (q, $^2J_{C\text{-}H}$ = 6, 4 C, *C*$_6$H$_2$), 157.4 (s, 2 C, *C*=S). IR data: 3177 (w), 3152 (w), 3094 (w), 2954 (w), 2919 (w), 2857 (w), 1607 (w), 1557 (w), 1484 (m), 1438 (w), 1415 (w), 1371 (s), 1281 (w), 1237 (m), 1165 (w), 1143 (w), 1120 (w), 1071 (s), 1042 (vs), 1028 (vs), 982 (m), 926 (m), 864 (m), 847 (s), 737 (s), 697 (s). ESI-MS (in MeCN): *m/z* = 781.36, $[Ag(IMesS)_2]^+$. Anal. Calc. for $C_{42}H_{48}AgBF_4N_4S_2$: C, 58.1; H, 5.6; N, 6.5. Found: C, 58.7; H, 5.6; N, 6.7%.

4.4.12. Synthesis of $[Ag(IMesS)_2]ClO_4$

A stirred solution of $AgClO_4$ (0.043 g, 0.209 mmol) in DI water (1 mL) was treated with a suspension of IMesS (0.138 g, 0.411 mmol) in acetonitrile (6 mL), resulting in the immediate formation of a white solid suspended in a colorless solution. The suspension was stirred for 24 h, concentrated under reduced pressure to *ca.* 1 mL, treated with diethyl ether (8 mL), and the product was isolated by filtration and dried *in vacuo* for 24 h (0.119 g, 66%). Mp = 316-318 °C (dec.). NMR data (in CD_2Cl_2): ^{1}H δ 2.00 (s, 24 H, C*H*$_3$), 2.31 (s, 12 H, C*H*$_3$), 7.02 (s, 12 H, imidazole *H* + C$_6$*H*$_2$); ^{13}C δ 17.8 (q, $^1J_{C\text{-}H}$ = 128, 8 C, *C*H$_3$), 21.3 (q, $^1J_{C\text{-}H}$ = 127, 4 C, *C*H$_3$), 121.1 (dd, $^1J_{C\text{-}H}$ = 202, $^2J_{C\text{-}H}$ = 11, 4 C, imidazole *C*), 130.4 (d, $^1J_{C\text{-}H}$ = 159, 8 C, *C*$_6$H$_2$), 132.1 (s, 4 C, *C*$_6$H$_2$), 135.5 (q, $^2J_{C\text{-}H}$ = 6, 8 C, *C*$_6$H$_2$), 141.5 (q, $^2J_{C\text{-}H}$ = 6, 4 C, *C*$_6$H$_2$), 157.2 (s, 2 C, *C*=S). IR data: 2973 (m), 2956 (m), 2865 (w), 1592 (w), 1519 (s), 1504 (m), 1476 (m), 1452 (m), 1399 (w), 1389 (w), 1361 (w), 1330 (m), 1319 (m), 1309 (s), 1299 (s), 1270 (m), 1255 (w), 1216 (m), 1207 (m), 1183 (w), 1150 (w), 1112 (w), 1102 (w), 1094 (s), 1079 (s), 1059 (s), 1048 (s), 960 (w), 939 (m), 931 (w), 921 (w), 853 (w), 842 (w), 809 (w), 800 (vs), 768 (w), 754 (s), 728 (w), 697 (w), 676 (w). Anal. Calc. for $C_{42}H_{48}AgClN_4O_4S_2$: C, 57.3; H, 5.5; N, 6.4. Found: C, 57.2; H, 5.5; N, 6.3%.

4.4.13. Synthesis of $[Ag(IMesS)_2]PF_6$

A stirred suspension of IMesS (0.115 g, 0.342 mmol) in acetonitrile (6 mL) was treated with a suspension of $AgPF_6$ (0.043 g, 0.170 mmol) in deionized H_2O (1 mL), resulting in the immediate formation of a colorless solution. After stirring for 24 h, the solution concentrated under reduced pressure to *ca.* 1 mL and treated with diethyl ether (8 mL),

leading to the separation of the product, which was isolated by filtration and dried *in vacuo* for 24 h (0.120 g, 76%). Mp = 319-322 °C (dec). NMR data (in CD_2Cl_2): ^{1}H δ 1.99 (s, 24 H, C*H*$_3$), 2.31 (s, 12 H, C*H*$_3$), 7.00 (s, 4 H, imidazole *H*), 7.02 (s, 8 H, C_6H_2); ^{13}C δ 17.8 (q, $^1J_{C\text{-}H}$ = 128, 8 C, *C*H$_3$), 21.4 (q, $^1J_{C\text{-}H}$ = 127, 4 C, *C*H$_3$), 121.0 (dd, $^1J_{C\text{-}H}$ = 202, $^2J_{C\text{-}H}$ = 11, 4 C, imidazole *C*), 130.4 (d, $^1J_{C\text{-}H}$ = 159, 8 C, *C*$_6$H$_2$), 132.1 (s, 4 C, *C*$_6$H$_2$), 135.5 (q, $^2J_{C\text{-}H}$ = 6, 8 C, *C*$_6$H$_2$), 141.6 (q, $^2J_{C\text{-}H}$ = 6, 4 C, *C*$_6$H$_2$), 157.3 (s, 2 C, *C*=S). IR data: 3179 (w), 3149 (w), 2972 (w), 2917 (w), 1607 (w), 1559 (w), 1484 (m), 1440 (w), 1415 (w), 1372 (s), 1292 (w), 1236 (m), 1167 (w), 1143 (w), 1075 (w), 1066 (w), 1038 (m), 984 (w), 929 (w), 864 (sh), 828 (vs), 739 (m), 693 (m). Anal. Calc. for $C_{42}H_{48}AgF_6N_4PS_2$: C, 54.5; H, 5.2; N, 6.1. Found: C, 54.7; H, 5.3; N, 6.0%.

4.4.14. Synthesis of [Ag(IMesSe)$_2$]NO$_3$

A stirred suspension of IMesSe (0.181 g, 0.472 mmol) in acetonitrile (6 mL) was treated with a solution of $AgNO_3$ (0.040 g, 0.235 mmol) in deionized H_2O (1 mL), resulting in the immediate formation of a colorless solution. After stirring for 24 h, the solution was concentrated under reduced pressure to *ca.* 1 mL and treated with diethyl ether (8 mL), leading to the separation of the product, which was isolated by filtration and dried *in vacuo* for 24 h (0.214 g, 97%). Mp = 291-294 °C (dec). NMR data (in CD_2Cl_2): ^{1}H δ 1.98 (s, 24 H, C*H*$_3$), 2.33 (s, 12 H, C*H*$_3$), 7.01 (s, 8 H, C_6H_2), 7.20 (s, 4 H, imidazole *H*); ^{13}C δ 17.9 (q, $^1J_{C\text{-}H}$ = 128, 8 C, *C*H$_3$), 21.4 (q, $^1J_{C\text{-}H}$ = 127, 4 C, *C*H$_3$), 123.0 (dd, $^1J_{C\text{-}H}$ = 202, $^2J_{C\text{-}H}$ = 11, 4 C, imidazole *C*), 130.3 (d, $^1J_{C\text{-}H}$ = 159, 8 C, *C*$_6$H$_2$), 133.0 (s, 4 C, *C*$_6$H$_2$), 135.3 (q, $^2J_{C\text{-}H}$ = 6, 8 C, *C*$_6$H$_2$), 141.5 (q, $^2J_{C\text{-}H}$ = 6, 4 C, *C*$_6$H$_2$), 150.3 (s, 2 C, *C*=Se). IR data: 3157 (w), 3118 (w), 3084 (w), 2972 (w), 2915 (w), 1606 (w), 1561 (w), 1483 (m),

1447 (m), 1415 (w), 1379 (sh), 1364 (s), 1341 (vs), 1234 (s), 1167 (w), 1134 (w), 1114 (m), 1103 (m), 1079 (m), 1032 (m), 979 (w), 961 (w), 927 (m), 903 (w), 855 (s), 831 (w), 746 (m), 734 (s), 689 (m), 650 (w), 625 (w), 593 (w), 573 (s), 557 (m), 549 (m), 543(m). Anal. Calc. for $C_{42}H_{48}AgN_5O_3Se_2$: C, 53.9; H, 5.2; N, 7.5. Found: C, 53.9; H, 5.2; N, 7.5%.

4.4.15. Synthesis of $[Ag(IMesSe)_2]BF_4$

A stirred suspension of $AgBF_4$ (0.033 g, 0.170 mmol) in DI water (~0.5 mL) was treated with a suspension of IMesSe (0.132 g, 0.344 mmol) in acetonitrile (5 mL), resulting in the immediate formation of a colorless solution, which was stirred for 24 h. Concentration of the solution under reduced pressure to *ca.* 1 mL and addition of diethyl ether (8 mL) led to the separation of the white product, which was isolated by filtration and dried *in vacuo* for 25 h (0.120 g, 72%). Mp = 312-315 °C (dec). NMR data (in CD_2Cl_2): ^{1}H δ 1.99 (s, 24 H, C*H*$_3$), 2.33 (s, 12 H, C*H*$_3$), 7.02 (s, 8 H, C_6H_2), 7.15 (s, 4 H, imidazole *H*); ^{13}C δ 17.9 (q, $^1J_{C\text{-}H}$ = 127, 8 C, *C*H$_3$), 21.5 (q, $^1J_{C\text{-}H}$ = 127, 4 C, *C*H$_3$), 122.9 (dd, $^1J_{C\text{-}H}$ = 202, $^2J_{C\text{-}H}$ = 11, 4 C, imidazole *C*), 130.4 (d, $^1J_{C\text{-}H}$ = 159, 8 C, C_6H_2), 133.1 (s, 4 C, C_6H_2), 135.4 (q, $^2J_{C\text{-}H}$ = 6, 8 C, C_6H_2), 141.6 (q, $^2J_{C\text{-}H}$ = 6, 4 C, C_6H_2), 150.6 (s, 2 C, *C*=Se). IR data: 3187 (w), 3163 (w), 3141 (w), 2973 (w), 2943 (w), 2917 (w), 2855 (w), 1607 (w), 1561 (w), 1483 (m), 1448 (w), 1417 (w), 1366 (m), 1342 (w), 1288 (w), 1234 (m), 1071 (sh), 1050 (vs), 1035 (vs), 928 (w), 856 (m), 744 (m), 689 (m), 649 (w). ESI-MS (in MeCN): *m/z* = 875.70, $[Ag(IMesSe)_2]^+$. Anal. Calc. for $C_{42}H_{48}AgBF_4N_4Se_2$: C, 52.5; H, 5.0; N, 5.8. Found: C, 52.7; H, 5.0; N, 5.9%.

4.4.16. Synthesis of $[Ag(IMesSe)_2]ClO_4$

A stirred suspension of $AgClO_4$ (0.050 g, 0.241 mmol) in DI water (1 mL) was treated with a suspension of IMesS (0.184 g, 0.480 mmol) in acetonitrile (6 mL), resulting in the immediate formation of a white solid suspended in a colorless solution. The suspension was stirred for 24 h, concentrated under reduced pressure to *ca.* 1 mL, treated with diethyl ether (8 mL), and the product was isolated by filtration and dried *in vacuo* for 24 h (0.134 g, 57%). Mp = 313-316 °C (dec). NMR data (in CD_2Cl_2): ^{1}H δ 2.00 (s, 24 H, C*H*$_3$), 2.34 (s, 12 H, C*H*$_3$), 7.02 (s, 8 H, C$_6$*H*$_2$), 7.16 (s, 4 H, imidazole *H*); ^{13}C δ 17.9 (q, $^1J_{C\text{-}H}$ = 128, 8 C, *C*H$_3$), 21.4 (q, $^1J_{C\text{-}H}$ = 127, 4 C, *C*H$_3$), 122.8 (dd, $^1J_{C\text{-}H}$ = 202, $^2J_{C\text{-}H}$ = 11, 4 C, imidazole *C*), 130.3 (d, $^1J_{C\text{-}H}$ = 159, 8 C, *C*$_6$H$_2$), 133.1 (s, 4 C, *C*$_6$H$_2$), 135.4 (q, $^2J_{C\text{-}H}$ = 6, 8 C, *C*$_6$H$_2$), 141.4 (q, $^2J_{C\text{-}H}$ = 6, 4 C, *C*$_6$H$_2$), 150.7 (s, 2 C, *C*=Se). IR data: 3184 (w), 3157 (w), 3134 (w), 3100 (w), 2970 (w), 2944 (w), 2915 (w), 2856 (w), 2734 (w), 1606 (w), 1561 (w), 1483 (m), 1446 (w), 1415 (w), 1365 (m), 1341 (w), 1297 (w), 1233 (m), 1166 (w), 1132 (w), 1090 (s), 1075 (vs), 1032 (m), 978 (w), 961 (w), 927 (w), 854 (m), 743 (m), 736 (sh), 722 (w), 689 (m), 648 (w), 622 (s), 593 (m), 572 (m), 537 (w), 525 (w). Anal. Calc. for $C_{42}H_{48}AgClN_4O_4Se_2$: C, 51.8; H, 5.0; N, 5.8. Found: C, 52.5; H, 5.20; N, 5.9%.

4.4.17. Synthesis of $[Ag(IMesSe)_2]PF_6$

A stirred solution of $AgPF_6$ (0.049 g, 0.194 mmol) in DI water (~0.5 mL) was treated with a suspension of IMesSe (0.148 g, 0.386 mmol) in acetonitrile (5 mL), resulting in the immediate formation of a white solid suspended in a colorless solution. The suspension was stirred for 24 h, concentrated under reduced pressure to *ca.* 1 mL, treated

with diethyl ether (8 mL), and the product was isolated by filtration and dried *in vacuo* for 24 h (0.118 g, 59%). Mp = 280-283 °C (dec). NMR data (in CD_2Cl_2): ^{1}H δ 2.00 (s, 24 H, C*H*$_3$), 2.34 (s, 12 H, C*H*$_3$), 7.03 (s, 8 H, C$_6$*H*$_2$), 7.14 (s, 4 H, imidazole *H*); ^{13}C δ 17.9 (q, $^1J_{C\text{-}H}$ = 128, 8 C, *C*H$_3$), 21.4 (q, $^1J_{C\text{-}H}$ = 127, 4 C, *C*H$_3$), 122.8 (dd, $^1J_{C\text{-}H}$ = 202, $^2J_{C\text{-}H}$ = 11, 4 C, imidazole *C*), 130.3 (d, $^1J_{C\text{-}H}$ = 159, 8 C, *C*$_6$H$_2$), 133.1 (s, 4 C, *C*$_6$H$_2$), 135.4 (q, $^2J_{C\text{-}H}$ = 6, 8 C, *C*$_6$H$_2$), 141.5 (q, $^2J_{C\text{-}H}$ = 6, 4 C, *C*$_6$H$_2$), 150.7 (s, 2 C, *C*=Se). IR data: 3183 (w), 3156 (w), 3025 (w), 2972 (w), 2946 (w), 2918 (w), 2857 (w), 1607 (w), 1557 (w), 1484 (m), 1440 (w), 1413 (w), 1377 (w), 1361 (m), 1342 (m), 1326 (w), 1295 (w), 1233 (m), 1164 (w), 1137 (w), 1031 (w), 978 (w), 930 (w), 830 (vs), 735 (m), 691 (m). Anal. Calc. for $C_{42}H_{48}AgF_6N_4PSe_2$: C, 49.5; H, 4.7; N, 5.5. Found: C, 50.0; H, 4.9; N, 5.6%.

4.4.18. Synthesis of [Ag(IDippS)$_2$]NO$_3$

A stirred suspension of IDippS (0.200 g, 0.475 mmol) in acetonitrile (5 mL) was treated with a solution of $AgNO_3$ (0.040 g, 0.235 mmol) in deionized H_2O (1 mL). After stirring for 24 h, the solvent was removed under reduced pressure from the resulting solution to give a white solid, which was washed with pentane (10 mL), separated by filtration and dried *in vacuo* for 24 h (0.198 g, 76%). Mp = 293-295 °C (dec.). NMR data (in CD_2Cl_2): ^{1}H δ 1.15 [d, $^3J_{H\text{-}H}$ = 6.9, 24 H, CH(C*H*$_3$)$_2$], 1.21 [d, $^3J_{H\text{-}H}$ = 6.9, 24 H, CH(C*H*$_3$)$_2$], 2.39 [septet, $^3J_{H\text{-}H}$ = 6.8, 8 H, C*H*(CH$_3$)$_2$], 7.12 (s, 4 H, imidazole *H*), 7.28 (d, $^3J_{H\text{-}H}$ = 7.7, 8 H, C$_6$*H*$_3$), 7.45 (t, $^3J_{H\text{-}H}$ = 7.8, 4 H, C$_6$*H*$_3$); ^{13}C δ 23.7 [q, $^1J_{C\text{-}H}$ = 127, 8 C, CH(*C*H$_3$)$_2$], 24.2 [q, $^1J_{C\text{-}H}$ = 127, 8 C, CH(*C*H$_3$)$_2$], 29.3 [d, $^1J_{C\text{-}H}$ = 127, 8 C, *C*H(CH$_3$)$_2$], 122.0 (dd, $^1J_{C\text{-}H}$ = 202, $^2J_{C\text{-}H}$ = 11, 4 C, imidazole *C*), 125.4 (d, $^1J_{C\text{-}H}$ = 160, 8 C, *C*$_6$H$_3$), 131.8 (d, $^1J_{C\text{-}H}$ =

162, 4 C, C_6H_3),132.0 (s, 4 C, C_6H_3), 146.3 (s, 8 C, C_6H_3), 160.3 (s, 2 C, *C*=S). IR data: 3159 (w), 3105 (w), 3061 (w), 2963 (m), 2928 (w), 2869 (w), 1593 (w), 1556 (w), 1457 (m), 1421 (m), 1361 (s), 1323 (s), 1272 (w), 1254 (w), 1214 (w), 1179 (w), 1120 (w), 1102 (w), 1059 (m), 1041 (w), 981 (w), 935 (m), 829 (w), 800 (s), 767 (m), 756 (m), 750 (m), 740 (m), 696 (m). Anal. Calc. for $C_{54}H_{72}AgN_5O_3S_2$: C, 64.1; H, 7.2; N, 6.9. Found: C, 63.9; H, 7.0; N, 6.8%.

4.4.19. Synthesis of $[Ag(IDippS)_2]BF_4$

A stirred suspension of IDippS (0.178 g, 0.423 mmol) in acetonitrile (5 mL) was treated with a solution of $AgBF_4$ (0.041 g, 0.211 mmol) in deionized H_2O (1 mL). After stirring for 24 h, the solvent was removed under reduced pressure from the resulting solution to give a white solid, which was washed with ether (10 mL) and dried *in vacuo* for 24 h (0.129 g, 59%). Mp = 331-334 °C (dec.). NMR data (in CD_2Cl_2): ^{1}H δ 1.15 [d, $^3J_{H-H}$ = 6.6, 24 H, CH(C*H*$_3$)$_2$], 1.20 [d, $^3J_{H-H}$ = 7.2, 24 H, CH(C*H*$_3$)$_2$], 2.37 [septet, $^3J_{H-H}$ = 6.9, 8 H, C*H*(CH$_3$)$_2$], 7.05 (s, 4 H, imidazole *H*), 7.25-7.49 (m, 12 H, C_6H_3); ^{13}C δ 23.7 [q, $^1J_{C-H}$ = 127, 8 C, CH(*C*H$_3$)$_2$], 24.2 [q, $^1J_{C-H}$ = 127, 8 C, CH(*C*H$_3$)$_2$], 29.3 [d, $^1J_{C-H}$ = 127, 8 C, *C*H(CH$_3$)$_2$], 122.0 (dd, $^1J_{C-H}$ = 202, $^2J_{C-H}$ = 11, 4 C, imidazole *C*), 125.5 (d, $^1J_{C-H}$ = 160, 8 C, C_6H_3), 131.9 (d, $^1J_{C-H}$ = 162, 4 C, C_6H_3),131.9 (s, 4 C, C_6H_3), 146.3 (s, 8 C, C_6H_3), 160.3 (s, 2 C, *C*=S). IR data: 3174 (w), 2962 (w), 2930 (w), 2871 (w), 1592 (w), 1560 (w), 1470 (w), 1458 (w), 1422 (w), 1377 (m), 1364 (m), 1331 (w), 1286 (w), 1256 (w), 1215 (w), 1182 (w), 1141 (w), 1099 (w), 1086 (w), 1050 (vs), 1038 (sh), 982 (w), 942 (w), 809 (m), 800 (w), 769 (w), 758 (w), 742 (w), 694 (w), 643 (w), 618 (w). Anal. Calc. for $C_{54}H_{72}AgBF_4N_4S_2$: C, 62.6; H, 7.0; N, 5.4. Found: C, 62.5; H, 7.0; N, 5.2%.

4.4.20. Synthesis of $[Ag(IDippS)_2]ClO_4$

A stirred suspension of IDippS (0.152 g, 0.361 mmol) in acetonitrile (5 mL) was treated with a solution of $AgClO_4$ (0.036 g, 0.174 mmol) in the same solvent (5 mL). After stirring for 24 h, the solvent was removed under reduced pressure from the resulting solution to give a white solid, which was washed with pentane (10 mL), separated by filtration, and dried *in vacuo* for 24 h (0.190 g, 93%). Mp = 317-320 °C (dec.). NMR data (in CD_2Cl_2): ^{1}H δ 1.15 [d, $^3J_{H-H}$ = 6.9, 24 H, CH(C*H*$_3$)$_2$], 1.21 [d, $^3J_{H-H}$ = 6.9, 24 H, CH(C*H*$_3$)$_2$], 2.38 [septet, $^3J_{H-H}$ = 6.9, 8 H, C*H*(CH$_3$)$_2$], 7.08 (s, 4 H, imidazole *H*), 7.28 (d, $^3J_{H-H}$ = 7.7, 8 H, C$_6$*H*$_3$), 7.46 (t, $^3J_{H-H}$ = 7.8, 4 H, C$_6$*H*$_3$); ^{13}C δ 23.7 [q, $^1J_{C-H}$ = 127, 8 C, CH(*C*H$_3$)$_2$], 24.2 [q, $^1J_{C-H}$ = 127, 8 C, CH(*C*H$_3$)$_2$], 29.3 [d, $^1J_{C-H}$ = 127, 8 C, *C*H(CH$_3$)$_2$], 122.0 (dd, $^1J_{C-H}$ = 202, $^2J_{C-H}$ = 11, 4 C, imidazole *C*), 125.5 (d, $^1J_{C-H}$ = 160, 8 C, *C*$_6$H$_3$), 131.9 (d, $^1J_{C-H}$ = 162, 4 C, *C*$_6$H$_3$), 131.9 (s, 4 C, *C*$_6$H$_3$), 146.3 (s, 8 C, *C*$_6$H$_3$), 160.3 (s, 2 C, *C*=S). IR data: 3165 (w), 3127 (w), 3063 (w), 2962 (m), 2928 (w), 2869 (w), 1591 (w), 1558 (w), 1465 (m), 1457 (m), 1422 (w), 1373 (s), 1362 (s), 1328 (w), 1273 (w), 1255 (w), 1215 (w), 1181 (w), 1139 (w), 1094 (vs), 1074 (vs), 1043 (sh), 982 (w), 935 (m), 801 (s), 769 (m), 757 (m), 738 (m), 694 (m), 621 (s). ESI-MS (in MeCN): *m/z* = 949.92, $[Ag(IDippS)_2]^+$. Anal. Calc. for $C_{54}H_{72}AgClN_4O_4S_2$: C, 61.9; H, 6.9; N, 5.3. Found: C, 62.1; H, 7.0; N, 5.2%.

4.4.21. Synthesis of $[Ag(IDippS)_2]PF_6$

A stirred suspension of IDippS (0.166 g, 0.395 mmol) in acetonitrile (5 mL) was treated with a solution of $AgPF_6$ (0.050 g, 0.198 mmol) in the same solvent (5 mL). After stirring for 24 h, the solvent was removed under reduced pressure from the resulting

solution to give a white solid, which was washed with pentane (10 mL), separated by filtration and dried *in vacuo* for 24 h (0.185 g, 84%). Mp = 295-298 °C (dec.). NMR data (in CD_2Cl_2): ^{1}H δ 1.16 [d, $^3J_{H-H}$ = 6.9, 24 H, CH(C*H*$_3$)$_2$], 1.22 [d, $^3J_{H-H}$ = 6.9, 24 H, CH(C*H*$_3$)$_2$], 2.39 [septet, $^3J_{H-H}$ = 6.8, 8 H, C*H*(CH$_3$)$_2$], 7.07 (s, 4 H, imidazole *H*), 7.29 (d, $^3J_{H-H}$ = 7.7, 8 H, C$_6$*H*$_3$), 7.46 (t, $^3J_{H-H}$ = 7.8, 4 H, C$_6$*H*$_3$); ^{13}C δ 23.7 [q, $^1J_{C-H}$ = 127, 8 C, CH(*C*H$_3$)$_2$], 24.2 [q, $^1J_{C-H}$ = 127, 8 C, CH(*C*H$_3$)$_2$], 29.4 [d, $^1J_{C-H}$ = 127, 8 C, *C*H(CH$_3$)$_2$], 122.0 (dd, $^1J_{C-H}$ = 202, $^2J_{C-H}$ = 11, 4 C, imidazole *C*), 125.5 (d, $^1J_{C-H}$ = 160, 8 C, *C*$_6$H$_3$), 131.9 (d, $^1J_{C-H}$ = 162, 4 C, *C*$_6$H$_3$),131.9 (s, 4 C, *C*$_6$H$_3$), 146.3 (s, 8 C, *C*$_6$H$_3$), 160.3 (s, 2 C, *C*=S). IR data: 3180 (w), 3155 (w), 2964 (m), 2928 (w), 2870 (w), 1592 (w), 1560 (w), 1522 (w), 1457 (m), 1423 (w), 1375 (m), 1364 (m), 1328 (w), 1256 (w) 1215 (w), 1181 (w), 1141 (w), 1122 (w), 1103 (w), 1059 (w), 1043 (w), 982 (w), 936 (w), 836 (vs), 800 (m), 767 (m), 756 (m), 737 (m), 694 (m). Anal. Calc. for $C_{54}H_{72}AgF_6N_4PS_2$: C, 59.3; H, 6.6; N, 5.1. Found: C, 59.1; H, 6.7; N, 5.1%.

4.4.22. Synthesis of [Ag(IDippS)$_2$]SbF$_6$

A stirred suspension of IDippS (0.209 g, 0.496 mmol) in acetonitrile (5 mL) was treated with a solution of $AgSbF_6$ (0.080 g, 0.233 mmol) in deionized H_2O (1 mL). After stirring for 24 h, the solvent was removed under reduced pressure from the resulting solution to give a white solid, which was washed with pentane (10 mL), separated by filtration, and dried *in vacuo* for 24 h (0.198 g, 71%). Mp = 317-320 °C (dec.). NMR data (in CD_2Cl_2): ^{1}H δ 1.15 [d, $^3J_{H-H}$ = 6.9, 24 H, CH(C*H*$_3$)$_2$], 1.21 [d, $^3J_{H-H}$ = 6.9, 24 H, CH(C*H*$_3$)$_2$], 2.38 [septet, $^3J_{H-H}$ = 6.9, 8 H, C*H*(CH$_3$)$_2$], 7.07 (s, 4 H, imidazole *H*), 7.28 (d, $^3J_{H-H}$ = 7.7, 8 H, C$_6$*H*$_3$), 7.46 (t, $^3J_{H-H}$ = 7.7, 4 H, C$_6$*H*$_3$); ^{13}C δ 23.7 [q, $^1J_{C-H}$ = 127, 8 C, CH(*C*H$_3$)$_2$], 24.2

[q, $^{1}J_{C\text{-}H}$ = 127, 8 C, CH(*C*H_3)$_2$], 29.4 [d, $^{1}J_{C\text{-}H}$ = 127, 8 C, *C*H(CH$_3$)$_2$], 122.0 (dd, $^{1}J_{C\text{-}H}$ = 202, $^{2}J_{C\text{-}H}$ = 11, 4 C, imidazole *C*), 125.5 (d, $^{1}J_{C\text{-}H}$ = 158, 8 C, *C*$_6$H$_3$), 131.9 (d, $^{1}J_{C\text{-}H}$ = 162, 4 C, *C*$_6$H$_3$), 131.9 (s, 4 C, *C*$_6$H$_3$), 146.3 (s, 8 C, *C*$_6$H$_3$), 160.3 (s, 2 C, *C*=S). IR data: 3177 (w), 3151 (w), 2962 (w), 2929 (w), 2870 (w), 1590 (w), 1560 (w), 1458 (m), 1421 (w), 1375 (s), 1363 (s), 1330 (w), 1289 (w), 1273 (w), 1256 (w), 1214 (w), 1183 (w), 1141 (w), 1124 (w), 1105 (w), 1061 (w), 1043 (w), 982 (w), 939 (w), 800 (m), 769 (w), 759 (m), 740 (w), 730 (m), 691 (m), 661 (s), 629 (vs). Anal. Calc. for $C_{54}H_{72}AgF_6N_4SbS_2$: C, 54.7; H, 6.1; N, 4.7. Found: C, 54.9; H, 6.3; N, 4.7%.

4.4.23. Synthesis of [Ag(IDippSe)$_2$]NO$_3$

A stirred suspension of IDippSe (0.220 g, 0.471 mmol) in acetonitrile (5 mL) was treated with a solution of $AgNO_3$ (0.040 g, 0.235 mmol) in deionized H_2O (1 mL). After stirring for 24 h, the solvent was removed under reduced pressure from the resulting solution to give a white solid, which was washed with pentane (10 mL), separated by filtration, and dried *in vacuo* for 24 h (0.227 g, 79%). Mp = 306-309 °C (dec.). NMR data (in CD_3CN): ^{1}H δ 1.12 [d, $^{3}J_{H\text{-}H}$ = 6.9, 24 H, CH(C*H*$_3$)$_2$], 1.23 [d, $^{3}J_{H\text{-}H}$ = 6.9, 24 H, CH(C*H*$_3$)$_2$], 2.35 [septet, $^{3}J_{H\text{-}H}$ = 6.9, 8 H, C*H*(CH$_3$)$_2$], 7.29-7.50 (m, 12 H, C$_6$*H*$_3$), 7.45 (s, 4 H, imidazole *H*); ^{13}C δ 23.8 [q, $^{1}J_{C\text{-}H}$ = 126, 8 C, CH(*C*H$_3$)$_2$], 24.3 [q, $^{1}J_{C\text{-}H}$ = 127, 8 C, CH(*C*H$_3$)$_2$], 29.9 [d, $^{1}J_{C\text{-}H}$ = 128, 8 C, *C*H(CH$_3$)$_2$], 125.0 (dd, $^{1}J_{C\text{-}H}$ = 204, $^{2}J_{C\text{-}H}$ = 11, 4 C, imidazole *C*), 126.0 (d, $^{1}J_{C\text{-}H}$ = 160, 8 C, *C*$_6$H$_3$), 132.3 (d, $^{1}J_{C\text{-}H}$ = 162, 4 C, *C*$_6$H$_3$),133.7 (s, 4 C, *C*$_6$H$_3$), 146.9 (s, 8 C, *C*$_6$H$_3$), 154.1 (s, 2 C, *C*=Se). IR data: 3164 (w), 3075 (w), 2962 (m), 2928 (w), 2869 (w), 1627 (w), 1591 (w), 1556 (w), 1457 (m), 1421 (m), 1385 (w), 1343 (vs), 1255 (w), 1212 (w), 1180 (w), 1148 (w), 1119 (w), 1061 (w), 1042 (w),

974 (w), 937 (w), 830 (w), 807 (m), 798 (m), 768 (w), 755 (m), 746 (m), 689 (m). Anal. Calc. for $C_{54}H_{72}AgN_5O_3Se_2$: C, 58.7; H, 6.6; N, 6.3. Found: C, 58.4; H, 6.7; N, 6.4%.

4.4.24. Synthesis of $[Ag(IDippSe)_2]BF_4$

A stirred suspension of IDippSe (0.223 g, 0.477 mmol) in acetonitrile (5 mL) was treated with a solution of $AgBF_4$ (0.046 g, 0.236 mmol) in deionized water (~0.5 mL), resulting in the immediate formation of a colorless solution. After stirring for 25 h, the solvent was removed under reduced pressure to give a white solid, which was washed with diethyl ether (10 mL) and dried *in vacuo* for 23 h (0.185 g, 69%). Mp = 327-330 °C (dec.). NMR data (in CD_2Cl_2): ^{1}H δ 1.14 [d, $^3J_{H-H}$ = 6.6, 24 H, CH(C*H*$_3$)$_2$], 1.24 [d, $^3J_{H-H}$ = 6.6, 24 H, CH(C*H*$_3$)$_2$], 2.37 [septet, $^3J_{H-H}$ = 6.9, 8 H, C*H*(CH$_3$)$_2$], 7.19 (s, 4 H, imidazole H), 7.25-7.53 (m, 12 H, C$_6$*H*$_3$); ^{13}C δ 23.7 [q, $^1J_{C-H}$ = 127, 8 C, CH(*C*H$_3$)$_2$], 24.4 [q, $^1J_{C-H}$ = 127, 8 C, CH(*C*H$_3$)$_2$], 29.4 [d, $^1J_{C-H}$ = 128, 8 C, *C*H(CH$_3$)$_2$], 123.8 (dd, $^1J_{C-H}$ = 202, $^2J_{C-H}$ = 11, 4 C, imidazole *C*), 125.5 (d, $^1J_{C-H}$ = 160, 8 C, *C*$_6$H$_3$), 131.8 (d, $^1J_{C-H}$ = 162, 4 C, *C*$_6$H$_3$), 132.9 (s, 4 C, *C*$_6$H$_3$), 146.1 (s, 8 C, *C*$_6$H$_3$), 154.5 (s, 2 C, *C*=Se). IR data: 3172 (w), 3146 (w), 3088 (w), 2964 (m), 2929 (w), 2871 (w), 1593 (w), 1557 (w), 1458 (m), 1423 (w), 1385 (w), 1365 (m), 1352 (m), 1329 (w), 1256 (w), 1214 (w), 1182 (w), 1118 (w), 1051 (vs), 976 (w), 944 (w), 937 (w), 801 (m), 768 (m), 756 (m), 744 (m), 691 (m). ESI-MS (in MeCN): *m/z* = 1043.86, $[Ag(IDippSe)_2]^+$. Anal. Calc. for $C_{54}H_{72}AgBF_4N_4Se_2$: C, 57.4; H, 6.4; N, 5.0. Found: C, 57.6; H, 6.4; N, 5.0%.

4.4.25. Synthesis of $[Ag(IDippSe)_2]ClO_4$

A stirred suspension of IDippSe (0.182 g, 0.389 mmol) in acetonitrile (5 mL) was treated with a solution of $AgClO_4$ (0.040 g, 0.193 mmol) in deionized H_2O (1 mL). After stirring

for 24 h, the solvent was removed under reduced pressure from the resulting solution to give a white solid, which was washed with pentane (10 mL), separated by filtration and dried *in vacuo* for 24 h (0.156 g, 69%). Mp = 316-319 °C (dec.). NMR data (in CD_2Cl_2): ^{1}H δ 1.14 [d, $^3J_{HH}$ = 6.9, 24 H, CH(C*H*$_3$)$_2$], 1.25 [d, $^3J_{HH}$ = 6.9, 24 H, CH(C*H*$_3$)$_2$], 2.37 [septet, $^3J_{HH}$ = 6.8, 8 H, C*H*(CH$_3$)$_2$], 7.23 (s, 4 H, imidazole H), 7.29 (d, $^3J_{HH}$ = 7.7, 8 H, C$_6$*H*$_3$), 7.48 (t, $^3J_{HH}$ = 7.8, 4 H, C$_6$*H*$_3$); ^{13}C δ 23.7 [q, $^1J_{C-H}$ = 127, 8 C, CH(*C*H$_3$)$_2$], 24.3 [q, $^1J_{C-H}$ = 127, 8 C, CH(*C*H$_3$)$_2$], 29.4 [d, $^1J_{C-H}$ = 127, 8 C, *C*H(CH$_3$)$_2$], 123.9 (dd, $^1J_{C-H}$ = 202, $^2J_{C-H}$ = 11, 4 C, imidazole *C*), 125.5 (d, $^1J_{C-H}$ = 162, 8 C, *C*$_6$H$_3$), 131.8 (d, $^1J_{C-H}$ = 163, 4 C, *C*$_6$H$_3$), 132.9 (s, 4 C, *C*$_6$H$_3$), 146.1 (s, 8 C, *C*$_6$H$_3$), 154.4 (s, 2 C, *C*=Se). IR data: 3165 (w), 3125 (w), 3085 (w), 3055 (w), 2963 (m), 2928 (w), 2869 (w), 1592 (w), 1556 (w), 1457 (m), 1422 (m), 1384 (m), 1364 (m), 1350 (m), 1328 (m), 1273 (w), 1255 (w), 1213 (w), 1181 (w), 1094 (vs), 1073 (vs), 975 (w), 943 (m), 936 (m), 800 (s), 767 (m), 755 (s), 743 (m), 690 (m). Anal. Calc. for $C_{54}H_{72}AgClN_4O_4Se_2$: C, 56.8; H, 6.4; N, 4.9. Found: C, 57.0; H, 6.5; N, 5.0%.

4.4.26. Synthesis of [Ag(IDippSe)$_2$]PF$_6$

A stirred suspension of IDippSe (0.185 g, 0.395 mmol) in acetonitrile (5 mL) was treated with a solution of $AgPF_6$ (0.051 g, 0.202 mmol) in the same solvent (5 mL). After stirring for 24 h, the solvent was removed under reduced pressure from the resulting solution to give a white solid, which was washed with pentane (10 mL), separated by filtration, and dried *in vacuo* for 24 h (0.161 g, 68%). Mp = 304-307 °C (dec.). NMR data (in CD_2Cl_2): ^{1}H δ 1.14 [d, $^3J_{H-H}$ = 6.9, 24 H, CH(C*H*$_3$)$_2$], 1.25 [d, $^3J_{H-H}$ = 6.9, 24 H, CH(C*H*$_3$)$_2$], 2.36 [septet, $^3J_{H-H}$ = 6.9, 8 H, C*H*(CH$_3$)$_2$], 7.19 (s, 4 H, imidazole *H*), 7.29 (d,

$^{3}J_{H\text{-}H}$ = 7.8, 8 H, C_6H_3), 7.48 (t, $^{3}J_{H\text{-}H}$ = 7.8, 4 H, C_6H_3); ^{13}C δ 23.7 [q, $^{1}J_{C\text{-}H}$ = 127, 8 C, $CH(CH_3)_2$], 24.3 [q, $^{1}J_{C\text{-}H}$ = 127, 8 C, $CH(CH_3)_2$], 29.4 [d, $^{1}J_{C\text{-}H}$ = 127, 8 C, $CH(CH_3)_2$], 123.8 (dd, $^{1}J_{C\text{-}H}$ = 202, $^{2}J_{C\text{-}H}$ = 11, 4 C, imidazole *C*), 125.5 (d, $^{1}J_{C\text{-}H}$ = 160, 8 C, C_6H_3), 131.8 (d, $^{1}J_{C\text{-}H}$ = 160, 4 C, C_6H_3), 132.9 (s, 4 C, C_6H_3), 146.2 (s, 8 C, C_6H_3), 154.5 (s, 2 C, *C*=Se). IR data: 3179 (w), 3154 (w), 2963 (w), 2928 (w), 2870 (w), 1592 (w), 1557 (w), 1458 (w), 1423 (w), 1384 (w), 1365 (w), 1353 (w), 1328 (w), 1256 (w), 1214 (w), 1180 (w), 1120 (w), 1060 (w), 1042 (w), 976 (w), 936 (w), 876 (w), 837 (vs), 800 (m), 766 (w), 755 (m), 741 (m), 689 (w), 640 (w). Anal. Calc. for $C_{54}H_{72}AgF_6N_4PSe_2$: C, 54.6; H, 6.1; N, 4.7. Found: C, 54.5; H, 6.1; N, 4.7%.

CHAPTER 5: CONCLUSIONS AND FUTURE WORK

5.1 Conclusions

A series of six IArE ligands have been prepared using various synthetic techniques, all of which display surprising stability in normal atmospheric conditions. Due to this, it is the metal center to which the coordination occurs that dictates how the reactions must be carried out. An inert atmosphere is required to synthesize all of the Cu(I) complexes to prevent oxidation. For the silver(I) complexes, the presence of light during synthesis or after collecting and drying the product has been found to degrade the complexes due to the reduction to Ag^0, depositing metallic silver to the sides of the reaction vessel. The coordination chemistry surrounding this set must be thoroughly exploited and their applications be determined. These are all rare examples of linear homoleptic copper(I) or silver(I) complexes supported by NHT or NHSe ligands.

The (IArE)CuX complexes were found to prefer a bent LCuX geometry with the sterics of the IArE ligands believed to have little impact, although it is possible that the smaller atomic radius of copper versus that of silver may be a contributing factor. The interactions between the metal centers and the rich π systems of the ligands' aromatic rings is close enough to have stabilizing effects for the complexes. The linear homoleptic charged $[Ag(IArE)_2]X$ complexes were confirmed to reflect the same geometry in the solution phase, confirmed by ESI-MS. The counterions are believed to have an effect on the electronic properties of these complexes in the solution phase as detected by ^1H NMR spectroscopy. The effect of the counterions also was directly related to the solubility in various solvents. Additionally, the Ag-S bond length for the complexes in this study tend

to be shorter (2.35-2.38 Å) than other reported two- (2.41-2.49 Å) and three-coordinate (2.35-2.57 Å) mononuclear Ag(I) complexes with monodentate NHT ligands. The same comparison cannot be made for complexes bearing NHSe ligands as there are no reported structures in literature with the same criteria.

The biological activity of several of the $[Ag(IArE)_2]X$ complexes was assessed via MTT assay to determine the relative cell viability following treatment of the compounds in 1% DMSO solutions. Many complexes displayed notable cytotoxicity against HeLa, MDA-MB-231, and PC3 cancer cell lines *in vitro* while the ligands and silver salts showed little to no cytotoxicity. The most promising complexes were then further tested to determine that their IC50 values. Currently, the IC_{50} values for the three selected $[Ag(IArE)_2]X$ complexes are between 2-7 μM across the three cell lines.

5.2 Future Work

5.2.1. Synthesis of *p*-Methoxyphenyl-Substituted NHE ligands

Additionally, the synthesis of a new ligand bearing *p*-methoxyphenyl aromatic substituents is of interest due to the previously mentioned paper by Che *et al.*, which describes significant cytotoxic capabilities containing a saturated imidazole backbone with these aromatic substituents. It is anticipated that the unsaturated version should show similar results. However, preliminary work on the synthesis of this ligand with *p*-methoxyphenyl aromatic substituents has shown to be troublesome and cannot be synthesized in a similar fashion to the IArE ligands due polymerization of the imidazolium salt at room temperature. An alternative synthetic route is currently being pursued for the synthesis of a new set of ligands, abbreviated as IpAnE (I = unsaturated imidazole; pAn = p-anisidine; E = S, Se). Upon successful isolation of this ligand, the

reactivity and biological activity will be assessed for both the thione and selone analogs with silver (Scheme 5.1).

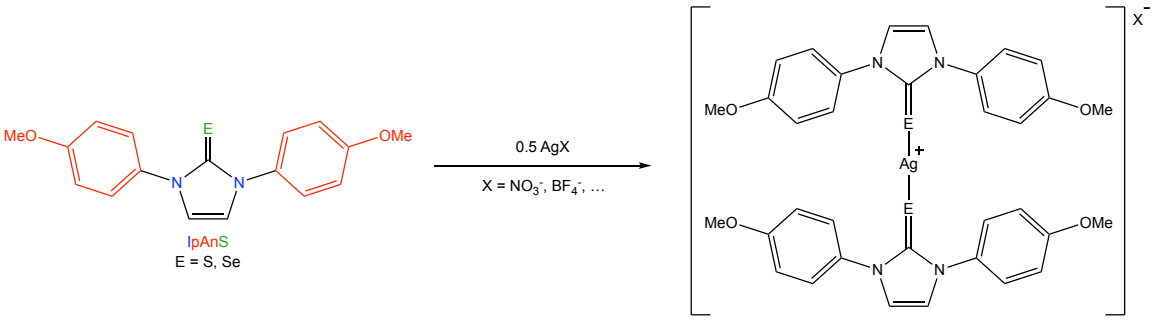

Scheme 5.1. Proposed synthesis of a series of new potentially cytotoxic $[Ag(IpAnE)_2]X$ complexes.

5.2.2. Synthesis of IArTe Ligands

It was an obvious decision to at least attempt to explore sulfur and selenium's atomically larger and heavier counterpart. Tellurium, a metalloid, shares similar chemical properties to sulfur and selenium but is slightly less electronegative and conversely more electropositive compared to the two lighter chalcogens. This translates to decreased overall reactivity towards most elements compared to the lighter analogues like sulfur, or oxygen that is known to bond with most elements of the periodic table. Also, due to tellurium's larger size, it tends to form weaker π bonds and has decreased tendency to form double bonds with second row elements. This suggests that the C-Te bond in imidazole tellones should be more of a single bond in character and be relatively longer than the lengths observed for thiones or selones.

Knowing that tellurium forms a weaker bond with carbon, a reflux in a primary alcohol seemed like a thermodynamically unfavorable route, but was still investigated employing the same reaction conditions used to synthesize the thione and selone ligand set with the substitution of methanol for ethanol to lower the reflux temperature. After 3-

4 days, small amounts of a white impure product was obtained. Next, the method outlined by Prabusankar *et al.* was used to synthesized the desired light green crystalline IDippTe ligand in acceptable yields. In the glovebox under an inert nitrogen atmosphere, IDippHCl was reacted with KOtBu and Te in THF for 2 days (Scheme 5.2).[75] Further recrystallization in a 60 °C hexane/toluene mixture yielded a bright white product that unfortunately showed conversion back to the imidazolium salt by ^{1}H NMR (Figure 5.1). The light green "crude" IDippTe ligand was also reported by Prabusankar as a green solid so further purification was deemed unnecessary. Instead, it was seen that the ligand does not exhibit high thermal stability in solution, and is in fact fairly labile. Additionally, this opens up potential for using these ligands as precursors to such materials as inorganic tellurides for photovoltaic materials and other practical applications.

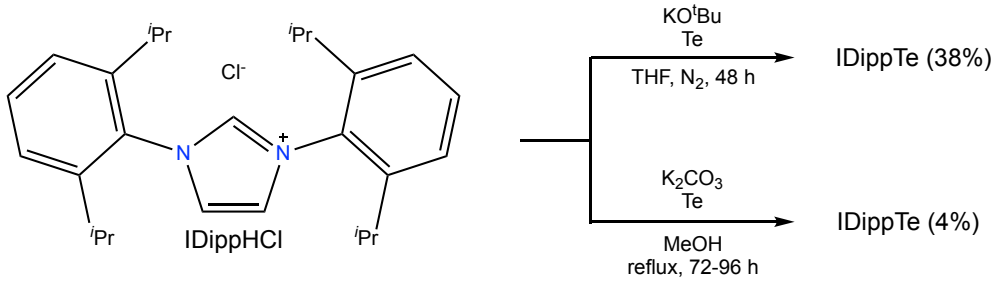

Scheme 5.2. Possible synthetic routes for the synthesis of IDippTe.

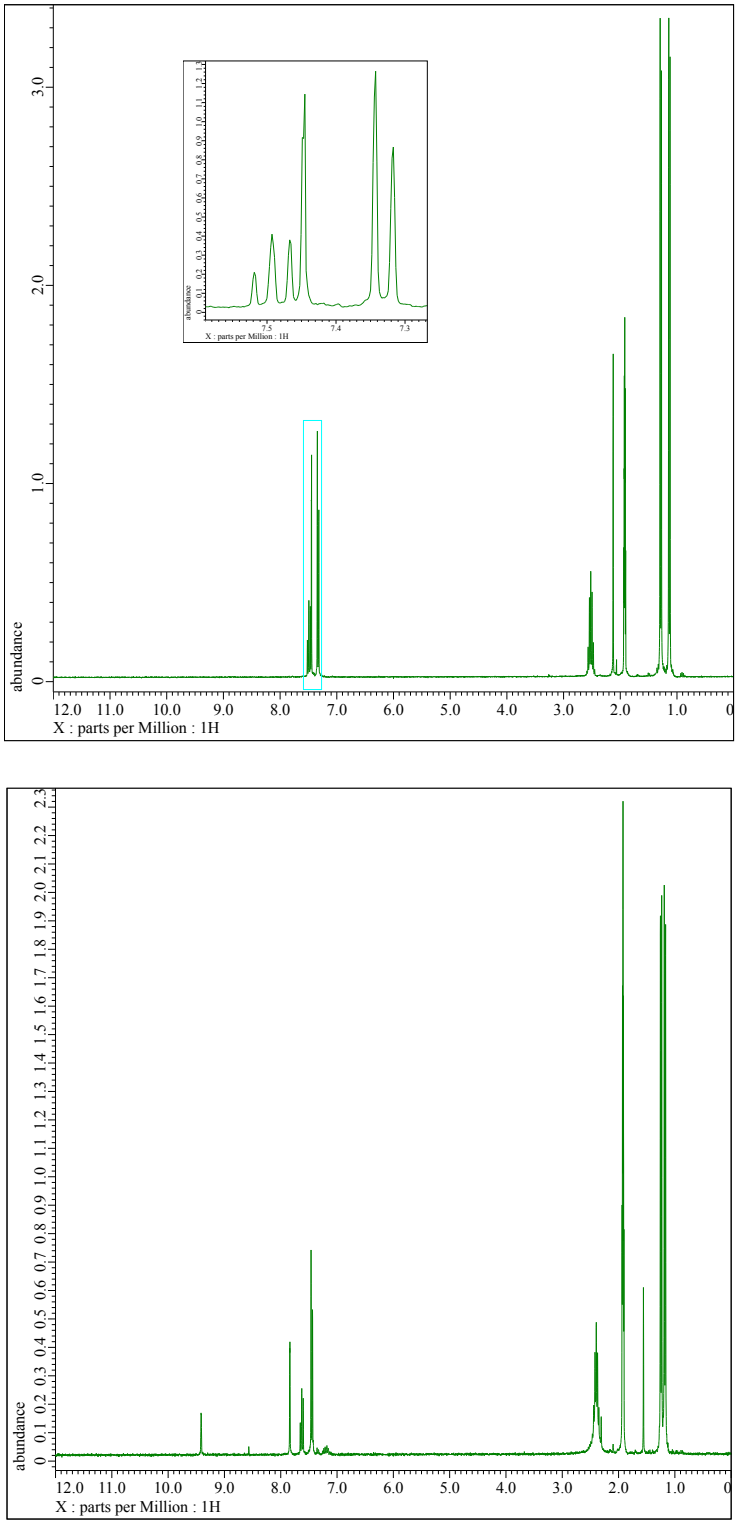

Figure 5.1. ^{1}H NMR spectra of IDippTe in CD_3CN prior to recrystallization in a 60 °C hexane/toluene mixture (top) and following the recrystallization (bottom) that shows a singlet around 9.4 ppm that corresponds to the methine proton of the imidazolium salt.

Upon obtaining the pure ligand in modest yields, crystals were obtained by slow evaporation in acetone and the structure was determined by single-crystal X-ray diffraction (Figure 5.2). Given that IMesTe was known, a search in the CSD showed there was no report of IXyTe, the 2,6-xylyl-substituted analog of this ligand. Employing the same synthetic technique used to synthesize and isolate IDippTe, IXyTe was obtained in relatively low yields as a fine brick red powder. Likewise, crystals were obtained of IXyTe as well, but this time in chloroform and its structure was obtained via XRD techniques (Figure 5.3). For the first time in the group, analysis was able to be completed that compared the structures of the telone ligands to that of the thione and selone analogs.

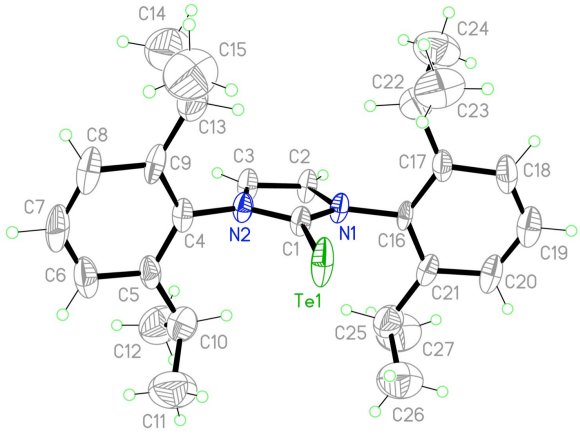

Figure 5.2. Molecular structure of IDippTe.

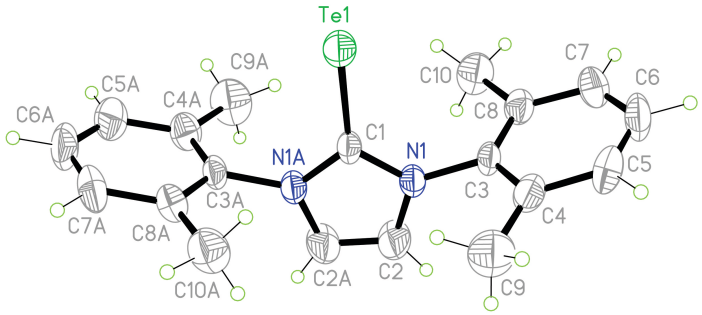

Figure 5.3. Molecular structure of IXyTe.

Compiling the relevant bond lengths and bond angles, it is noted there are deviations in several parameters (Table 5.1). As predicted, the length of the C=Te bond is significantly longer than that of the C=Se and C=S bond in both the 2,6-xylyl and Dipp substituted ligands. This can be explained by the polarizability of the C=E bond, with tellurium being the softest of the three it is expected to have a less polar bond and allow for stronger σ-donation to a metal, but lowered π-accepting ability. As previously noted, tellurium's lowered electronegativity will result in a bond that is more similar in nature to a C-Te single bond, but still displays double-bond character.

Table 5.1. Selected bond lengths (Å) and angles (°) for IArE (Ar = Xy, Dipp; E = S, Se, Te) ligands.

	C=E (Å)	C=C (Å)	N–C–N (°)	N–C=E (°)
IXyS	1.68	1.34	104.8	127.6
IXySe	1.83	1.35	105.2	127.4
IXyTe	2.05	1.32	106.3	126.9
IDippS	1.68	1.35	104.7	127.6
IDippSe	1.83	1.35	104.9	128.3
IDippTe	2.08	1.37	106.6	126.7*

* average of two values

The longer C=E bond and larger atomic radius also has the effect of lowering the steric hindrance around the metal center. Space-filling models can also accurately display the effect of the aromatic substituents and how the bulkier Dipp substituents work to encapsulate the metal center to provide higher electronic and kinetic stabilization, especially upon coordination to a metal center (Figure 5.4).

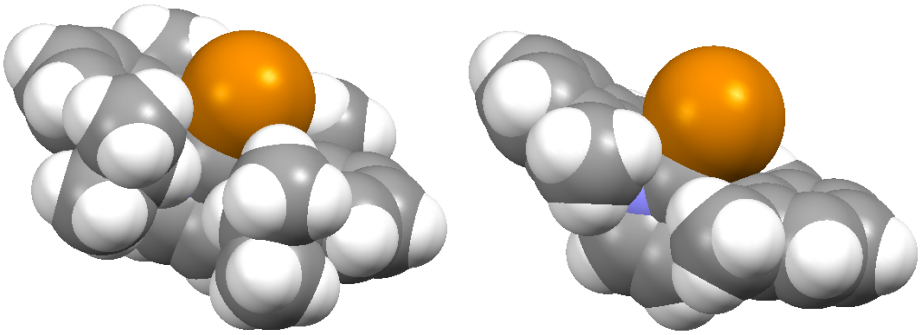

Figure 5.4. Space-filling diagrams of IDippTe (left) and IXyTe (right).

Upon comparing the bond length of the C=C bond of the imidazole backbone, it can be seen there is no significant deviation with the length only varying by 0.01-0.03 Å. This suggests that most of the electronics in the back of the imidazole remain relatively unaffected regardless of the chalcogen donor and there is no significant ring expansion. However, it is observed that the N-C-N bond angle increases significantly down the group, an indication of the aforementioned donor ability of the ligands. Upon calculating the summation of the two N-C-Te bond angles and N-C-N angle for the IXyTe and IDippTe, it is evident that the tellurium atom lies in the same plane of the imidazole ring with values of 359.9° and 360.0°, respectively.

One ligand, IDippTe, was chosen to investigate the reactivity of this ligand set under similar reaction conditions as used for the synthesis of the $[Ag(IArE)_2]X$ (E = S, Se) complexes. A stirred solution of IDippTe in acetonitrile was added dropwise to a stirred suspension of $AgBF_4$ in DI water and allowed to stir for approximately 10 minutes. The resulting colorless solution was concentrated under reduced pressure to near dryness and washed with diethyl ether prior to being isolated by filtration. The sample was then dried *in vacuo* for 24 h to afford a fine white powder. A crystal of

[Ag(IDippTe)2]BF_4 suitable for XRD studies was obtained by slow evaporation of the compound in acetone-d_6.

It is evident that the linear mononuclear cationic structure is still the preferred geometry as the chalcogen donor atom is altered. It was worthwhile to investigate the deviation in the bond lengths and angles between the three IArE ligands that contain a BF_4^- counterion to quantify the electronic and steric effects across the series (Table 5.2).

Table 5.2. Selected bond lengths and angles for [Ag(IDippE)$_2$]BF_4.

	C=E (Å)	Ag-E (Å)	Ag···Cent.‡ (Å)	Ag-E-C (°)
[Ag(IDippS)$_2$]BF_4	1.71	2.38	3.18	108.0
[Ag(IDippSe)$_2$]BF_4	1.87	2.48*	3.20	105.6
[Ag(IDippTe)$_2$]BF_4	2.08	2.63	3.22	102.5

‡ distance between silver atom and the centroid of the nearest aromatic ring
* average of two values

5.2.3. Reactivity Studies of Copper(I) Complexes

In a paper by Nolan *et al*., the reactivity of 5-membered NHCs with unsaturated backbones was investigated through the generation of a (NHC)CuOH intermediate.[76] Monomeric copper(I) alkoxide complexes are rare in literature and reported to catalyze the reduction of CO_2 to CO quite effectively through a series of transformations.[77,78] It was shown that this (NHC)CuOH intermediate was able to produce a myriad of novel complexes through the sequential displacement of the hydroxyl ligand and coordination of an incoming species with a labile proton, to form water as a byproduct. It has been theorized that this same general schema can be applied to our NHT and NHSe ligands.

Upon generation of the (IArE)CuX species, one equivalent is reacted with excess CsOH to generate the (IArE)CuOH intermediate. A number of novel complexes supported by NHT or NHSe ligands are possible, utilizing such coordinating reagents as alkoxides, phosphines, thiocarbamates, thiols, selenols, etc. (Scheme 5.3).

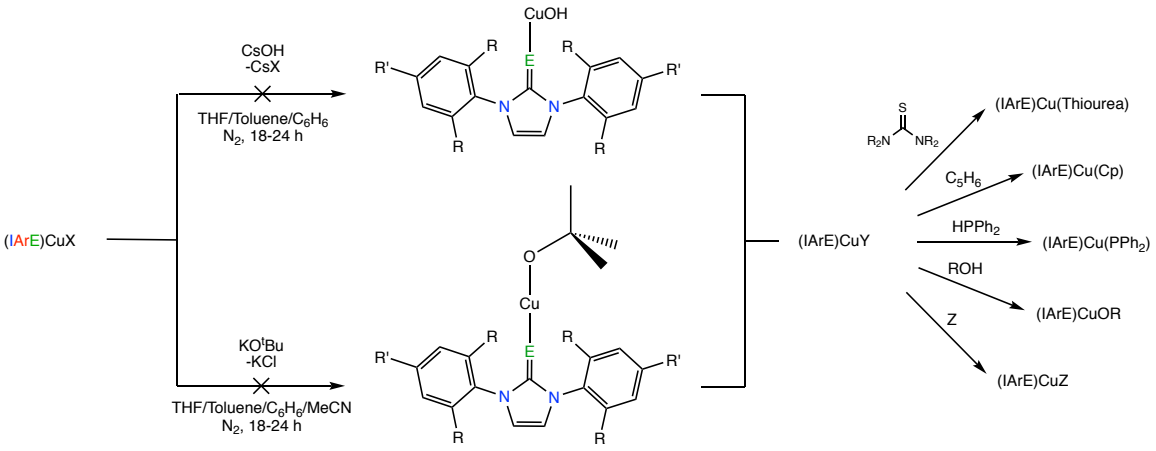

Scheme 5.3. Proposed reactivity of (IArE)CuX.

However, numerous attempts at synthesizing the (IArE)CuOH intermediate were unsuccessful, so an alternate synthetic route was developed utilizing potassium *tert*-butoxide to act as both a base and coordinating species to produce KX (X = Cl, Br, I) as a byproduct. This synthetic route also proved to be unsuccessful.

The displacement of an alkoxide ligand instead of a hydroxide ligand will be more favored due to the formation of the corresponding alcohol, in place of water. Future attempts will employ other metal alkoxides. Cuprous tert-butoxide was even synthesized via a salt metathesis reaction between anhydrous CuCl and KO^{t}Bu.[79] Regardless, equimolar reactions of this impure (CuO^{t}Bu)$_4$ with the (IArE)CuX complexes was also unsuccessful at producing the desired (IArE)CuO^{t}Bu intermediate. The explanation for this occurrence comes from hard-soft acid-base theory.

5.2.4. Synthesis of (IArE)AgOAc

It is also worth noting that a large portion of current cytotoxic Ag(I)-NHC complexes in the literature have an acetate ligand coordinated to the other side of the silver center in monomeric fashion. It was our initial goal to focus on the synthesis of (IArE)AgOAc complexes considering current research has pointed to this ligand being somewhat promising for cancer research. Early attempts made at synthesizing this heteroleptic complex proved challenging, as complete degradation was observed visually with the product turning from a bright white powdery solid to dark gray in less than 24 h, even in the complete absence of light. Several attempts were made to grow crystals of this compound to see the adopted molecular geometry, only to have all attempts fail. This part of the project was left on hold for some time until recently, a crystal suitable for single-crystal X-ray diffraction was obtained for (IDippSe)AgOAc and (IDippS)AgOAc by slow evaporation of acetonitrile in complete darkness. This initiated later attempts at synthesizing and isolating the pure product. Reacting the IDippE ligands in a 1:1 molar ratio with AgOAc in methanol for 1 h was determined to be an effective method as white fine powders were obtained.

5.2.5. Synthesis of (IArE)AuCl and (IArE)$AuCl_3$

Gold(I) complexes have a well-known role in the treatment of arthritis with many FDA-approved drugs currently on the market.[17] Notably, gold(I) thiosulfates such as sodium aurothiomalate, aurothioglucose, sodium aurothiopropanol sulfonate, and sodium aurothiosulfate have been used since the early 20th century for the treatment of arthritis. Possibly the most well-known gold(I) metallodrug is auranofin (tetraacetyl-β-D-

thioglucose-gold(I)-thioethylphosphine), a monomeric, lipophilc neutral coordination compound that is administered orally in a capsule (Figure 5.5).

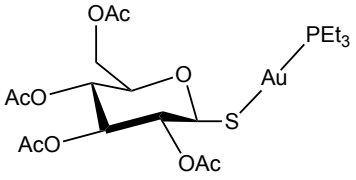

Figure 5.5. Structural diagram of auranofin.

Remarkably, auranofin and many other gold complexes have shown anticancer activity.[80,81] Gold anticancer drugs are said to interact with the mitochondria and pathways of phosphorylation to generally lead to apoptosis.[82] Gold(I) complexes tend to inhibit the seleno-enzyme TrxR, similarly to Ag(I) compounds discussed previously.[83]

Given gold's diverse therapeutic applications and reports of Au-NHCs possessing anticancer potential it is of interest to synthesize a series of new complexes bearing our IArE ligands with the ultimate goal of exploring any pertinent biological applications. A synthetic route has been proposed to synthesize a series of novel (IArE)$AuCl_3$ complexes. Typically, gold(III) complexes require the use of a multidentate ligand to stabilize the complex and prevent the reduction to Au^I or Au^0 *in vivo*. Nevertheless, reacting Au metal in aqua regia will form the desired $HAuCl_4$ intermediate that is then isolated and reacted with one equivalent of IArE in THF for several hours. Gold(I) complexes will also be synthesized by reacting one equivalent of (tht)AuCl (tht = tetrahydrathiophene) with one equivalent of ligand to form (IArE)AuCl via a ligand substitution pathway (Scheme 5.4).

$$\text{(tht)AuCl + IArE} \xrightarrow[\text{-tht}]{Et_2O} \text{(IArE)AuCl}$$

$$HAuCl_4 + \text{IArE} \xrightarrow{\text{THF}} \text{(IArE)}AuCl_3 + HCl$$

Scheme 5.4. Synthesis of (IArE)AuCl and (IArE)$AuCl_3$ for future cancer studies.

5.2.6. Additional Biological Studies

Following the investigation of the biological activity of the $[Ag(IArE)_2]X$ complexes, it should be beneficial to expand this scope to include other ligands from within the Rabinovich group. It is hypothesized that ligands with a saturated imidazole or pyrimidine backbone would also offer positive results across cancer cell lines due to similar electronic properties. This would further reinforce the claim that the ligands coordinated to the metal atom have significant properties that influence cytotoxicity. Expanding the studies to include complexes of Cu(I), Au(I), and Au(III) supported by NHT or NHSe ligands will also provide insight into the significance of the metal on the cytotoxicity of the complexes.

Specifically, for the $[Ag(IArE)_2]X$ complexes, the mechanism of action must be determined in an effort to gain understanding on the significance of complexation. If it can be understood how these complexes trigger cell death, the ligands can be fine-tuned to increase their biological activity across a more diverse set of cancers *in vitro*. This can be conducted through the use of appropriate metallomic studies. *In vivo* testing will then be completed to assess the effectiveness of the compounds in living subjects. This will also provide valuable information on the toxicity of these complexes and their individual components in a living system.

REFERENCES

1. Singh, M. S. *Reactive Intermediates in Organic Chemistry: Structure, Mechanism, and Reactions*; Wiley-VCH: Weinheim, 2014.
2. Doering, W. V. E.; Hoffmann, A. K. *J. Am. Chem. Soc*. **1954**, *76*, 6162-6165.
3. Skell, P. S.; Sandler, S. R. *J. Am. Chem. Soc.* **1958**, *80*, 2024-2025.
4. Fischer, E. O.; Maasböl, A. *Angew. Chem. Int. Ed.* **1964**, *3*, 580-581.
5. Arduengo, A. J., III; Harlow, R. L.; Kline, M. *J. Am. Chem. Soc.* **1991**, *113*, 361-363.
6. Bourissou, D.; Guerret, O.; Gabbaï, F. P.; Bertrand, G. *Chem. Rev*. **2000**, *100*, 39-92.
7. Hirai, K.; Itoh, T.; Tomioka, H. *Chem. Rev.* **2009**, *109*, 3275-3332.
8. Johnson, N. A.; Southerland, M. R.; Youngs, W. J. *Molecules* **2017**, *22*, 1263-1283.
9. Hopkinson, M. N.; Richter, C.; Schedler, M.; Glorius, F. *Nature* **2014**, *510*, 485-496.
10. Lehmann, J. F.; Urquhart, S. G.; Ennis, L. E.; Hitchcock, A. P.; Hatano, K.; Gupta, S.; Denk, M. K. *Organometallics* **1999**, *18*, 1862-1872.
11. Tafipolsky, M.; Scherer, W.; Öfele, K.; Artus, G.; Pederson, B.; Herrmann, W. A.; McGrady, G. S. *J. Am. Chem. Soc.* **2002**, *124*, 5865-5880.
12. Herrmann, W. A.; Köcher, C. *Angew. Chem. Int. Ed. Engl*. **1997**, *36*, 2162-2187.

13. *Handbook of Chalcogen Chemistry: New Perspectives in Sulfur, Selenium and Tellurium*; Devillanova, F. A.; Du Mont, W., Eds.; Royal Society of Chemistry: Cambridge, 2013.
14. Rong, Y.; Al-Harbi, A.; Kriegel, B.; Parkin, G. *Inorg. Chem.* **2013**, *52*, 7172-7182.
15. Marinelli, M.; Santini, C.; Pellei, M. *Curr. Top. Med. Chem*. **2016**, *16*, 2995-3017.
16. Monteiro, D. C. F.; Phillips, R. M.; Crossley, B. D.; Fielden, J.; Willans, C. E. *Dalton Trans.* **2012**, *41*, 3720-3725.
17. Medvetz. D. A.; Hindi, K. M.; Pazner, M. J.; Ditto, A. J.; Youngs, W. J. *Met.-Based Drugs* **2008**, *2008*, 1-7.
18. Bourassa, M. W.; Miller, L. M. *Metallomics* **2012**, *4*, 721-738.
19. Anderson, C. J.; Welch, M. J. *Chem. Rev.* **1999**, *99*, 2219-2234.
20. Mounicou, S.; Szpunar, J.; Lobinski, R. *Chem. Soc. Rev*. **2009**, *38*, 1119-1138.
21. Szpunar, J. *Analyst* **2005**, *130*, 442-465.
22. Sankararamakrishnan, R.; Verma, S.; Kumar, S. *Proteins* **2005**, *58*, 211-221.
23. Coste, F.; Malinge, J.-M.; Serre, L.; Shepard, W.; Roth, M.; Leng, M.; Zelwer, C. *Nucleic Acids Res.* **1999**, *27*, 1837-1846.
24. Tretyakova, N. Y.; Groehler IV, A.; Ji, S. *Acc. Chem. Res.* **2015**, *48*, 1631-1644.
25. Mjos, K. D.; Orvig, C. *Chem. Rev.* **2014**, *114*, 4540-4563.
26. Rosenberg, B.; Renshaw, E.; Vancamp, L.; Hartwick, J.; Drobnik, J. *J. Bacteriol*. **1967**, *93*, 716-721.

27. Rosenberg, B.; VanCamp, L.; Trosko, J. E.; Mansour, V. H. *Nature* **1969**, *222*, 385-386.

28. Zaki, M.; Arjmand, F.; Tabassum, S. *Inorg. Chim. Acta* **2016**, *444*, 1-22.

29. Alessio, E. *Eur. J. Inorg. Chem.* **2017**, 1549-1560.

30. Ang, W. H.; Casini, A.; Sava, G.; Dyson, P. J. *J. Organomet. Chem*. **2011**, *696*, 989-998.

31. Leijen, S.; Burgers, S. J.; Baas, P.; Pluim, D.; Tibben, M.; Werkhoven, E.; Alessio, E.; Sava, G.; Beijnen, J. H.; Schellens, J. H. M. *Invest. New Drugs* **2015**, *33*, 201-204.

32. Hill, W. R. *Argyria – The Pharmacology of Silver*; Williams and Wilkins: 1939.

33. Medici, S.; Peana, M.; Crisponi, G.; Nurchi, V. M.; Lachowicz, J. I.; Remelli, M.; Zoroddu, M. A. *Coord. Chem. Rev.* **2016**, *328*, 349-359.

34. Silver, S. *Microbiol. Rev*. **2003**, *27*, 341-353.

35. Zhang, S.; Du, C.; Wang, Z.; Han, X.; Zhang, K.; Liu, L. *Toxicol. In Vitro* **2013**, *27*, 739-744.

36. Boselli, L.; Ader, I.; Carraz, M.; Hemmert, C.; Cuvillier, O.; Gornitzka, H. *Eur. J. Med. Chem.* **2014**, *85*, 87-94.

37. Haque, R. A.; Choo, S. Y.; Budagumpi, S.; Iqbal, M. A.; Abdullah, A. A.-A. *Eur. J. Med. Chem.* **2015**, *90*, 82-92.

38. Srivastava, M.; Singh, S.; Self W. T. *Environ. Health Perspect*. **2012**, *120*, 56-61.

39. Eloy, L.; Jarrousse, A.-S.; Teyssot, M.-L.; Gautier, L. M.; Jolivalt, C.; Cresteil, T.; Roland, S. *ChemMedChem* **2012**, *7*, 805-814.

40. Sandtorv, A. H.; Leitch, C.; Bedringaas, S. L.; Gjertsen, B. T.; Bjørsvik, H.-R. *ChemMedChem* **2015**, *10*, 1522-1527.

41. Yan, K.; Lok, C.-N.; Bierla, K.; Che, C.-M. *Chem. Commun*. **2010**, *46*, 7691-7693.

42. Zulikha, H. Z.; Haque, R. A.; Budagumpi, S.; Majid, A.M.S. A. *Inorg. Chim. Acta* **2011**, *411*, 40-47.

43. Hussaini, S. Y.; Haque, R. A.; Asekunowo, P. O.; Majid, A.M.S. A.; Agha, M. T.; Razali, M. R. *J. Organomet. Chem.* **2017**, *840*, 56-62.

44. Gandin, V.; Pellei, M.; Marinelli, M.; Marzano, C.; Dolmella, A.; Giorgetti, M.; Santini, C. *J. Inorg. Biochem.* **2013**, *129*, 135-144.

45. Citta, A.; Schuh, E.; Mohr, F.; Folda, A.; Massimino M. L.; Bindoli, A.; Casini, A.; Rigobello, M. P. *Metallomics* **2013**, *5*, 1006-1015.

46. Shahini, C. R.; Achar, G.; Budagumpi, S.; Tacke, M.; Patil, S. A. *Appl. Organometal. Chem*. **2017**, *31*, 1-15.

47. Yang, D.; Chen, Y.-C.; Zhu, N.-Y. *Org. Lett.* **2004**, *6*, 1577-1580.

48. Ramnial, T.; Taylor, S. A.; Bender, M. L.; Gorodetsky, B.; Lee, P. T. K.; Dickie, D. A.; McCollum, B. M.; Pye, G. C.; Walsby, C. J.; Clyburne, J. A. C. *J. Org. Chem.* **2008**, *73*, 801-812.

49. Zhang, L.-M.; Li, H.-Y.; Li, H.-X.; Young, D. J.; Wang, Y.; Lang, J.-P. *Inorg. Chem.* **2017**, *56*, 11230-11243.

50. Huang, J.; Schanz, H.-J.; Stevens, E. D.; Nolan, S. P.; Capps, K. B.; Bauer, A.; Hoff, C. D. *Inorg. Chem.* **2000**, *39*, 1042-1045.

51. Wei, S.; Wei, X.-G., Su, X.; You, J.; Ren, Y. *Chem. Eur. J.* **2011**, *17*, 5965-5971.

52. Tretiakov, M.; Shermolovich, Y. G.; Pratap Singh, A.; Samuel, P. P.; Roesky, H. W.; Niepötter, B.; Visscher, A.; Stalke, D. *Dalton Trans.* **2013**, *42*, 12940-12946.

53. Zhang, F.; Zhang, J.; Zhou, X. *Inorg. Chem.* **2017**, *56*, 2070-2077.

54. Vummaleti, S. V. C.; Nelson, D. J.; Poater, A.; Gómez-Suárez, A.; Cordes, D. B.; Slawin, A. M. Z.; Nolan, S. P.; Cavallo, L. *Chem. Sci*. **2015**, *6*, 1895-1904.

55. Liske, A.; Verlinden, K.; Buhl, H.; Schaper, K.; Ganter, C. *Organometallics* **2013**, *32*, 5269-5272.

56. Nelson, D. J.; Nahra, F.; Patrick, S. R.; Cordes, D. B.; Slawin, A. M. Z.; Nolan S. P. *Organometallics* **2014**, *33*, 3640−3645.

57. Nelson, D. J.; Collado, A.; Manzini, S.; Meiries, S.; Slawin, A. M. Z.; Cordes, D. B.; Nolan S. P. *Organometallics* **2014**, *33*, 2048−2058.

58. Kocherga, M. B.S. Honors Thesis, The University of North Carolina at Charlotte, Charlotte, North Carolina, 2016.

59. Sola, J.; Lopez, A.; Coxall, R. A.; Clegg, W. *Eur. J. Inorg. Chem.* **2004**, 4871-4881.

60. Ghassemzadeh, M.; Sharifi, A.; Malakootikhah, J.; Neumüller, B.; Iravani, E. *Inorg. Chim. Acta* **2004**, *357*, 2245-2252.

61. Nöth, H.; Beck, W.; Burger, K. *Eur. J. Inorg. Chem.* **1998**, 93-99.

62. Cingolani, A.; Marchetti, F.; Pettinari, C.; Pettinari, R.; Skelton, B. W.; White, A. H. *Inorg. Chem.* **2002**, *41*, 1151-1161.

63. Molloy, K. C.; Mahon, M. F.; Barret, M. C. *Acta Cryst.* **1999**, *C55*, 555-557.

64. Aslanidis, P.; Karagiannidis, P.; Akrivos, P. D.; Krebs, B.; Läge, M. *Inorg. Chim. Acta* **1997**, *254*, 277-284.

65. Batsala, G. K.; Dokorou, V.; Kourkoumelis, N.; Manos, M. J.; Tasiopoulos, A. J.; Mavromoustakos, T.; Simčič, M.; Golič-Grdadolnik, S.; Hadjikakou, S. K. *Inorg. Chim. Acta* **2012**, *382*, 146-157.

66. Ferrari, M. B.; Fava, G. G.; Tani, M. E. V. *Cryst. Struct. Commun.* **1981**, *10*, 571-575.

67. Bowmaker, G. A.; Pakawatchai, C.; Saithong, S.; Skelton, B. W.; White, A. H. *Dalton Trans.* **2009**, 2588-2598.

68. Jia, D.; Zhang, Y.; Deng, J.; Ji, M. *J. Coord. Chem*. **2007**, *60*, 833-841.

69. Zhu, Q.; Chu, W.; Huang, R.; Zhang, J.; Xu, Y. *J. Coord. Chem.* **2008**, *61*, 3390-3400.

70. Bowmaker, G. A.; Chaichit, N.; Pakawatchai, C.; Skelton, B. W.; White, A. H. *Can. J. Chem.* **2009**, *87*, 161-170.

71. Lobana, T. S.; Sultana, R.; Butcher, R. J.; Jasinski, J. P.; Akitsu, T. *Z. Anorg. Allg. Chem.* **2014**, *640*, 1688-1695.

72. Casas, J. S.; Martínez, E. G.; Sánchez, A.; González, A. S.; Sordo, J.; Casellato, U.; Graziani, R. *Inorg. Chim. Acta* **1996**, *241*, 117-123.

73. Hintermann, L. *Beilstein J. Org. Chem.* **2007**, *3*, 1-5.

74. Fulmer, G. R.; Miller, A. J. M.; Sherden, N. H.; Gottlieb, H. E.; Nudelman, A.; Stoltz, B. M.; Bercaw, J. E.; Goldberg, K. I. *Organometallics* **2010**, *29*, 2176-2179.

75. Srinivas, K.; Suresh, P.; Babu, C. N.; Sathyanarayana, A.; Prabusankar, G. *RSC Adv.* **2015**, *5*, 15579-15590.

76. Fortman, G. C.; Slawin, A. M. Z.; Nolan, S. P. *Organometallics* **2010**, *29*, 3966-3972.

77. Goj, L. A.; Blue, E. D.; Munro-Leighton, C.; Gunnoe, T. B.; Petersen, J. L. *Inorg. Chem*. **2005**, *44*, 8647-8649.

78. Laitar, D. S.; Muller, P.; Sadighi, J. P. *J. Am. Chem. Soc*. **2005**, *127*, 17196-17197.

79. Tsuda, T.; Hashimoto, T.; Saegusa, T. *J. Am. Chem. Soc.* **1972**, *94*, 658-659.

80. *Metallo-Drugs: Development and Action of Anticancer Agents*; Sigel, A., Sigel, H., Freisinger, E., Sigel, R. K. O., Eds.; Walter de Gruyter: Berlin, 2018.

81. Simon, T. M.; Kunishima, D. H.; Vibert, G. J.; Lorber, A. *Cancer* **1979**, *44*, 1965-1975.

82. Barnard, P. J.; Berners-Price, S. J.; *Coord. Chem. Rev.* **2007**, *251*, 1889-1902.

83. Berners-Price, S. J.; Filipovska, A. *Metallomics* **2011**, *3*, 863-873.

APPENDIX A: CRYSTAL DATA FOR (IDippS)CuCl

Empirical formula	$C_{27}H_{36}ClCuN_2S$	
Formula weight	519.65	
Temperature	100(2) K	
Wavelength	0.71073 Å	
Crystal system, space group	Monoclinic, $P2_1/c$ (No. 14)	
Unit cell dimensions	a = 10.3965(4) Å	$\alpha = 90°$
	b = 19.9146(7) Å	$\beta = 91.8110(10)°$
	c = 12.8869(4) Å	$\gamma = 90°$
Volume	2666.80(16) $Å^3$	
Z, Calculated density	4, 1.294 Mg/m^3	
Absorption coefficient	1.014 mm^{-1}	
Crystal size	0.18 x 0.15 x 0.10 mm^3	
Crystal color / habit	colorless / block	
Theta range for data collection	3.16 to 26.38°	
Reflections collected / unique	30895 / 5384 [R(int) = 0.0360]	
Completeness to theta = 25.000°	99.6 %	
Absorption correction	multi-scan / sadabs	
Refinement method	Full-matrix least-squares on F^2	
Goodness-of-fit on F^2	1.009	
Final R indices [I>2sigma(I)]	R1 = 0.0279, wR2 = 0.0706	
R indices (all data)	R1 = 0.0382, wR2 = 0.0768	
Largest diff. peak and hole	0.362 and -0.246 $e.Å^{-3}$	

APPENDIX B: CRYSTAL DATA FOR (IXyS)CuBr

Empirical formula	$C_{19}H_{20}BrCuN_2S$	
Formula weight	451.89	
Temperature	200(2) K	
Wavelength	0.71073 Å	
Crystal system, space group	Monoclinic, *Cc* (No. 9)	
Unit cell dimensions	a = 11.6245(8) Å	$\alpha = 90°$
	b = 8.1462(8) Å	$\beta = 105.901(4)°$
	c = 21.1234(18) Å	$\gamma = 90°$
Volume	1923.8(3) $Å^3$	
Z, Calculated density	4, 1.560 Mg/m^3	
Absorption coefficient	3.323 mm^{-1}	
Crystal size	0.21 x 0.20 x 0.18 mm^3	
Crystal color / habit	colorless / block	
Theta range for data collection	3.09 to 25.73°	
Reflections collected / unique	23462 / 3643 [R(int) = 0.0413]	
Completeness to theta = 25.000°	99.9 %	
Absorption correction	multi-scan / sadabs	
Refinement method	Full-matrix least-squares on F^2	
Goodness-of-fit on F^2	1.049	
Final R indices [I>2sigma(I)]	R1 = 0.0185, wR2 = 0.0433	
R indices (all data)	R1 = 0.0209, wR2 = 0.0446	
Largest diff. peak and hole	0.202 and -0.242 $e.Å^{-3}$	

APPENDIX C: CRYSTAL DATA FOR (IMesS)CuBr

Empirical formula	$C_{21}H_{24}BrCuN_2S$	
Formula weight	479.94	
Temperature	200(2) K	
Wavelength	0.71073 Å	
Crystal system, space group	Monoclinic, $P2_1/c$ (No. 14)	
Unit cell dimensions	a = 11.1896(9) Å	$\alpha = 90°$
	b = 15.3084(13) Å	$\beta = 112.869(2)°$
	c = 13.5541(10) Å	$\gamma = 90°$
Volume	2139.2(3) $Å^3$	
Z, Calculated density	4, 1.490 Mg/m^3	
Absorption coefficient	2.993 mm^{-1}	
Crystal size	0.21 x 0.14 x 0.08 mm^3	
Crystal color / habit	colorless / block	
Theta range for data collection	3.09 to 25.75°	
Reflections collected / unique	39881 / 4069 [R(int) = 0.0493]	
Completeness to theta = 25.000°	99.8 %	
Absorption correction	multi-scan / sadabs	
Refinement method	Full-matrix least-squares on F^2	
Goodness-of-fit on F^2	1.070	
Final R indices [I>2sigma(I)]	R1 = 0.0336, wR2 = 0.0778	
R indices (all data)	R1 = 0.0510, wR2 = 0.0887	
Largest diff. peak and hole	0.619 and -0.719 $e.Å^{-3}$	

APPENDIX D: CRYSTAL DATA FOR (IDippS)CuBr

Empirical formula	$C_{27}H_{36}BrCuN_2S$	
Formula weight	564.10	
Temperature	100(2) K	
Wavelength	0.71073 Å	
Crystal system, space group	Monoclinic, $P2_1/c$ (No. 14)	
Unit cell dimensions	a = 10.9860(11) Å	$\alpha = 90°$
	b = 17.3661(18) Å	$\beta = 97.799(3)°$
	c = 14.3283(15) Å	$\gamma = 90°$
Volume	2708.3(5) $Å^3$	
Z, Calculated density	4, 1.383 Mg/m^3	
Absorption coefficient	2.376 mm^{-1}	
Crystal size	0.28 x 0.10 x 0.05 mm^3	
Crystal color / habit	colorless / plate	
Theta range for data collection	1.85 to 26.45°	
Reflections collected / unique	26669 / 5548 [R(int) = 0.0778]	
Completeness to theta = 25.000°	100.0 %	
Absorption correction	multi-scan / sadabs	
Refinement method	Full-matrix least-squares on F^2	
Goodness-of-fit on F^2	1.039	
Final R indices [I>2sigma(I)]	R1 = 0.0474, wR2 = 0.1024	
R indices (all data)	R1 = 0.0940, wR2 = 0.1213	
Largest diff. peak and hole	0.568 and -0.592 $e.Å^{-3}$	

APPENDIX E: CRYSTAL DATA FOR (IDippSe)CuBr

Empirical formula	$C_{27}H_{36}BrCuN_2Se$	
Formula weight	611.00	
Temperature	200(2) K	
Wavelength	1.54178 Å	
Crystal system, space group	Monoclinic, $P2_1/c$ (No. 14)	
Unit cell dimensions	a = 11.1093(18) Å	$\alpha = 90°$
	b = 17.570(3) Å	$\beta = 98.300(5)°$
	c = 14.502(2) Å	$\gamma = 90°$
Volume	2801.1(8) $Å^3$	
Z, Calculated density	4, 1.449 Mg/m^3	
Absorption coefficient	4.365 mm^{-1}	
Crystal size	0.22 x 0.20 x 0.18 mm^3	
Crystal color / habit	colorless / block	
Theta range for data collection	3.98 to 68.47°	
Reflections collected / unique	38023 / 5101 [R(int) = 0.0335]	
Completeness to theta = 68.25°	99.1 %	
Absorption correction	multi-scan / sadabs	
Refinement method	Full-matrix least-squares on F^2	
Goodness-of-fit on F^2	1.021	
Final R indices [I>2sigma(I)]	R1 = 0.0328, wR2 = 0.0901	
R indices (all data)	R1 = 0.0352, wR2 = 0.0934	
Largest diff. peak and hold	0.413 and -0.612 $e.Å^{-3}$	

APPENDIX F: CRYSTAL DATA FOR $[Ag(IXyS)_2]NO_3$

Empirical formula	$C_{38}H_{40}AgN_5O_3S_2$	
Formula weight	786.75	
Temperature	297(2) K	
Wavelength	0.71073 Å	
Crystal system, space group	Monoclinic, $P2_1/c$ (No. 14)	
Unit cell dimensions	a = 8.6018(5) Å	$\alpha = 90°$
	b = 14.4276(9) Å	$\beta = 98.193(2)°$
	c = 15.1787(8) Å	$\gamma = 90°$
Volume	1864.50(19) $Å^3$	
Z, Calculated density	2, 1.401 Mg/m^3	
Absorption coefficient	0.695 mm^{-1}	
Crystal size	0.400 x 0.320 x 0.250 mm^3	
Crystal color / habit	colorless / block	
Theta range for data collection	2.938 to 25.718°	
Reflections collected / unique	75483 / 3563 [R(int) = 0.0277]	
Completeness to theta = 25.000°	99.8 %	
Absorption correction	multi-scan / sadabs	
Refinement method	Full-matrix least-squares on F^2	
Goodness-of-fit on F^2	1.010	
Final R indices [I>2sigma(I)]	R1 = 0.0359, wR2 = 0.0954	
R indices (all data)	R1 = 0.0440, wR2 = 0.1088	
Largest diff. peak and hole	0.330 and -0.397 $e.Å^{-3}$	

APPENDIX G: CRYSTAL DATA FOR $[Ag(IXySe)_2]NO_3$

Empirical formula	$C_{38}H_{40}AgN_5O_3Se_2$	
Formula weight	880.54	
Temperature	200(2) K	
Wavelength	0.71073 Å	
Crystal system, space group	Monoclinic, $P2_1/n$ (No. 11)	
Unit cell dimensions	a = 14.4198(15) Å	$\alpha = 90°$
	b = 8.4407(9) Å	$\beta = 90.142(3)°$
	c = 30.680(3) Å	$\gamma = 90°$
Volume	3734.2(7) $Å^3$	
Z, Calculated density	4, 1.566 Mg/m^3	
Absorption coefficient	2.532 mm^{-1}	
Crystal size	0.300 x 0.150 x 0.100 mm^3	
Crystal color / habit	colorless / block	
Theta range for data collection	2.873 to 25.391°	
Reflections collected / unique	125003 / 6848 [R(int) = 0.0505]	
Completeness to theta = 25.000°	99.9 %	
Absorption correction	multi-scan / sadabs	
Refinement method	Full-matrix least-squares on F^2	
Goodness-of-fit on F^2	1.080	
Final R indices [I>2sigma(I)]	R1 = 0.0296, wR2 = 0.0667	
R indices (all data)	R1 = 0.0393, wR2 = 0.0720	
Largest diff. peak and hole	0.577 and -0.674 $e.Å^{-3}$	

APPENDIX H: CRYSTAL DATA FOR $[Ag(IXyS)_2]BF_4$

Empirical formula	$C_{38}H_{40}AgBF_4N_4S_2$	
Formula weight	811.55	
Temperature	297(2) K	
Wavelength	0.71073 Å	
Crystal system, space group	Monoclinic, *C*2/*c* (No. 15)	
Unit cell dimensions	a = 19.799(3) Å	$\alpha = 90°$
	b = 8.5943(14) Å	$\beta = 90.437(4)°$
	c = 22.900(3) Å	$\gamma = 90°$
Volume	3896.7(10) $Å^3$	
Z, Calculated density	4, 1.383 Mg/m^3	
Absorption coefficient	0.675 mm^{-1}	
Crystal size	0.220 x 0.200 x 0.180 mm^3	
Crystal color / habit	colorless / block	
Theta range for data collection	3.133 to 25.389°	
Reflections collected / unique	41550 / 3563 [R(int) = 0.0425]	
Completeness to theta = 25.000°	99.7 %	
Absorption correction	multi-scan / sadabs	
Refinement method	Full-matrix least-squares on F^2	
Goodness-of-fit on F^2	1.062	
Final R indices [I>2sigma(I)]	R1 = 0.0463, wR2 = 0.1349	
R indices (all data)	R1 = 0.0623, wR2 = 0.1546	
Largest diff. peak and hole	0.584 and -0.442 $e.Å^{-3}$	

APPENDIX I: CRYSTAL DATA FOR $[Ag(IXySe)_2]BF_4$

Empirical formula	$C_{38}H_{40}AgBF_4N_4Se_2$	
Formula weight	905.34	
Temperature	200(2) K	
Wavelength	0.71073 Å	
Crystal system, space group	Triclinic, $P\bar{1}$ (No. 2)	
Unit cell dimensions	a = 8.176(4) Å	α = 115.719(13)°
	b = 15.175(7) Å	β = 91.885(15)°
	c = 16.901(7) Å	γ = 97.044(15)°
Volume	1866.2(14) $Å^3$	
Z, Calculated density	2, 1.611 Mg/m^3	
Absorption coefficient	2.543 mm^{-1}	
Crystal size	0.200 x 0.180 x 0.150 mm^3	
Crystal color / habit	colorless / block	
Theta range for data collection	2.970 to 25.552°	
Reflections collected / unique	50222 / 6875 [R(int) = 0.0464]	
Completeness to theta = 25.000°	99.8 %	
Absorption correction	multi-scan / sadabs	
Refinement method	Full-matrix least-squares on F^2	
Goodness-of-fit on F^2	1.025	
Final R indices [I>2sigma(I)]	R1 = 0.0391, wR2 = 0.0928	
R indices (all data)	R1 = 0.0594, wR2 = 0.1096	
Largest diff. peak and hole	0.984 and -0.916 $e.Å^{-3}$	

APPENDIX J: CRYSTAL DATA FOR $[Ag(IMesS)_2]BF_4$

Empirical formula	$C_{42}H_{48}AgBF_4N_4S_2$	
Formula weight	867.66	
Temperature	297(2) K	
Wavelength	0.71073 Å	
Crystal system, space group	Monoclinic, *C*2/*c* (No. 15)	
Unit cell dimensions	a = 20.317(2) Å	$\alpha = 90°$
	b = 8.4130(9) Å	$\beta = 99.964(4)°$
	c = 24.811(3) Å	$\gamma = 90°$
Volume	4177.1(8) $Å^3$	
Z, Calculated density	1, 1.380 Mg/m^3	
Absorption coefficient	0.635 mm^{-1}	
Crystal size	0.290 x 0.200 x 0.180 mm^3	
Crystal color / habit	colorless / block	
Theta range for data collection	2.846 to 25.426°	
Reflections collected / unique	41895 / 3846 [R(int) = 0.0286]	
Completeness to theta = 25.000°	99.8 %	
Absorption correction	multi-scan / sadabs	
Refinement method	Full-matrix least-squares on F^2	
Goodness-of-fit on F^2	1.047	
Final R indices [I>2sigma(I)]	R1 = 0.0310, wR2 = 0.0850	
R indices (all data)	R1 = 0.0350, wR2 = 0.0883	
Largest diff. peak and hole	0.327 and -0.257 $e.Å^{-3}$	

APPENDIX K: CRYSTAL DATA FOR $[Ag(IDippS)_2]BF_4$

Empirical formula	$C_{54}H_{72}AgBF_4N_4S_2$	
Formula weight	1035.95	
Temperature	200(2) K	
Wavelength	0.71073 Å	
Crystal system, space group	Triclinic, $P\bar{1}$ (No. 2)	
Unit cell dimensions	a = 10.976(4) Å	α = 104.306(10)°
	b = 13.912(4) Å	β = 97.625(11)°
	c = 19.739(6) Å	γ = 102.177(10)°
Volume	2799.9(15) $Å^3$	
Z, Calculated density	2, 1.229 Mg/m^3	
Absorption coefficient	0.484 mm^{-1}	
Crystal size	0.230 x 0.220 x 0.200 mm^3	
Crystal color / habit	colorless / block	
Theta range for data collection	2.979 to 25.677°	
Reflections collected / unique	112907 / 10578 [R(int) = 0.0485]	
Completeness to theta = 25.000°	99.8 %	
Absorption correction	multi-scan / sadabs	
Refinement method	Full-matrix least-squares on F^2	
Goodness-of-fit on F^2	1.035	
Final R indices [I>2sigma(I)]	R1 = 0.0438, wR2 = 0.1116	
R indices (all data)	R1 = 0.0560, wR2 = 0.1227	
Largest diff. peak and hole	1.081 and -0.857 $e.Å^{-3}$	

APPENDIX L: CRYSTAL DATA FOR $[Ag(IDippSe)_2]BF_4$

Empirical formula	$C_{54}H_{72}AgBF_4N_4Se_2$	
Formula weight	1129.77	
Temperature	200(2) K	
Wavelength	0.71073 Å	
Crystal system, space group	Monoclinic, *C*2/*c* (No. 15)	
Unit cell dimensions	a = 19.384(7) Å	$\alpha = 90°$
	b = 16.617(6) Å	$\beta = 114.734(10)°$
	c = 20.160(11) Å	$\gamma = 90°$
Volume	5898(4) $Å^3$	
Z, Calculated density	4, 1.272 Mg/m^3	
Absorption coefficient	1.623 mm^{-1}	
Crystal size	0.240 x 0.220 x 0.220 mm^3	
Crystal color / habit	colorless / block	
Theta range for data collection	3.154 to 25.384°	
Reflections collected / unique	94115 / 5407 [R(int) = 0.0427]	
Completeness to theta = 25.000°	99.8 %	
Absorption correction	multi-scan / sadabs	
Refinement method	Full-matrix least-squares on F^2	
Goodness-of-fit on F^2	1.083	
Final R indices [I>2sigma(I)]	R1 = 0.0385, wR2 = 0.0987	
R indices (all data)	R1 = 0.0517, wR2 = 0.1131	
Largest diff. peak and hole	0.960 and -0.897 $e.Å^{-3}$	

APPENDIX M: CRYSTAL DATA FOR $[Ag(IXyS)_2]ClO_4$

Empirical formula	$C_{38}H_{40}AgClN_4O_4S_2$	
Formula weight	824.20	
Temperature	200(2) K	
Wavelength	0.71073 Å	
Crystal system, space group	Triclinic, $P\bar{1}$ (No. 2)	
Unit cell dimensions	a = 8.1853(8) Å	α = 115.900(3)°
	b = 15.0590(16) Å	β = 92.016(3)°
	c = 16.7356(17) Å	γ = 96.927(3)°
Volume	1833.2(3) $Å^3$	
Z, Calculated density	2, 1.493 Mg/m^3	
Absorption coefficient	0.783 mm^{-1}	
Crystal size	0.290 x 0.220 x 0.180 mm^3	
Crystal color / habit	pale yellow / block	
Theta range for data collection	2.978 to 25.771°	
Reflections collected / unique	47439 / 6968 [R(int) = 0.0281]	
Completeness to theta = 25.000°	99.8 %	
Absorption correction	multi-scan / sadabs	
Refinement method	Full-matrix least-squares on F^2	
Goodness-of-fit on F^2	1.034	
Final R indices [I>2sigma(I)]	R1 = 0.0335, wR2 = 0.0861	
R indices (all data)	R1 = 0.0412, wR2 = 0.0935	
Largest diff. peak and hole	0.651 and -0.862 $e.Å^{-3}$	

APPENDIX N: CRYSTAL DATA FOR $[Ag(IXySe)_2]ClO_4$

Empirical formula	$C_{38}H_{40}AgClN_4O_4Se_2$	
Formula weight	917.99	
Temperature	200(2) K	
Wavelength	0.71073 Å	
Crystal system, space group	Triclinic, $P\bar{1}$ (No. 2)	
Unit cell dimensions	a = 8.161(3) Å	α = 115.295(13)°
	b = 15.162(5) Å	β = 92.086(14)°
	c = 16.871(6) Å	γ = 97.470(14)°
Volume	1861.4(11) $Å^3$	
Z, Calculated density	2, 1.638 Mg/m^3	
Absorption coefficient	2.614 mm^{-1}	
Crystal size	0.320 x 0.180 x 0.170 mm^3	
Crystal color / habit	colorless / block	
Theta range for data collection	2.860 to 25.789°	
Reflections collected / unique	47927 / 7059 [R(int) = 0.0421]	
Completeness to theta = 25.000°	99.9 %	
Absorption correction	multi-scan / sadabs	
Refinement method	Full-matrix least-squares on F^2	
Goodness-of-fit on F^2	1.024	
Final R indices [I>2sigma(I)]	R1 = 0.0301, wR2 = 0.0745	
R indices (all data)	R1 = 0.0421, wR2 = 0.0829	
Largest diff. peak and hole	0.555 and -0.822 $e.Å^{-3}$	

APPENDIX O: CRYSTAL DATA FOR $[Ag(IMesS)_2]ClO_4$

Empirical formula	$C_{42}H_{48}AgClN_4O_4S_2$	
Formula weight	880.30	
Temperature	200(2) K	
Wavelength	0.71073 Å	
Crystal system, space group	Monoclinic, *C*2/*c* (No. 15)	
Unit cell dimensions	a = 20.0304(17) Å	$\alpha = 90°$
	b = 8.4201(6) Å	$\beta = 99.830(5)°$
	c = 24.9694(17) Å	$\gamma = 90°$
Volume	4149.5(5) $Å^3$	
Z, Calculated density	4, 1.409 Mg/m^3	
Absorption coefficient	0.696 mm^{-1}	
Crystal size	0.400 x 0.350 x 0.220 mm^3	
Crystal color / habit	colorless / block	
Theta range for data collection	3.013 to 25.377°	
Reflections collected / unique	64838 / 4028 [R(int) = 0.0375]	
Completeness to theta = 25.000°	99.7 %	
Absorption correction	multi-scan / sadabs	
Refinement method	Full-matrix least-squares on F^2	
Goodness-of-fit on F^2	1.067	
Final R indices [I>2sigma(I)]	R1 = 0.0334, wR2 = 0.0903	
R indices (all data)	R1 = 0.0393, wR2 = 0.0942	
Largest diff. peak and hole	0.312 and -0.332 $e.Å^{-3}$	

APPENDIX P: CRYSTAL DATA FOR $[Ag(IMesSe)_2]ClO_4$

Empirical formula	$C_{42}H_{48}AgClN_4O_4Se_2$	
Formula weight	974.09	
Temperature	200(2) K	
Wavelength	0.71073 Å	
Crystal system, space group	Monoclinic, *C*2/*c* (No. 15)	
Unit cell dimensions	a = 19.975(6) Å	$\alpha = 90°$
	b = 8.573(2) Å	$\beta = 98.602(10)°$
	c = 24.937(8) Å	$\gamma = 90°$
Volume	4222(2) $Å^3$	
Z, Calculated density	4, 1.532 Mg/m^3	
Absorption coefficient	2.310 mm^{-1}	
Crystal size	0.390 x 0.360 x 0.350 mm^3	
Crystal color / habit	colorless / block	
Theta range for data collection	2.988 to 25.748°	
Reflections collected / unique	64838 / 4028 [R(int) = 0.0375]	
Completeness to theta = 25.000°	99.8 %	
Absorption correction	multi-scan / sadabs	
Refinement method	Full-matrix least-squares on F^2	
Goodness-of-fit on F^2	1.061	
Final R indices [I>2sigma(I)]	R1 = 0.0302, wR2 = 0.0708	
R indices (all data)	R1 = 0.0358, wR2 = 0.0741	
Largest diff. peak and hole	0.504 and -0.404 $e.Å^{-3}$	

APPENDIX Q: CRYSTAL DATA FOR $[Ag(IDippS)_2]ClO_4$

Empirical formula	$C_{54}H_{72}AgClN_4O_4S_2$	
Formula weight	1048.62	
Temperature	200(2) K	
Wavelength	0.71073 Å	
Crystal system, space group	Monoclinic, *C*2/*c* (No. 15)	
Unit cell dimensions	a = 19.834(5) Å	$\alpha = 90°$
	b = 16.399(4) Å	$\beta = 114.284(8)°$
	c = 20.174(6) Å	$\gamma = 90°$
Volume	5981(3) $Å^3$	
Z, Calculated density	4, 1.245 Mg/m^3	
Absorption coefficient	0.499 mm^{-1}	
Crystal size	0.280 x 0.20 x 0.120 mm^3	
Crystal color / habit	colorless / block	
Theta range for data collection	3.127 to 25.550°	
Reflections collected / unique	75092 / 5533 [R(int) = 0.0526]	
Completeness to theta = 25.000°	99.7 %	
Absorption correction	multi-scan / sadabs	
Refinement method	Full-matrix least-squares on F^2	
Goodness-of-fit on F^2	1.026	
Final R indices [I>2sigma(I)]	R1 = 0.0444, wR2 = 0.1161	
R indices (all data)	R1 = 0.0578, wR2 = 0.1261	
Largest diff. peak and hole	0.809 and -0.792 $e.Å^{-3}$	

APPENDIX R: CRYSTAL DATA FOR $[Ag(IDippSe)_2]ClO_4$

Empirical formula	$C_{54}H_{72}AgClN_4O_4Se_2$	
Formula weight	1142.41	
Temperature	297(2) K	
Wavelength	0.71073 Å	
Crystal system, space group	Triclinic, $P\bar{1}$ (No. 2)	
Unit cell dimensions	a = 11.0819(9) Å	α = 104.230(4)°
	b = 13.9167(11) Å	β = 97.489(4)°
	c = 19.7234(16) Å	γ = 100.880(4)°
Volume	2845.1(4) $Å^3$	
Z, Calculated density	2, 1.333 Mg/m^3	
Absorption coefficient	1.725 mm^{-1}	
Crystal size	0.290 x 0.150 x 0.150 mm^3	
Crystal color / habit	colorless / block	
Theta range for data collection	2.949 to 25.412°	
Reflections collected / unique	10331 / 10331 [R(int) = 0.0427]	
Completeness to theta = 25.000°	99.8 %	
Absorption correction	multi-scan / sadabs	
Refinement method	Full-matrix least-squares on F^2	
Goodness-of-fit on F^2	1.084	
Final R indices [I>2sigma(I)]	R1 = 0.0460, wR2 = 0.0863	
R indices (all data)	R1 = 0.0800, wR2 = 0.1039	
Largest diff. peak and hole	0.76 and -0.54 $e.Å^{-3}$	

APPENDIX S: CRYSTAL DATA FOR $[Ag(IXyS)_2]PF_6$

Empirical formula	$C_{38}H_{40}AgF_6N_4PS_2$	
Formula weight	869.71	
Temperature	297(2) K	
Wavelength	0.71073 Å	
Crystal system, space group	Triclinic, $P\bar{1}$ (No. 2)	
Unit cell dimensions	a = 8.3415(11) Å	α = 116.284(4)°
	b = 15.2406(18) Å	β = 91.073(6)°
	c = 17.011(3) Å	γ = 96.788(4)°
Volume	1919.3(5) $Å^3$	
Z, Calculated density	2, 1.505 Mg/m^3	
Absorption coefficient	0.738 mm^{-1}	
Crystal size	0.140 x 0.200 x 0.300 mm^3	
Crystal color / habit	colorless / block	
Theta range for data collection	2.98 to 25.42°	
Reflections collected / unique	7022 / 7022 [R(int) = 0.0371]	
Completeness to theta = 25.000°	99.1 %	
Absorption correction	multi-scan / sadabs	
Refinement method	Full-matrix least-squares on F^2	
Goodness-of-fit on F^2	1.004	
Final R indices [I>2sigma(I)]	R1 = 0.0499, wR2 = 0.1389	
R indices (all data)	R1 = 0.0764, wR2 = 0.1677	
Largest diff. peak and hole	0.509 and -0.554 $e.Å^{-3}$	

APPENDIX T: CRYSTAL DATA FOR $[Ag(IDippS)_2]PF_6$

Empirical formula	$C_{54}H_{72}AgF_6N_4PS_2$	
Formula weight	1094.11	
Temperature	200(2) K	
Wavelength	0.71073 Å	
Crystal system, space group	Triclinic, $P\bar{1}$ (No. 2)	
Unit cell dimensions	a = 11.0203(17) Å	α = 104.082(6)°.
	b = 13.9506(15) Å	β = 96.231(6)°.
	c = 19.992(2) Å	γ = 102.533(7)°.
Volume	2867.6(6) $Å^3$	
Z, Calculated density	2, 1.267 Mg/m^3	
Absorption coefficient	0.508 mm^{-1}	
Crystal size	0.260 x 0.200 x 0.200 mm^3	
Crystal color / habit	colorless / block	
Theta range for data collection	2.953 to 25.391°.	
Reflections collected / unique	91585 / 10442 [R(int) = 0.0352]	
Completeness to theta = 25.000°	99.8 %	
Absorption correction	multi-scan / sadabs	
Refinement method	Full-matrix least-squares on F^2	
Goodness-of-fit on F^2	1.041	
Final R indices [I>2sigma(I)]	R1 = 0.0360, wR2 = 0.0943	
R indices (all data)	R1 = 0.0484, wR2 = 0.1075	
Largest diff. peak and hole	0.150 and -0.633 e. $Å^{-3}$	

APPENDIX U: CRYSTAL DATA FOR $[Ag(IDippSe)_2]PF_6$

Empirical formula	$C_{54}H_{72}AgF_6N_4PSe_2$	
Formula weight	1187.91	
Temperature	200(2) K	
Wavelength	0.71073 Å	
Crystal system, space group	Triclinic, $P\bar{1}$ (No. 2)	
Unit cell dimensions	a = 11.057(3) Å	α = 104.328(11)°
	b = 13.978(4) Å	β = 96.030(12)°
	c = 19.887(5) Å	γ = 101.122(12)°
Volume	2884.1(14) Å3	
Z, Calculated density	2, 1.368 Mg/m^3	
Absorption coefficient	1.695 mm^{-1}	
Crystal size	0.260 x 0.200 x 0.200 mm^3	
Crystal color / habit	colorless / block	
Theta range for data collection	2.967 to 25.371°	
Reflections collected / unique	52171 / 10530 [R(int) = 0.0351]	
Completeness to theta = 25.000°	99.8 %	
Absorption correction	multi-scan / sadabs	
Refinement method	Full-matrix least-squares on F^2	
Goodness-of-fit on F^2	1.076	
Final R indices [I>2sigma(I)]	R1 = 0.0347, wR2 = 0.0797	
R indices (all data)	R1 = 0.0552, wR2 = 0.0949	
Largest diff. peak and hole	0.774 and -0.525 e.$Å^{-3}$	

APPENDIX V: CRYSTAL DATA FOR $[Ag(IXyS)_2]SbF_6$

Empirical formula	$C_{38}H_{40}AgF_6N_4S_2Sb$	
Formula weight	960.50	
Temperature	200(2) K	
Wavelength	0.71073 Å	
Crystal system, space group	Triclinic, $P\bar{1}$ (No. 2)	
Unit cell dimensions	a = 8.2449(7) Å	α = 116.355(3)°
	b = 15.4281(15) Å	β = 90.728(3)°
	c = 17.0404(16) Å	γ = 97.254(3)°
Volume	1921.0(3) $Å^3$	
Z, Calculated density	2, 1.661 Mg/m^3	
Absorption coefficient	1.384 mm^{-1}	
Crystal size	0.240 x 0.220 x 0.200 mm^3	
Crystal color / habit	colorless / block	
Theta range for data collection	2.979 to 25.764°	
Reflections collected / unique	50752 / 7316 [R(int) = 0.0349]	
Completeness to theta = 25.000°	99.8 %	
Absorption correction	multi-scan / sadabs	
Refinement method	Full-matrix least-squares on F^2	
Goodness-of-fit on F^2	1.045	
Final R indices [I>2sigma(I)]	R1 = 0.0249, wR2 = 0.0558	
R indices (all data)	R1 = 0.0342, wR2 = 0.0617	
Largest diff. peak and hole	0.494 and -0.574 $e.Å^{-3}$	

APPENDIX W: CRYSTAL DATA FOR $[Ag(IDippS)_2]SbF_6$

Empirical formula	$C_{54}H_{72}AgF_6N_4S_2Sb$	
Formula weight	1184.92	
Temperature	297(2) K	
Wavelength	0.71073 Å	
Crystal system, space group	Triclinic, $P\bar{1}$ (No. 2)	
Unit cell dimensions	a = 11.2306(19) Å	α = 84.497(4)°
	b = 13.859(2) Å	β = 88.643(4)°
	c = 28.811(5) Å	γ = 77.403(4)°
Volume	4356.1(13) $Å^3$	
Z, Calculated density	3, 1.355 Mg/m^3	
Absorption coefficient	0.930 mm^{-1}	
Crystal size	0.200 x 0.200 x 0.130 mm^3	
Crystal color / habit	colorless / block	
Theta range for data collection	2.932 to 25.561°	
Reflections collected / unique	139073 / 16189 [R(int) = 0.0606]	
Completeness to theta = 25.000°	99.8 %	
Absorption correction	multi-scan / sadabs	
Refinement method	Full-matrix least-squares on F^2	
Goodness-of-fit on F^2	1.213	
Final R indices [I>2sigma(I)]	R1 = 0.0748, wR2 = 0.1570	
R indices (all data)	R1 = 0.1114, wR2 = 0.1704	
Largest diff. peak and hole	1.170 and -1.483 $e.Å^{-3}$	